

UNCLASSIFIED

AD 286 318

*Reproduced
by the*

**ARMED SERVICES TECHNICAL INFORMATION AGENCY
ARLINGTON HALL STATION
ARLINGTON 12, VIRGINIA**



UNCLASSIFIED

NOTICE: When government or other drawings, specifications or other data are used for any purpose other than in connection with a definitely related government procurement operation, the U. S. Government thereby incurs no responsibility, nor any obligation whatsoever; and the fact that the Government may have formulated, furnished, or in any way supplied the said drawings, specifications, or other data is not to be regarded by implication or otherwise as in any manner licensing the holder or any other person or corporation, or conveying any rights or permission to manufacture, use or sell any patented invention that may in any way be related thereto.

286 318

63-1-2

286318

U. S. A R M Y
TRANSPORTATION RESEARCH COMMAND
FORT EUSTIS, VIRGINIA

CATALOGUED BY ADIIR

AS AD NO.

TCREC TECHNICAL REPORT 62-35

**OVERLAND AIR-CUSHION VEHICLE STABILITY
AND CONTROL WIND TUNNEL EXPERIMENTS**

Task 9R99-01-005-02

Contract DA 44-177-TC-709

November 1961

prepared by:

AERONUTRONIC
A Division of Ford Motor Company
Ford Road
Newport Beach, California



DISCLAIMER NOTICE

When Government drawings, specifications, or other data are used for any purpose other than in connection with a definitely related Government procurement operation, the United States Government thereby incurs no responsibility nor any obligation whatsoever; and the fact that the Government may have formulated, furnished, or in any way supplied the said drawings, specifications, or other data is not to be regarded by implication or otherwise as in any manner licensing the holder or any other person or corporation, or conveying any rights or permission, to manufacture, use, or sell any patented invention that may in any way be related thereto.

ASTIA AVAILABILITY NOTICE

Qualified requesters may obtain copies of this report from

Armed Services Technical Information Agency
Arlington Hall Station
Arlington 12, Virginia

This report has been released to the Office of Technical Services, U. S. Department of Commerce, Washington 25, D. C., for sale to the general public.

The information contained herein will not be used for advertising purposes.

The findings and recommendations contained in this report are those of the contractor and do not necessarily reflect the views of the Chief of Transportation or the Department of the Army.

Publication No. U-1447
Dated: 10 November 1961

SPECIAL PROGRAMS OPERATIONS

Submitted to:

U. S. Army Transportation Research Command
Fort Eustis, Virginia

CONTRACT NO. DA 44-177-TC-709

TECHNICAL REPORT

OVERLAND AIR-CUSHION VEHICLE
STABILITY AND CONTROL
WIND TUNNEL EXPERIMENTS

Prepared by:

B. H. Carmichael

B. H. Carmichael

D. E. McNay

D. E. McNay

Approved by:

M. F. Southcote

M. F. Southcote, Manager
Air Transportation

AERONUTRONIC

A DIVISION OF *Ford Motor Company*


FORD ROAD/NEWPORT BEACH, CALIFORNIA

HEADQUARTERS
U. S. ARMY TRANSPORTATION RESEARCH COMMAND
Fort Eustis, Virginia

The contemplated Army missions for Ground Effect Machines require that the ground clearances be greater and the overall machine dimensions be smaller, leading to a higher value of h/d ratio than has usually been investigated for air cushion concepts. Since the annular jet and plenum chamber configurations normally become unstable at h/d ratios above 0.05 to 0.1, this investigation was undertaken to determine the static stability of a generalized annular jet in hovering and forward flight and to evaluate various modifications which would improve the stability. In addition to stability, data were generated on control forces and performance.

The results of this investigation indicate that inherent stability can be achieved in the GEM at the operating heights believed to be necessary for overland use.

FOR THE COMMANDER:


KENNETH B. ABEL
1st Lt., TC
Assistant Adjutant

APPROVED BY:


WILLIAM D. HINSHAW
Project Engineer

TABLE OF CONTENTS

	<u>PAGE</u>
LIST OF ILLUSTRATIONS	1
LIST OF SYMBOLS	4
SUMMARY	7
CONCLUSIONS	9
INTRODUCTION	10
DESCRIPTION OF EXPERIMENTAL EQUIPMENT	11
EXPERIMENTAL PROCEDURE	16
EXPERIMENTAL RESULTS	25
(1) EFFECT OF FORWARD SPEED - MODEL STRAIGHT AND LEVEL	25
(2) STATIC LONGITUDINAL STABILITY	43
(3) STATIC LATERAL STABILITY	57
(4) STATIC DIRECTIONAL STABILITY	63
(5) STATIC CROSS-TERMS IN YAW	71
(6) LONGITUDINAL CONTROL	78
(7) LATERAL CONTROL	79
(8) DIRECTIONAL CONTROL AND BRAKING	80
ACKNOWLEDGMENTS	88
BIBLIOGRAPHY	89

LIST OF ILLUSTRATIONS

	<u>PAGE</u>
1. Drawing of Basic Jet Segmented Model.	19-a
2. Drawing of Skirted and Flap Segmented Model.	19-b
3. Drawing of High Speed Configuration.	19-c
4. Photograph of Faired Model.	
5. Photograph of Faired Model with Simulated Jet.	
6. Photograph of Basic Jet Segmented Model.	
7. Photograph of Skirted and Flap Segmented Model.	
8. Photograph of Model with Propulsion Fans and Tail.	
9. Photograph of Model with Extended Tail.	
10. Photograph of Model with Open Front Skirt and Forward Jets Sealed.	
11. Photograph of High Speed Model with Tilted Propulsion Fans.	
12. Photograph of Model with G. E. Type Inlet Louvers.	
13. Photograph of Model with 60° β Vanes in Jets.	
14. Base and Jet Instrumentation Identification.	20
15. Base and Jet Pressure Tap Areas of Influence.	21
16. Upper Model Pressure Tap Distribution.	22
17. Side Model Pressure Tap Distribution.	23
18. Pressure Distribution About Model.	24
19. Effect of Flight Speed on Lift.	32
20. Calculated vs. Measured Momentum Drag.	33
21. Effect of Flight Speed on Center of Pressure Location.	34

LIST OF ILLUSTRATIONS, continued...

	<u>PAGE</u>
22. Effect of Intake Flow on Longitudinal Pressure Distribution.	35
23. Longitudinal Pressure Distribution for Basic and High Speed Configuration.	36
24. Effect of Model Buildup on Longitudinal Trim Problem.	37
25. Effect of Skirt and Jet Modifications on Longitudinal Trim Problem.	38
26. Lift Drag Ratio for Standard and High Speed Configuration.	39
27. Effect of Height, Speed, and Configuration on L/D.	40
28. Performance Cost of Segmenting Jet Stabilization.	41
29. Ground Effect Power Factor in Hovering.	42
30. Effect of Height and Speed on Static Longitudinal Stability (J).	48
31. Effect of Pitch on Pressure Distribution.	49
32. Effect of Height and Speed on Static Longitudinal Stability (S).	50
33. Effect of Height and Speed on Static Longitudinal Stability (J/2 S 3/4).	51
34. Effect of B Vanes on Static Longitudinal Stability.	52
35. Effect of Propulsion Nacelles on Static Longitudinal Stability.	53
36. Effect of Location on Horizontal Tail Effectiveness.	54
37. Effect of Jet and Skirt Modifications on Static Longitudinal Stability.	55
38. Effect of Jet and Skirt Modifications on Static Longitudinal Stability.	56
39. Effect of Height and Speed on Static Lateral Stability (J).	59
40. Effect of Height and Speed on Static Lateral Stability (S).	60
41. Effect of Height and Speed on Static Lateral Stability (J/2 S 3/4).	61
42. Effect of Configuration Changes on Static Lateral Stability.	62

LIST OF ILLUSTRATIONS, continued....

	<u>PAGE</u>
43. Effect of Model Buildup on Directional Neutral Point (Faired Model).	66
44. Effect of Model Buildup on Directional Neutral Point (Blowing Model).	67
45. Effect of Yaw on External Pressure Distribution.	68
46. Effect of Propulsion Fan Mode on Directional Neutral Point.	69
47. Directional Stabilization Power of Vertical Tails and Propulsion Nacelles.	70
48. Effect of Yaw on Lateral g and Longitudinal g .	74
49. Effect of Yaw on Roll Trim and Pitch Trim.	75
50. Effect of Yaw on Lateral g and Longitudinal g .	76
51. Effect of Yaw on Roll Trim and Pitch Trim.	77
52. Longitudinal Control Power of Tail, Jet and Propulsion Nacelles.	82
53. Effect of Location on Horizontal Tail Control Power.	83
54. Lateral Control Power.	84
55. Power and Cost of Lateral Control.	85
56. Power and Cost of Lateral Control.	86
57. Directional Control Power.	87

LIST OF SYMBOLS

<u>Symbol</u>	<u>Description</u>	<u>Units</u>
AR	Aspect ratio (of tail) = b_t^2/S_T	--
b	Characteristic length (base + jets)	ft
Δb	Distance between center of pressure and moment center	ft
c	Chord (of tail or nacelle in x direction)	ft
C. G.	Center of Gravity (moment center) in % b	%
C. P.	Center of Pressure in % b or % W	%
c_p	Pressure coefficient = $(p_{local} - p_{ambient})/q$	--
C_L	Lift coefficient = L/qS	--
C_D	Drag coefficient = D/qS	--
C_Y	Side force coefficient = Y/qS	--
C_m	Pitching moment coefficient = M/qSb	--
C_l	Rolling moment coefficient = l/qSW	--
C_N	Yawing moment coefficient = N/qSW	--
C_L	Centerline	--
d	Effective vehicle diameter = $\sqrt{4S/\pi}$	ft
d	Nacelle diameter	ft
D	Drag force	lbs
G	Ground effect power factor (see Page)	--
g	Acceleration of gravity	32.2 ft/sec ²

LIST OF SYMBOLS, continued...

<u>Symbol</u>	<u>Description</u>	<u>Units</u>
h	Clearance height (base to ground)	ft
HP	Horsepower = $P/550$	HP
i_t	Incidence angle of the tail	deg
l	Peripheral length of jet at jet Q_L	ft
l	Rolling moment	ft lbs
L	Lift force	lbs
L/D	Lift drag ratio (see Figure)	--
M	Pitching Moment	ft lbs
N	Yawing Moment	ft lbs
NP	Yawing neutral point location in % b	%
p	Static pressure	lbs/ft ²
\bar{p}_{tj}	Average jet total pressure	lbs/ft ²
P	Power	ft lbs/sec
Q	Volume flow of air	ft ³ /sec
q	Flight dynamic pressure = $\frac{\rho}{2} v^2$	lbs/ft ²
RPM	Revolutions per minute (of the fan)	RPM
S	Reference area (base plus jet)	ft ²
S_{frontal}	Vehicle frontal area	ft ²
t_e	Jet thickness	ft
V	Flight velocity	ft/sec
V_j	Jet velocity	ft/sec
w	Characteristic width (base + jets)	ft

LIST OF SYMBOLS, continued...

<u>Symbols</u>	<u>Description</u>	<u>Units</u>
X	Force in the flight direction	lbs
Y	Side force	lbs
α	Angle of attack (pitch plane)	deg
ϕ	Angle of roll	deg
ψ	Angle of Yaw	deg
θ	Jet angle (from the vertical)	deg
β	Beta vane angle (from the vertical)	deg
ϵ	Downwash angle (from the horizontal)	deg
ρ	Mass density of air	lb sec ² /ft ⁴
Δ	Increment or change	--
—	Any area averaged value when used over a symbol	

SIGN CONVENTIONS

<u>Angles and Moments</u>	<u>Plane</u>
Positive nose up	Pitch
Positive Right side down	Roll
Positive nose right	Yaw
Positive trailing edge down	Control

<u>Forces</u>	<u>Axis</u>
Positive up	Vertical force
Positive aft	Longitudinal force
Positive out to right	Side force

SUMMARY

Wind tunnel tests of a peripheral jet air-cushion vehicle model at heights primarily greater than 10% of the diameter have been conducted. The 3-foot by 2-foot model employed separate lift and propulsion systems.

Inherent, static longitudinal and lateral stability was achieved at all heights (up through 20% of the diameter) and all speeds (up through flight dynamic pressure = 1.10 jet total pressure). This was accomplished by base centerline segmenting jets. A second successful method consisted of base centerline segmenting flaps in combination with a peripheral skirt of length equal to 10% of the vehicle length. Twin shrouded propulsion fans at the rear of the model provided static directional stability. Degree of stability required is still to be determined.

The model was out of trim in pitch (nose up) at all forward speeds for the full peripheral jet model. Increasing forward speed results in a reduction in base pressure at the nose providing a nose down pitch contribution. The upper surface airloads due to both the flow about the model and the inflow to the lift fans provided a nose up pitch. The large net nose up tendency was corrected for the cruise condition by employing lift system jets in only the rear half of the model together with a peripheral skirt of length equal to 10% of the model length at the sides and rear of the model. The skirt was not employed across the front of the model. The effective lift to drag ratio of the model was also doubled by this modification.

It was anticipated that the turn maneuver would be accomplished by yawing the model. Lateral accelerations of up to 1 g were obtained at 45° yaw for the model with propulsion fans on. This would provide excellent turning radius. The model level yaw runs also revealed, however, strong roll into the turn and strong nose down pitching moment. Both were beyond the capability of the control system at $\psi = 45^\circ$. The breakdown on contributions was the same as in the case of nose up pitch at $\psi = 0^\circ$.

Closure of front or rear jets did not provide adequate longitudinal control at forward speeds. The control power of a horizontal tail of area equal to 11.5% of planform area and tail length equal to half the model length provided the anticipated control power, which was, however, unable to correct the very high nose up pitch mentioned above. The horizontal tail was almost completely ineffectual as a stabilization device when mounted above the propulsion fans. Some effectiveness was obtained when mounted between the vertical tails. Tilting the propulsion fans provided the best longitudinal control power. Both thrust and normal force components on the propulsion nacelles contribute. Mechanical feasibility of this system is yet to be proven. Control surfaces placed behind propulsion fans would provide a simpler system. Closure of side jet controls provided moderate lateral control but at an unacceptable penalty in lift. Differential thrust of the propulsion fans provided adequate directional control. Windmilling of the propulsion fans resulted in zero thrust. The drag of the model then provided a 0.28 g braking deceleration at $q/p_t = .55$ and $h/S = 0.64$. Reversing the propulsion fans provided a 0.75 g braking deceleration but lead to static directional instability at small yaw angles. Dynamic calculations would be required to determine whether the powerful directional control and vehicle inertia would permit full braking action. This degree of braking represents a reverse thrust 70% in excess of the forward thrust at the same RPM.

Summing up, it appears that 3 axis static stability can be achieved for a limited class of jet air-cushion vehicles over a large height and speed range. It should be noted that the segmenting flap and skirt solution was obtained with rigid devices. The effect of flexibility remains to be determined. Considerable analytical method development is required to enable generalization of these test results. The control aspects of the problem require further study concentrating on control schemes not associated with the peripheral jet exit.

CONCLUSIONS

It is concluded that static longitudinal, lateral and directional stability can be achieved for peripheral jet air-cushion vehicles operating at heights up to and including 20% of their effective diameters and at flight dynamic pressures up to and in excess of jet total pressure with modest cost in performance.

Typical peripheral jet models experienced a large nose up pitching moment due to forward speed. Strong pitch and roll due to yaw hamper the flat yawing turn maneuver. Configuration changes leading to reduction of these undesirable effects require further study.

It is concluded that peripheral jet controls should not be used in forward flight due to limited control power and high lift loss. Controllable shrouded propulsion fans or control surfaces behind the propulsion fans are suggested instead. Considerable additional study is required to evolve a satisfactory control system.

The performance penalty associated with the momentum drag of the large quantities of air required for operation at the heights and speeds of this study indicate that the designer must give careful consideration to the selection of the propulsion system (i. e. , external vs. internal propulsion). For vehicle missions which entail a majority of high speed operation, it is desirable to reduce the cushion contribution to lift to a minimum and maximize external lift production. The configuration must then be compromised to provide adequate low speed performance and maneuverability. The resulting vehicle may be considerably different from one evolved from the hovering concept and will have its own set of stability and control problems. Since both these vehicle concepts are likely to have an air-cushion for at least a portion of its operation, the results of this study should be useful in estimating the cushion contributions to stability and control problems.

INTRODUCTION

Army transportation is faced with the problem of providing improved amphibious and off-road vehicles. The air-cushion vehicle has been suggested for this role. The rough country, off-road mission requires a vehicle of modest size with larger relative ground clearance than has been typical of air-cushion study to date.

Aeronutronic has, at the request of U. S. Army Transportation Research Command, conducted a study of the stability and control problems of overland air-cushion vehicles at height diameter ratios greater than 10%. The hovering phase of the project is reported in Reference 1. This work was used as the basis for the wind tunnel model design. The results of the analysis of the wind tunnel tests are herein reported. The basic force and pressure data are available in tabular form at Aeronutronic. Vought will provide a basic data report in plotted form. This report will be forwarded to U. S. Army Transportation Research Command by mid-December 1961.

DESCRIPTION OF EXPERIMENTAL EQUIPMENT

1. Tunnel Description

The program was conducted in the Chance Vought low speed wind tunnel at Dallas, Texas. The tunnel was of the atmospheric pressure, single return, closed throat variety. The test section was 7 feet high, 10 feet wide, and 16 feet long. A ground board was installed parallel to and two feet above the tunnel floor. It extended four feet fore and aft of the model support post and almost spanned the tunnel laterally as shown in Figure 4.

2. Model Mounting

The model was mounted right side up, above the ground board, on a single post support which pierced the ground board. The base of the model support was rigidly bolted to the top of the pyramid type balance system just below the tunnel floor. The upper end of the support post passed through a trunion in the model base, and extended to near the top of the model shell. Two electrical actuators tied into the top of the support post enabling the model to be rotated remotely in pitch and roll. The air supply for the tip jet fans was fed through the hollow support post and distributed to the fans through flexible hoses. The tip jet air supply was brought aboard the pyramid balance with a trapeze which made the force and moment inputs a minimum. In addition, the system was calibrated over a range of feed pressures to permit air-tares to be subtracted. The model was rotated remotely in yaw by the Chance Vought turntable. A swivel in the supply air line permitted this rotation. A close tolerance gap limited the air cushion leakage about the support strut to a negligible amount. Fairings shielded the support strut from tunnel wind loads. A typical fouling warning circuit was employed. Electrical leads from the four scanni-valves, pressure leads from four monitoring total pressure tubes, electrical leads from six fan RPM monitoring devices, and electrical leads from the pitch and roll actuators and from their position indicators were brought out of the tunnel along the outside of the support tube.

3. Model Description

The annular jet air cushion model was of rectangular planform with a length 50% greater than the width. The basic body height was about a third of the width. The body may be described as aerodynamically blunt with rounded corners.

Lift power was provided by four 7-inch diameter tip jet air driven fans mounted horizontally in the model. Flush and louvered inlets in the upper model surface were investigated during the tests. The fans were each capable of producing 60 pounds of static thrust at 24,000 RPM when operating free and fed with 1 lb/sec of 250 psi air.

The contract schedule required rapid model fabrication and use of existing fans. The model design criteria called for a high speed, uniform, peripheral jet. The tip jet fans loaned by Chance Vought solved the problem nicely. The lift fans discharged vertically into plenum chambers and through screens into the jets. A uniform, high velocity jet was obtained at the cost of low internal efficiency.

Propulsion and braking power was provided by two shrouded 7-inch diameter tip jet air driven fans mounted vertically at the rear of the model.

Longitudinal and lateral stabilization was provided by base segmenting jets along the model longitudinal and lateral centerline. A second system, consisting of a peripheral skirt and base segmenting flaps extending partially to the ground beneath the model base was also investigated. Directional stabilization was provided by the shrouded propulsion fans. A second system using conventional twin vertical tails was also investigated.

Longitudinal control was investigated by narrowing the forward or aft peripheral jet. Variable incidence horizontal tail and propulsion fan tilt were also investigated for longitudinal control in forward flight.

Lateral control was accomplished by narrowing the side peripheral jet.

Directional control was achieved through differential thrust of the rear propulsion fans.

The principal geometric characteristics of the model are defined in Table A. Further geometric description is found in the instrumentation section. Scale drawings of the model are shown in Figures 1 through 3. Photographs of several model configurations are shown in Figures 4 through 13.

4. Model Configurations Tested

<u>No Power</u>	<u>Propulsion Power Only</u>	<u>Lift Power Only</u>	<u>Lift and Pro- pulsion Power</u>
F	FP	J	JP
F _{with sim jet}	FPT	JL _L	JPT
		J B ₃₀ & 60	J/2 S ^{3/4} P + 15°
F S ^{3/4}		JVT	
		J EXT T	
		J/2 S ^{3/4}	
		S	

Where:

F	Faired model - no jets
J	Peripheral jet and base segmenting jets operating
J/2	Rear jet, rear half of side jets, and rear longitudinal jet operating
P	Twin propulsion fans operating
PT	Horizontal tail mounted above propulsion fans
VT	Horizontal tail mounted between vertical tails

EXT T	Horizontal and vertical tails mounted on extended booms
S	Skirt around vehicle - base segmented with flaps
S 3/4	Skirt around rear half, side walls on, front open
B ₃₀ & 60	30° and 60° Beta vanes in all longitudinal jets
P + 15°	Propulsion fans tilted 15° for longitudinal trim

5. Instrumentation

a. Force and Moment Data

The total forces and moments on the model were obtained directly from the Vought pyramid type balance. All six components (lift, drag, side force, pitching moment, rolling moment, and yawing moment) were measured in the wind axis system. The moments were measured about the resolving center which lies in the center of the tunnel cross sectional area. Moment transfers were made to the assumed model center of gravity which was located six inches above the model base. The transfer distances were different for each model height.

The Vought computer also transferred the data to the body axis system with the exception of the pure roll runs for which they had not had a previous requirement.

b. Pressure Data

The model lift system was powered with tip jet fans. The model jet exits flow consisted of 20% tip jet flow (which had been fed to the fans through the hollow model support pipe) and 80% flow induced by the fans through the inlets in the model upper surface. There was no simple measurement that could be made to obtain the exit power of the lift system. It was necessary to install total head tube and static head tube pairs at 28

locations in the jet exits as shown in Figure 14 to obtain the jet exit power, flow quantities, jet velocities, and jet reactions. There were also 36 flush static taps in the base of the model which together with the jet taps previously mentioned allowed integration of the cushion contributions to lift and moment through use of the area-arm information of Figure 15.

There were also 93 additional flush static taps in the sides and top of the model (as called out in Figures 16 and 17) with which the upper external load distributions could be monitored. †

The 185 pressures were conducted to a scani-valve assembly consisting of four 48 port valves. Each valve employed a ± 2.5 psi differential pressure transducer in which the measured pressures were bucked against the free stream ambient level. The spare tap on each valve had a known pressure imposed which gave a check of the complete scani-valve and readout system. All pressures were converted to units of pounds per square foot and (for all non-hovering runs) were also converted to pressure coefficients form $(\frac{P_{local} - P_{ambient}}{\text{flight dynamic pressure}})$.

In general, the pressure monitoring system performed well in spite of the fact that it was being operated at much lower pressure levels than were typical for Vought high speed tunnel work. There was a small range of allowable sealing oil quantity which would prevent leaks without causing small pressure values to be masked by hang up. Some data was lost through malfunction but not in an amount significant to the analysis of the test results.

† A typical upper external load distribution is presented in Figure 18. Note the high negative pressures around the corners and on the upper nose region.

EXPERIMENTAL PROCEDURE

The air feed to the lift fans was turned on with the tunnel shut down. The individual lift fans were adjusted with the valves provided in the model until the static rolling and pitching moments were near zero. The total feed was adjusted with the master valve until the monitoring total head tubes indicated the peripheral jet was at the design total pressure level. Since previous work had shown that properly non-dimensionalized results were independent of the absolute pressure level, no systematic variations of pressure level were made in this experiment. The average peripheral jet total pressure level was held at about 30 pounds per square foot. The supply air controls were held fixed once set as other variables such as model attitude and tunnel speed were varied. For most configurations, this procedure resulted in the same jet total pressure at a given tunnel speed throughout the program. An exception occurred with the J/2 S 3/4 configuration. The ram air entering the open front skirt caused an increase in the back pressure and a decrease in the flow at the jet exit, thus the total pressure rose due to the fan characteristics. Thus, although the air feed was the same, and the tunnel speed was the same as for the basic configuration, the ratio of q/\bar{p}_{tj} was different.

When propulsion fans were added, the procedure was as follows. At the intermediate speed ($q/\bar{p}_{tj} = 0.55$) the propulsion fans were adjusted with the wind tunnel running to just cancel out the total drag (unaccelerated flight) and were individually adjusted to produce zero yawing moment. At the high speed condition ($q/p_{tj} = 1.10$) the fixed pitch propulsion fans were not able to completely cancel the drag so were run wide open.

The remote control of pitch, roll, and yaw angle permitted very rapid execution of stability runs. The model was built and constructed for rapid model changes. The average time consumed by Mr. F. F. Kerns (in all but the few elaborate configuration changes) was one to two minutes. All model components including the remote pitch and roll actuation system functioned perfectly.

The tip jet fans burned out bearings on eight occasions early in the program due to dirt in the air supply. After this initial trouble, the remaining three-fourths of the program was carried out without further mishap.

The Vought force balance system functioned without trouble. The pressure monitoring scani-valve system caused trouble throughout the program. Each day's tests were preceded by several hours of scani-valve maintenance and checkout. Delays were often encountered in the testing due to some portion of pressure pickup or readout equipment. Due to the continuous and vigorous effort on the part of Vought personnel, sufficient pressure data was salvaged from the program to permit evaluation of performance as well as stability and control aspects of the program.

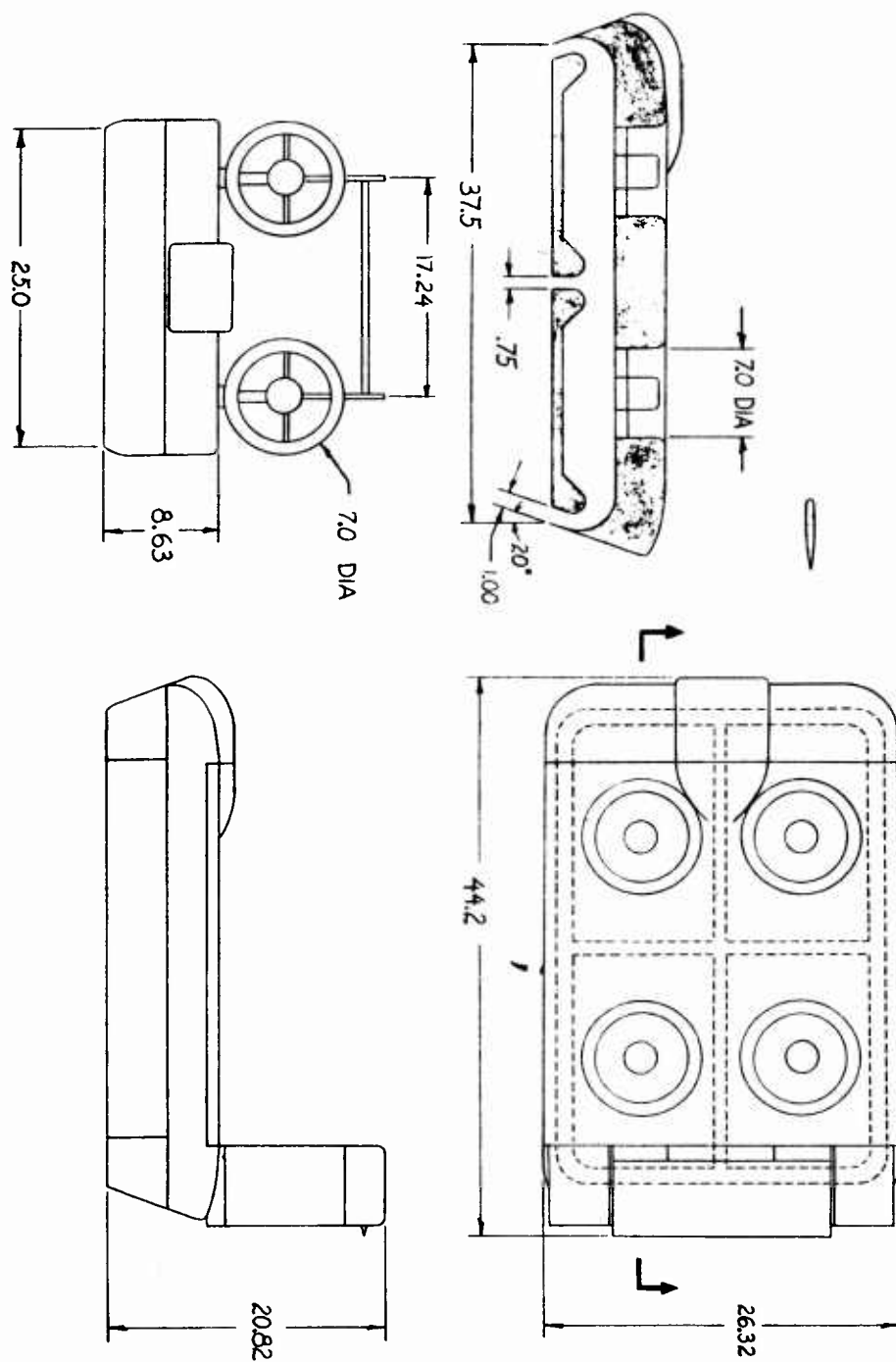
TABLE A

MODEL DIMENSIONS

<u>ITEM</u>	<u>DEFINITION</u>	<u>IN. or IN.²</u>	<u>FT. or FT.²</u>
Characteristic Length	Base + Peripheral Jet	37.5	3.12
Characteristic Width	Base + Peripheral Jet	25.0	2.08
Characteristic Area	Base + Peripheral Jet	925.0	6.43
Characteristic Pressure	Design Jet Total Pressure	5.8" H ₂ O	30 lb/ft ²
Overall Length	Including cab and tail	45.63	3.8
Overall Width		26.38	2.2
Overall Height	Including propulsion fans	20.88	1.74
Planform Area		1107.0	7.69
Total Weight	Including support post	-	200 lbs
Body Height	Base to Basic model top	8.63	.72
Base Length		35.38	2.94
Base Width		22.88	1.91
Base Area	Including Segmenting jets	802.5	5.57
Body Frontal Area	Including cab	232	1.61
Body Side Area	Including Cab	368	2.56
Peripheral Jet Width	Perpendicular to jet	1.0	.083
Peripheral Jet Length	On jet centerline	115.6	9.61
Peripheral Jet Area	Perpendicular to jet	115.6	.80
Peripheral Jet Angle	Measured from perpendicular	-	20°
Segmenting Jet Width	Perpendicular to jet	.75	.0625
Segmenting Jet Length	Longitudinal + lateral	43.0	3.58
Segmenting Jet Area	Perpendicular to jet	32.2	.224
Segmenting Jet Angle	Measured from perpendicular	-	0°
Fan Outer Diameter		7.0	.584
Fan Hub Diameter		2.63	.219
Fan Area	One fan	33.10	.23
Fan Area	Four lift fans	132.7	.92
Total Jet Area	Segmenting Jets open	147.5	1.024
Exit Area/Inlet Area	Segmenting Jets open	-	1.11
Skirt & Flap Length	Perpendicular to base	3.66	.305
Center of Gravity	From Longitudinal Centerline	0	0
Center of Gravity	From Lateral Centerline	0	0
Center of Gravity	Above base plane	6.0	.50

TABLE A, Continued...

<u>ITEM</u>	<u>DEFINITION</u>	<u>IN. or IN. ²</u>	<u>FT. or FT. ²</u>
Propulsion Fans	Height of Centerline above deck	7.5	.625
Propulsion Fans	Width between centers	17.25	1.44
Propulsion Fans	Distance of face aft of C. G.	17.25	1.44
Propulsion Nacelle	Diameter (each of two)	8.2	.684
Propulsion Nacelle	Chord (each of two)	6.5	.541
Propulsion Nacelle	Tail Length (C. G. to C. P.)	18.3	1.53
Horizontal Tail Span		17.25	1.44
Horizontal Tail Chord		6.20	0.516
Horizontal Tail Area		107.00	0.743
Horizontal Tail Length (Standard)	(C. P. to C. G.)	18.30	1.53
Horizontal Tail Length (Extended)	(C. P. to C. G.)	34.30	2.86
Vertical Tail Span	(each of two)	11.69	.973
Vertical Tail Chord	(each of two)	6.50	.541
Vertical Tail Area	(each of two)	76.00	.528
Vertical Tail Length (Standard)	(C. P. to C. G.)	18.30	1.53



STABILITY AND CONTROL WIND TUNNEL MODEL
BASIC DIMENSIONS

FIGURE 1. DRAWING OF BASIC JET SEGMENTED MODEL
19-a

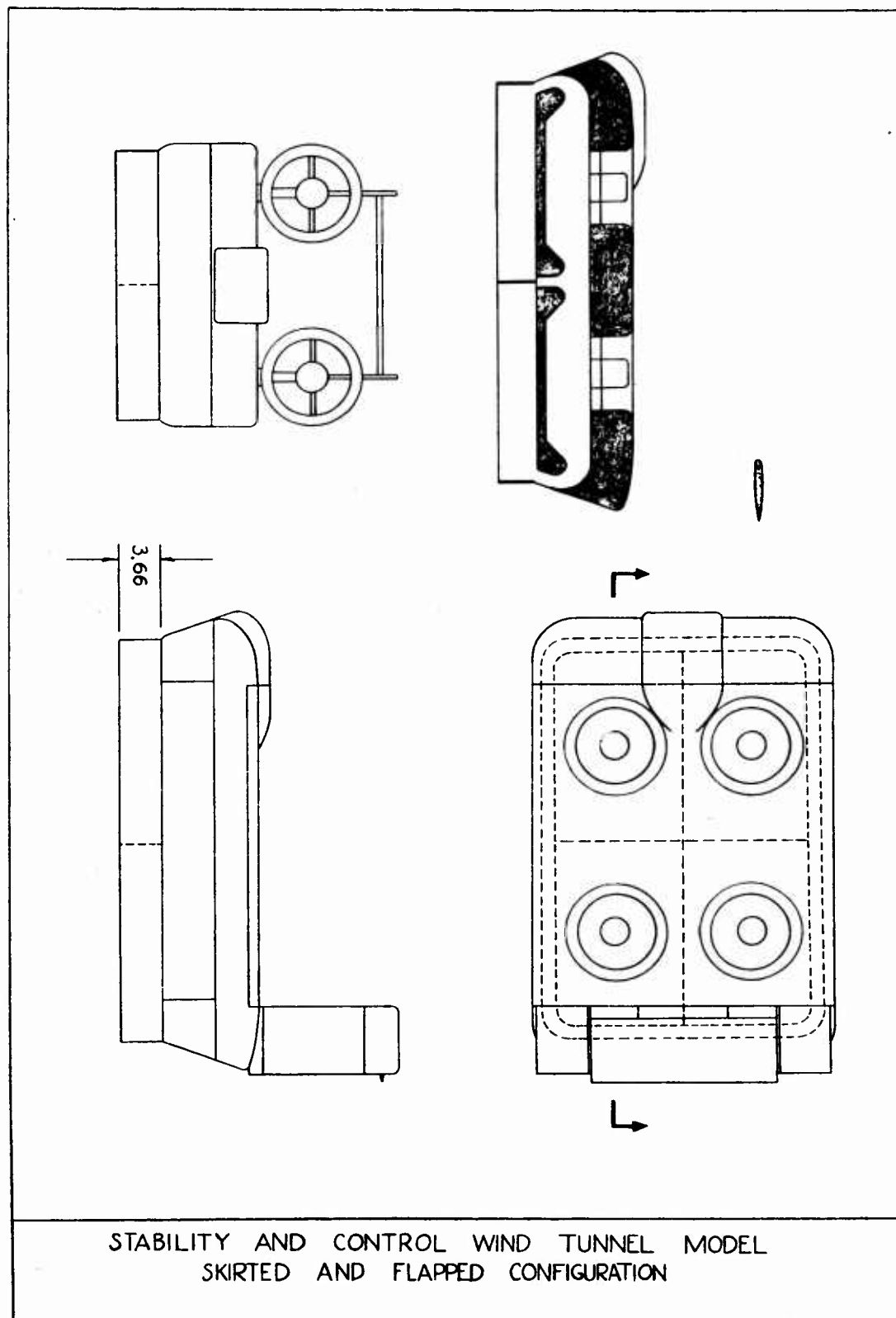


FIGURE 2. DRAWING OF SKIRTED AND FLAP SEGMENTED MODEL

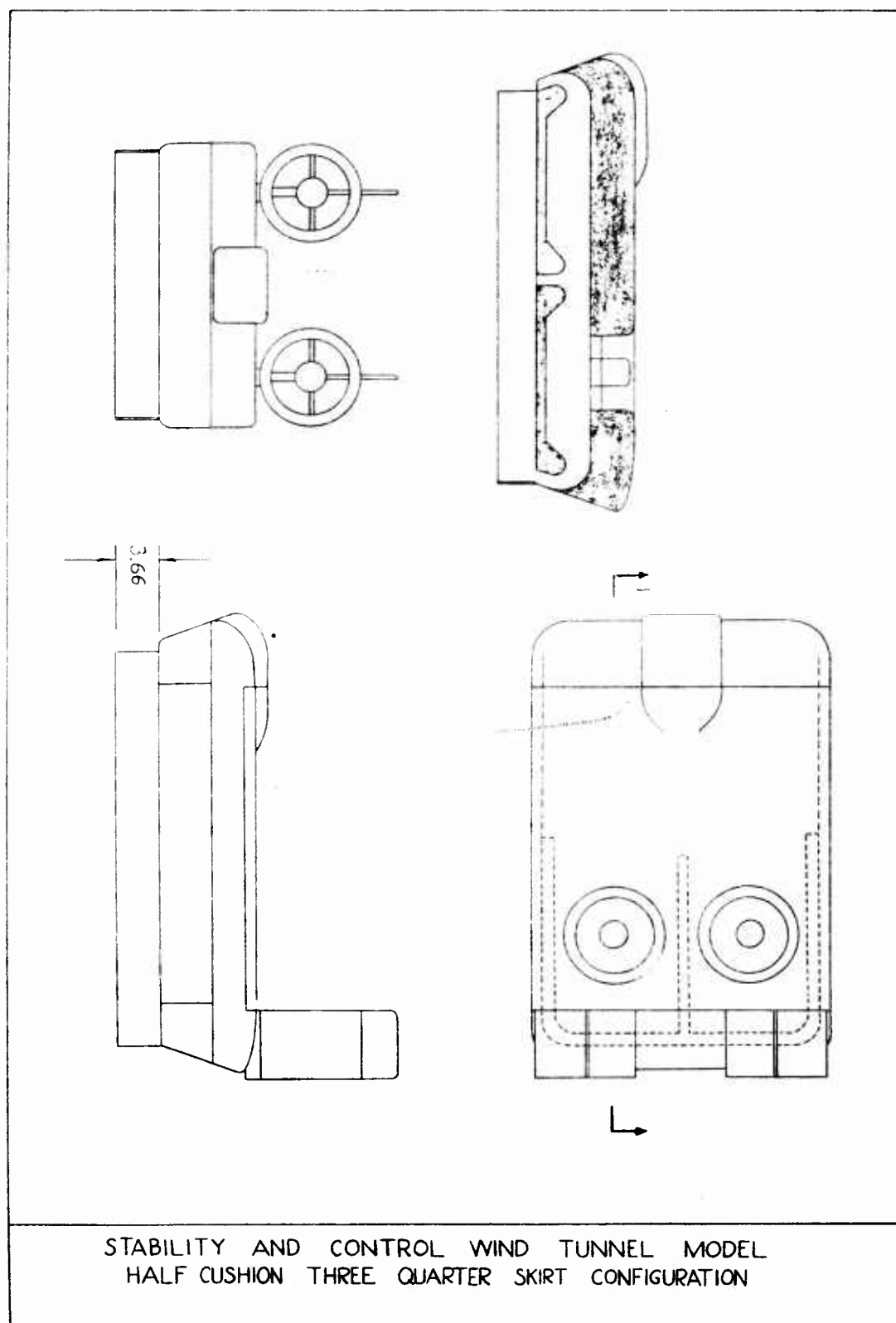


FIGURE 3. DRAWING OF HIGH SPEED CONFIGURATION
19-c

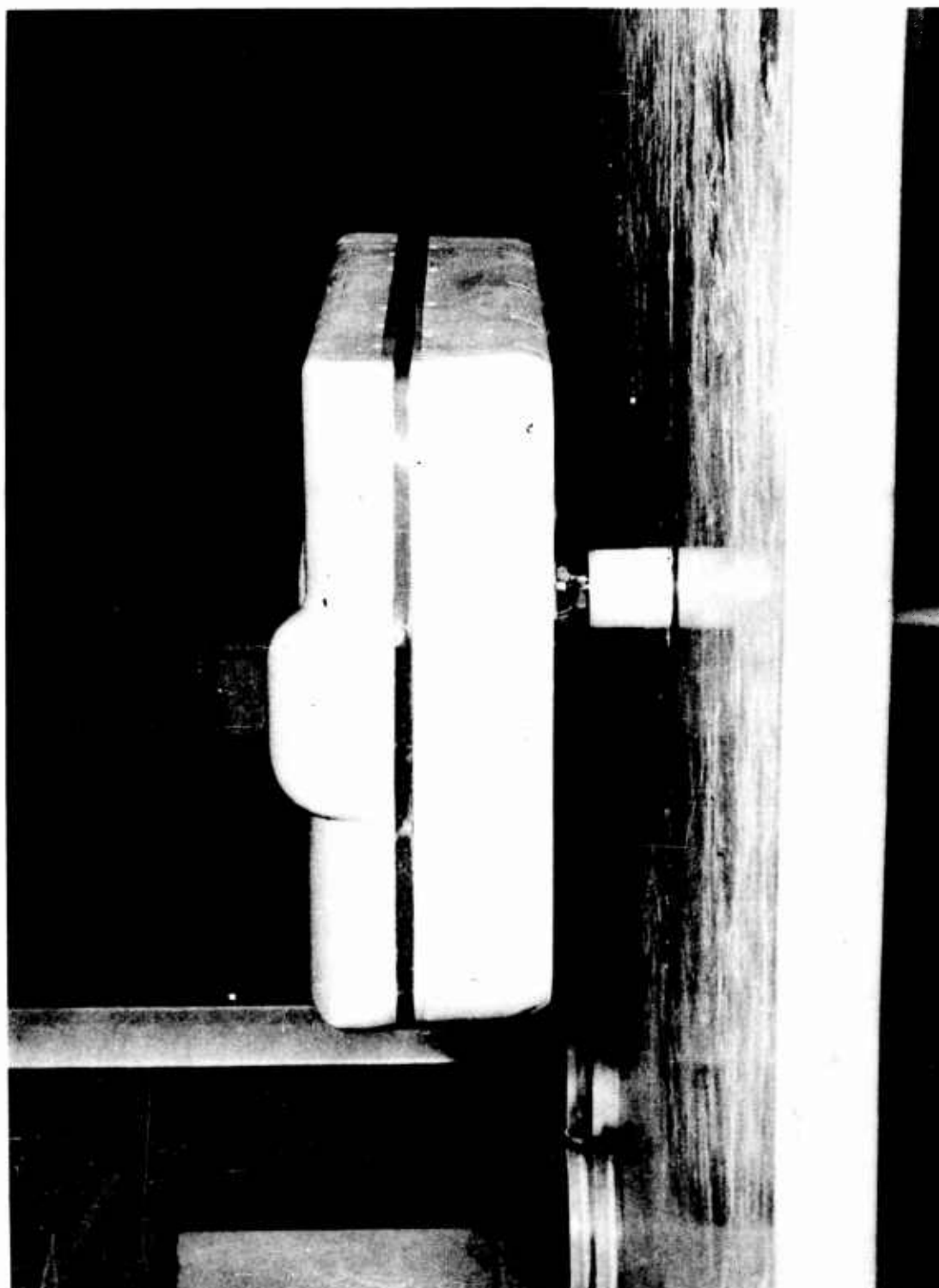


FIGURE 4. FAIRED MODEL

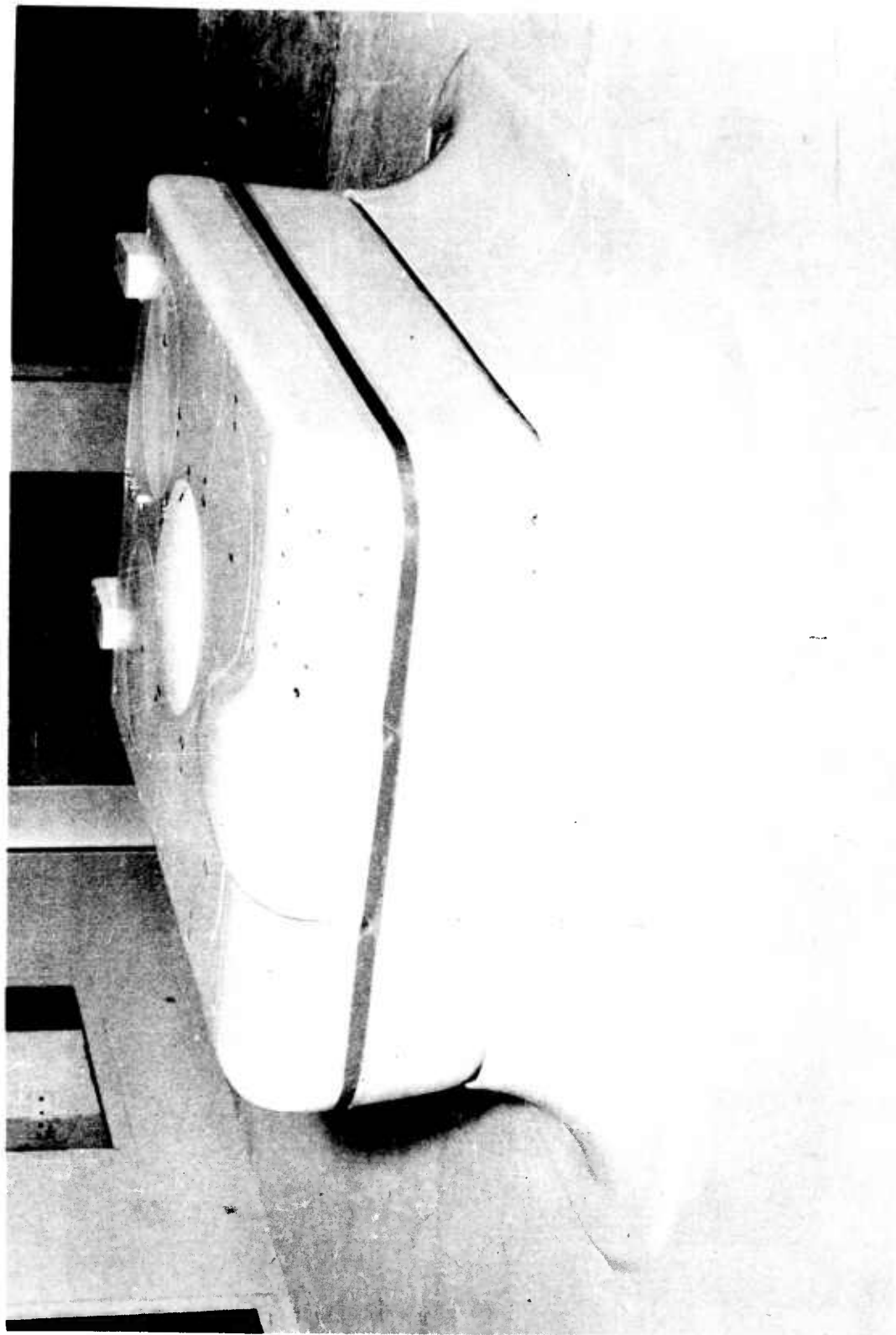


FIGURE 5. FAIRED MODEL WITH SIMULATED JET

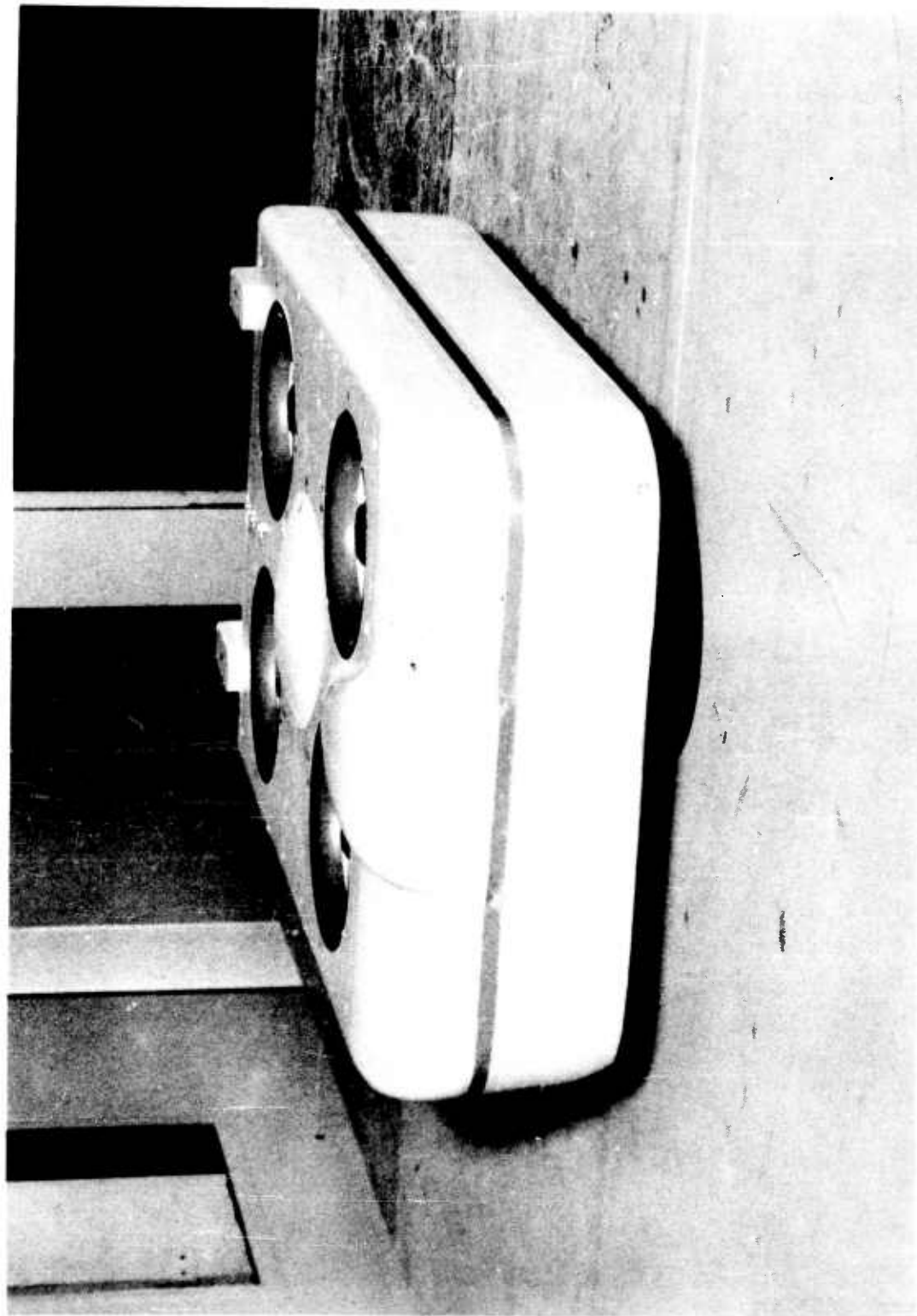


FIGURE 6. BASIC JET SEGMENTED MODEL

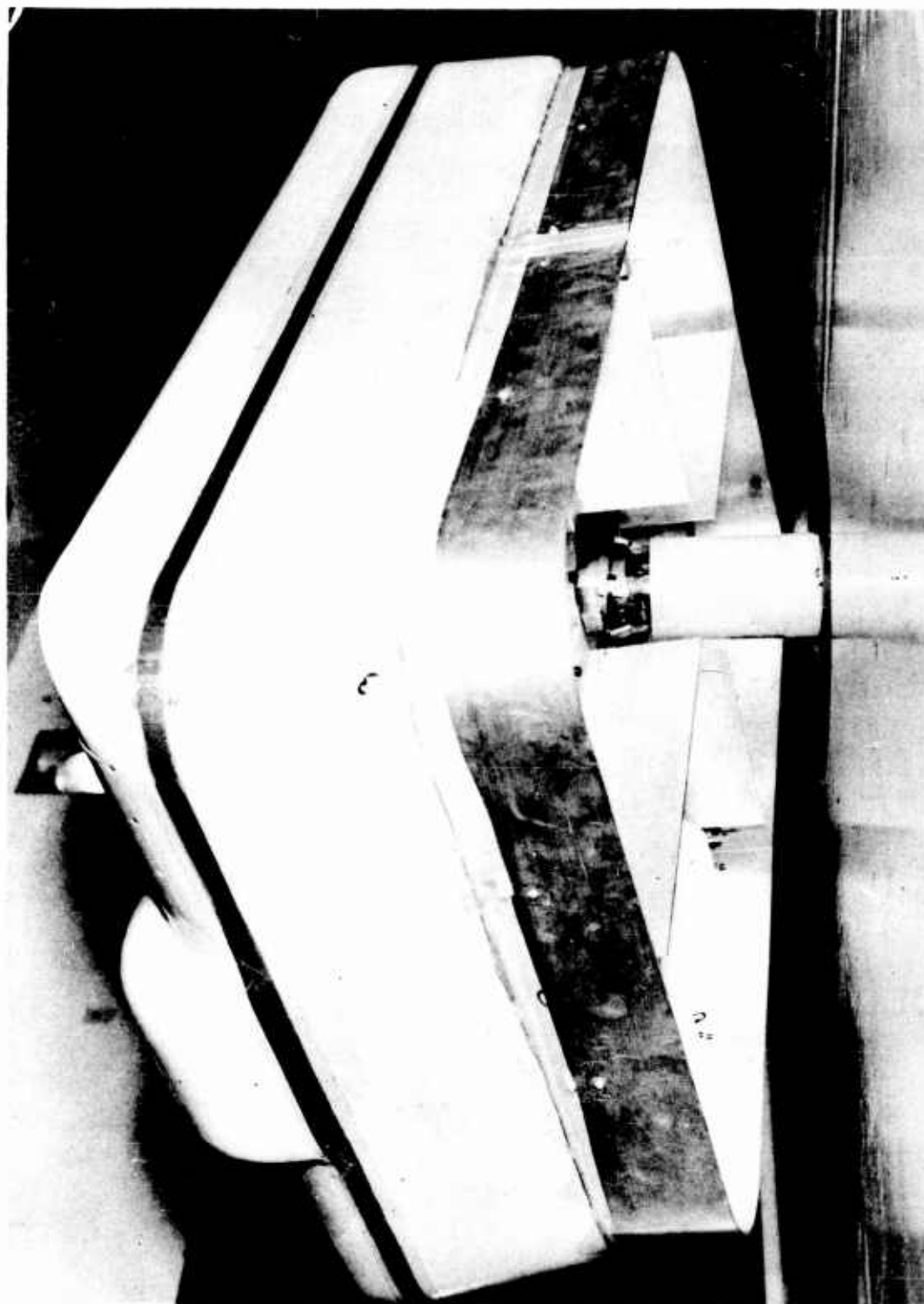


FIGURE 7. SKIRTED AND FLAP SEGMENTED MODEL

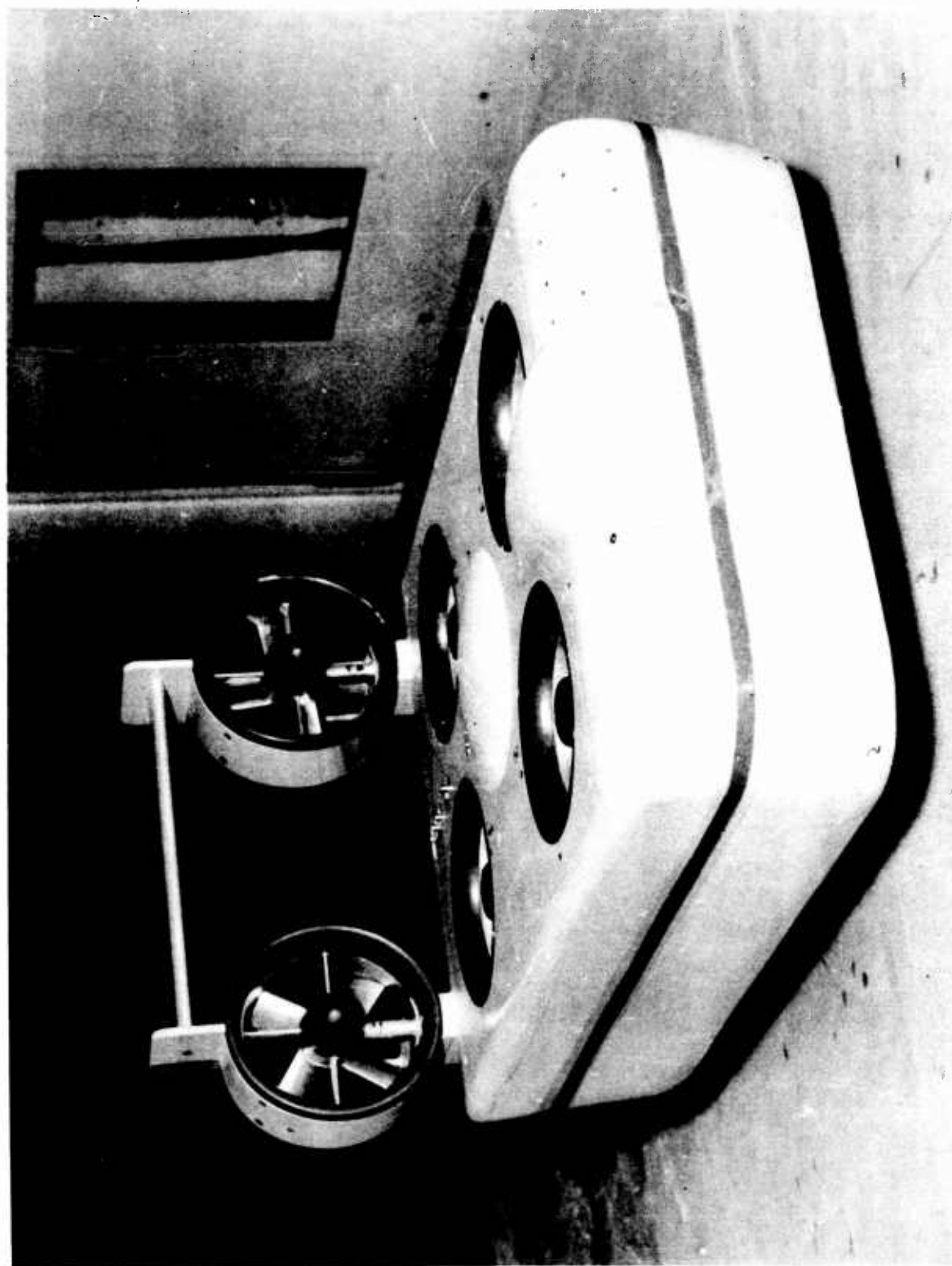


FIGURE 8. MODEL WITH PROPULSION FANS AND TAIL

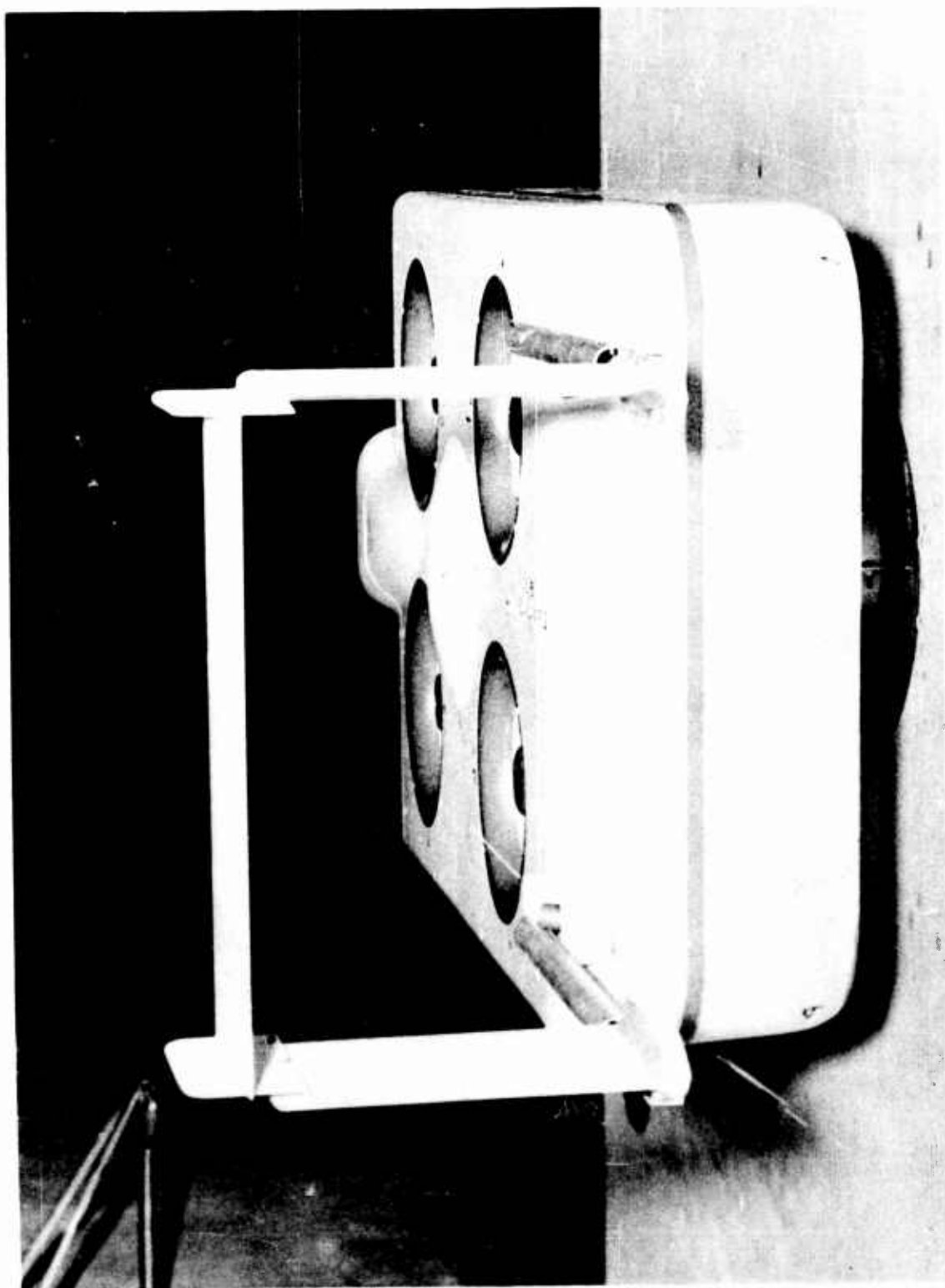


FIGURE 9. MODEL WITH EXTENDED TAIL

19-i

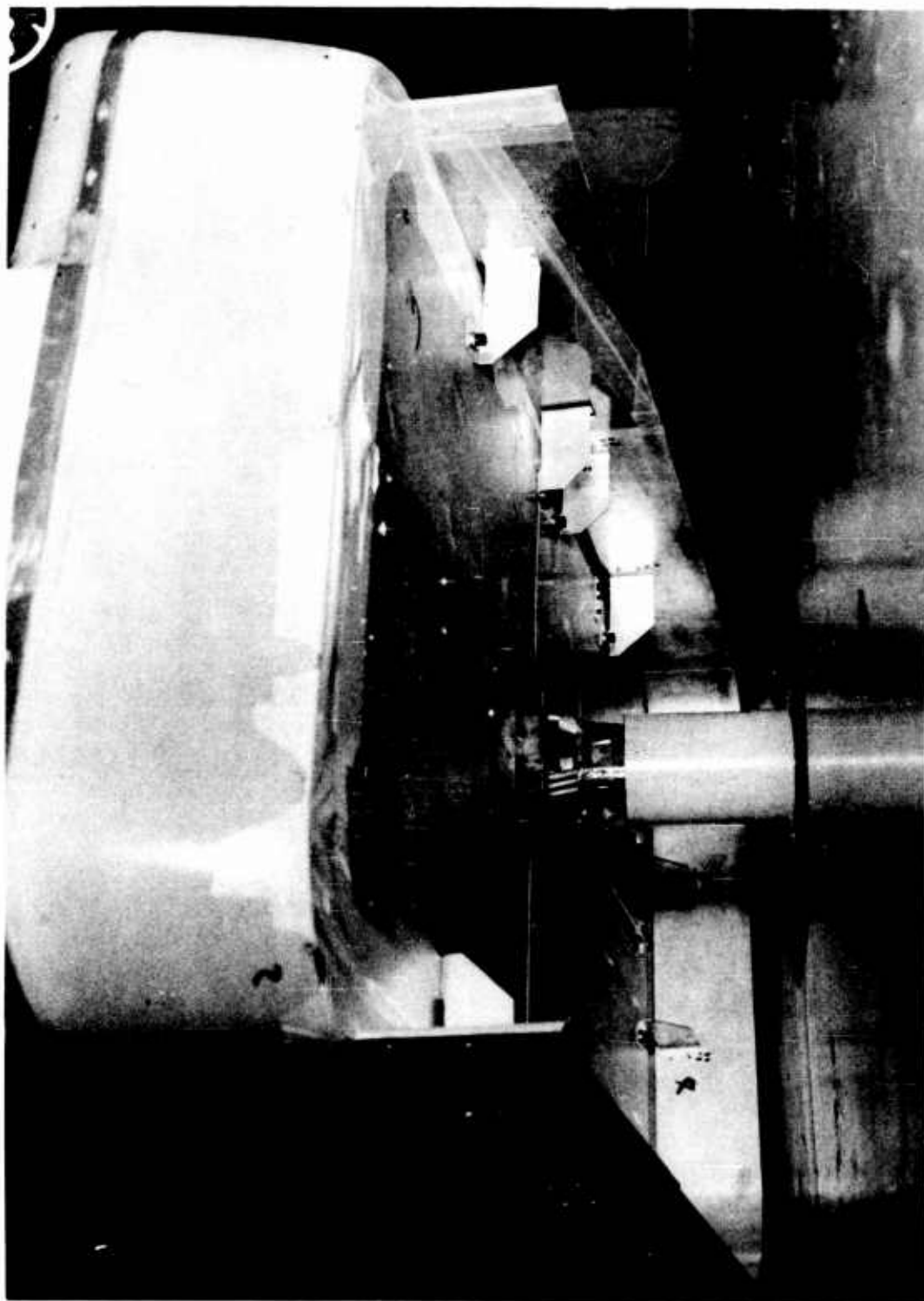


FIGURE 10. MODEL WITH OPEN FRONT SKIRT AND FORWARD JETS SEALED

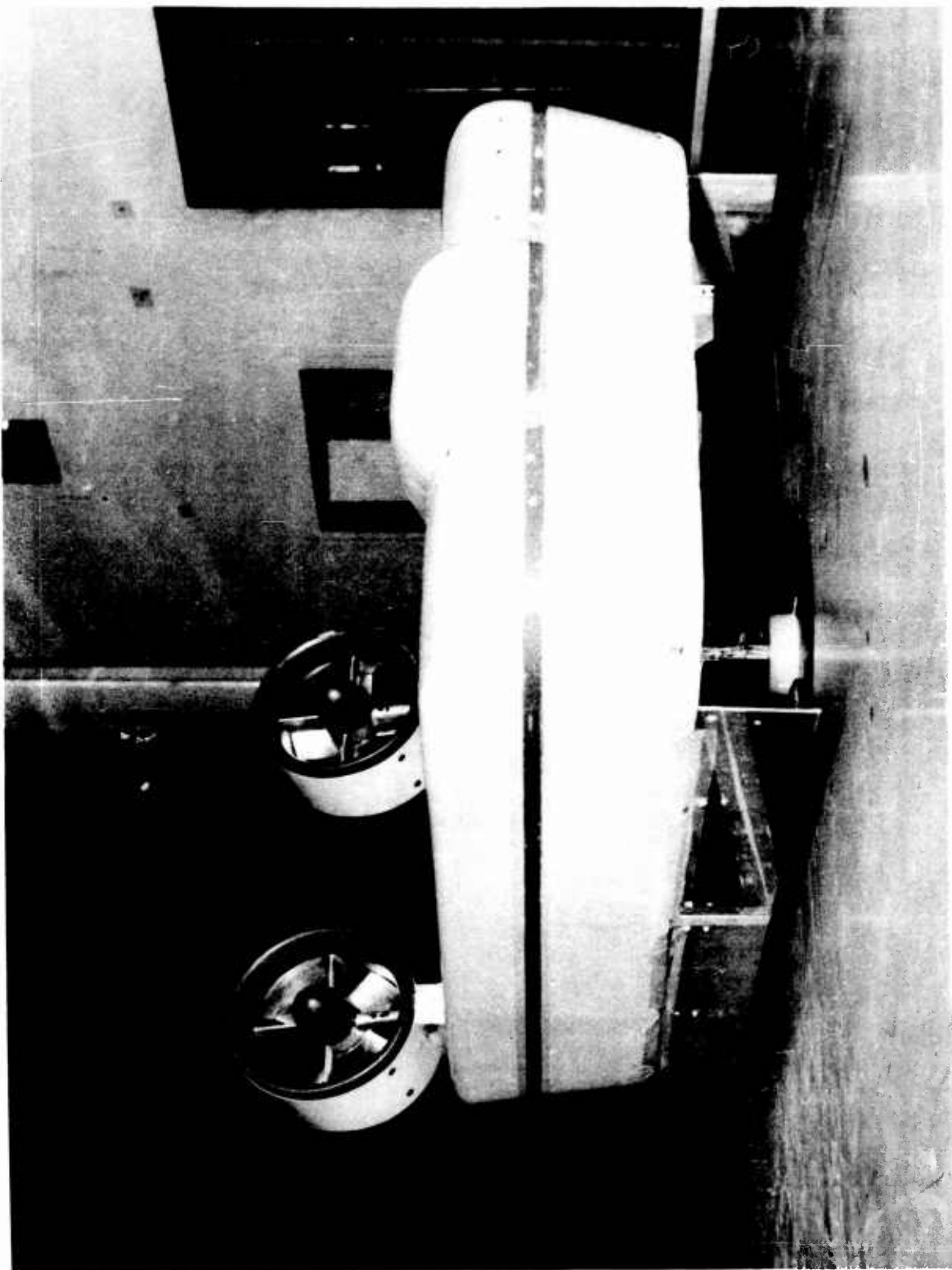


FIGURE 11. HIGH SPEED MODEL WITH TILTED PROPULSION FANS

19-k

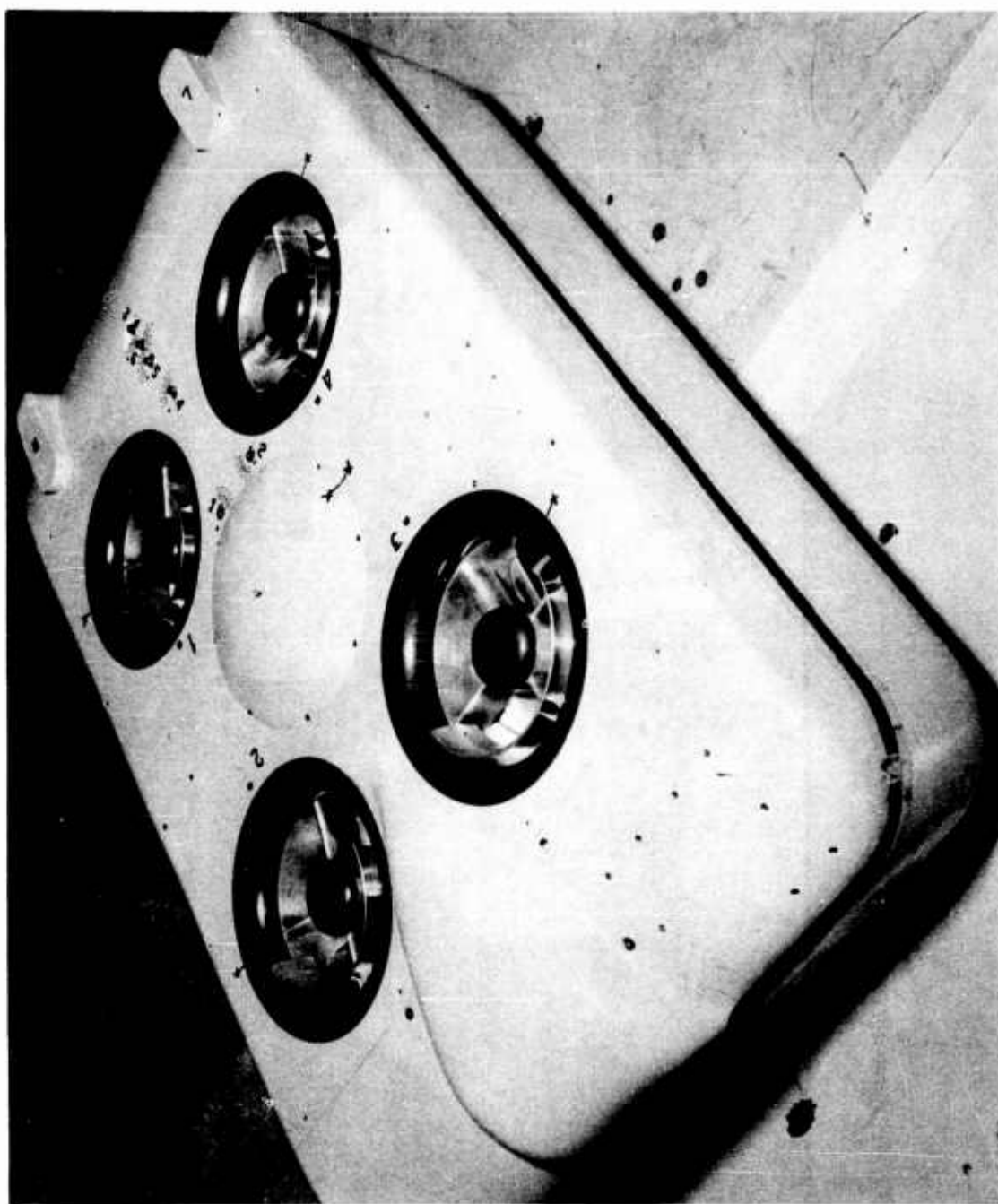


FIGURE 12. MODEL WITH G.E. TYPE INLET LOUVERS

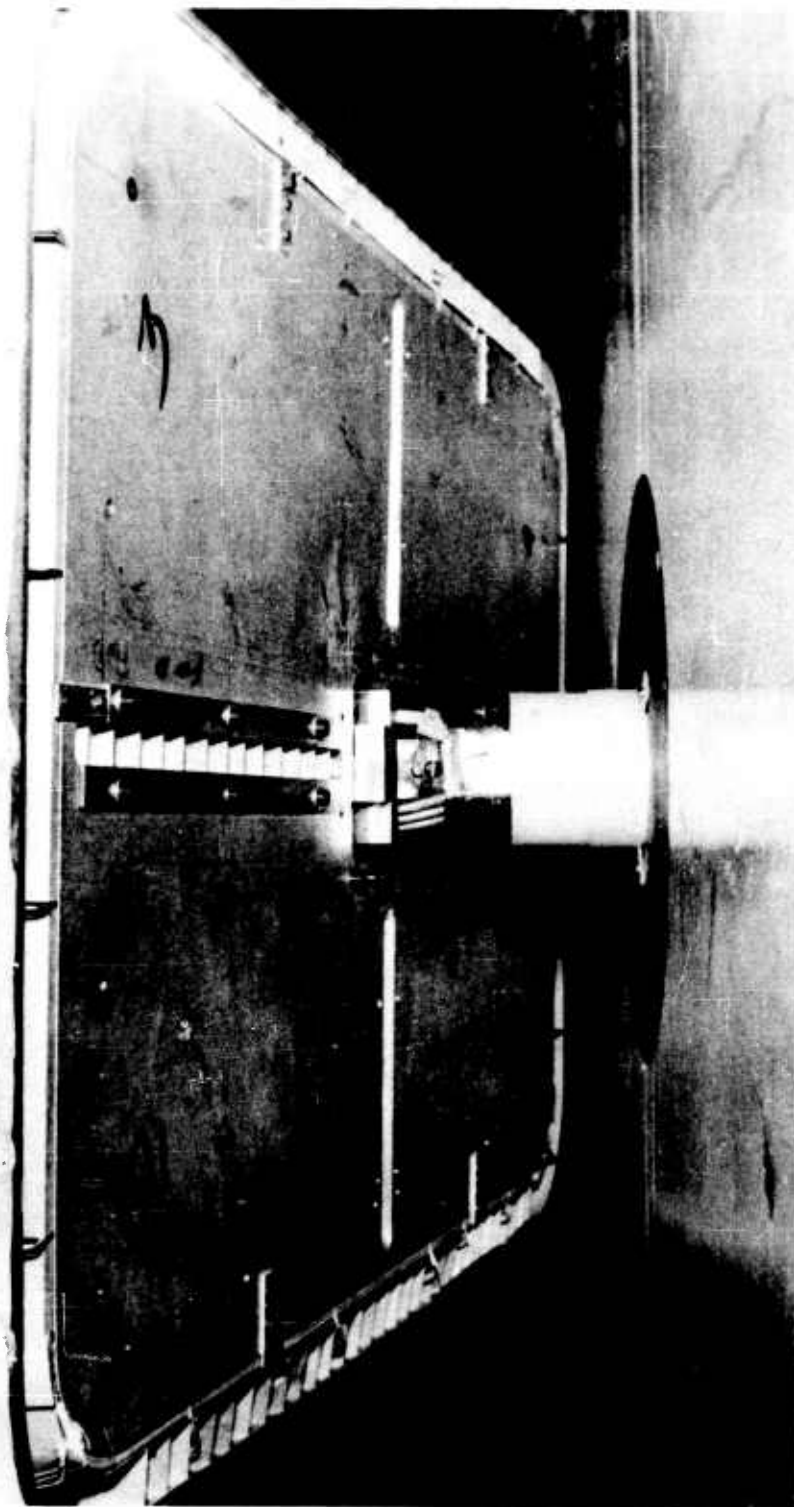
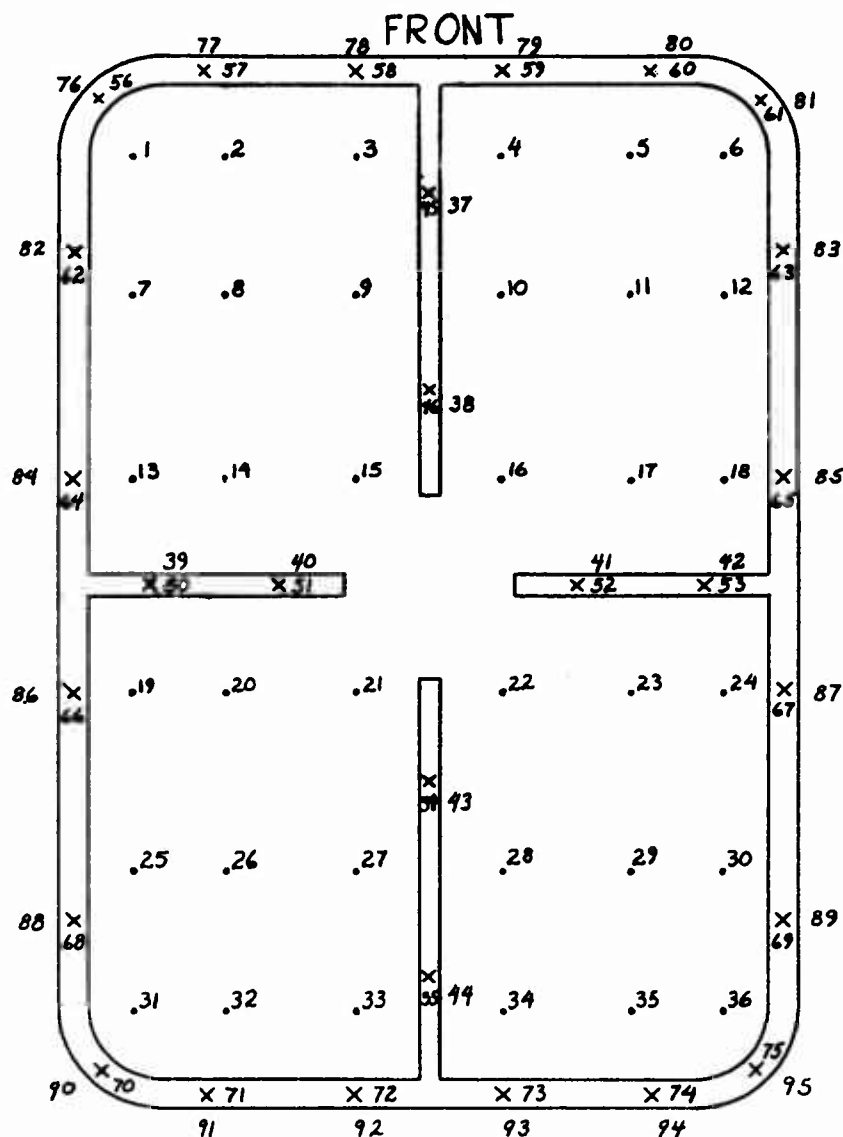


FIGURE 13. MODEL WITH 60° *B* VANES IN JETS

BASE AND JET INSTRUMENTATION IDENTIFICATION

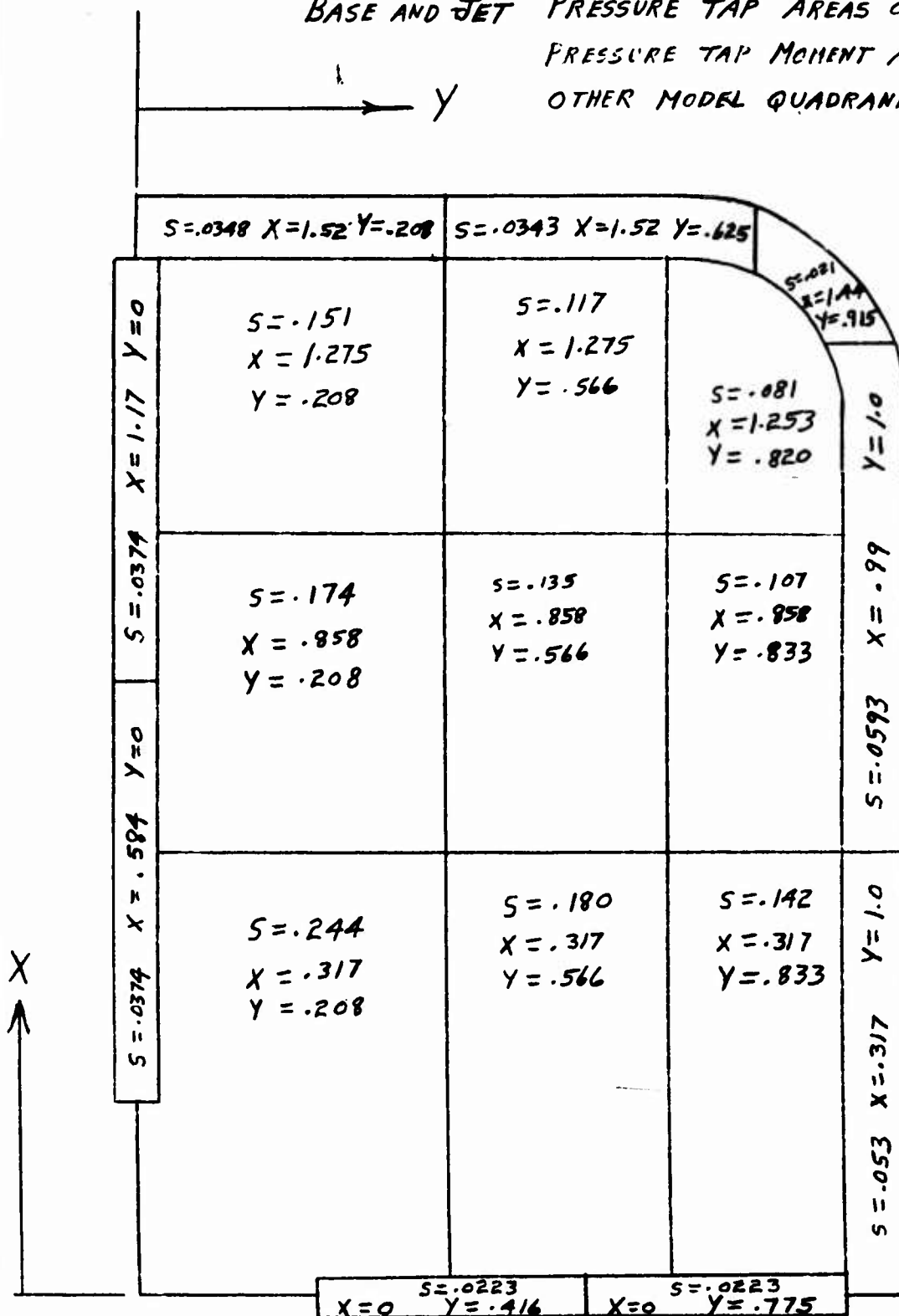
VIEW FROM ABOVE



NOTE: NUMBERS INSIDE JET DENOTE TOTAL HEAD TUBES
NUMBERS OUTSIDE JET DENOTE STATIC TUBES

FIG 15

BASE AND JET PRESSURE TAP AREAS OF INFLUENCE ~ FT²
 PRESSURE TAP MOMENT ARMS ~ FT
 OTHER MODEL QUADRANTS IDENTICAL



UPPER MODEL
PRESSURE TAP DISTRIBUTION

NOTE: SYMMETRICAL DISTRIBUTION
ALL FOUR QUADRANTS

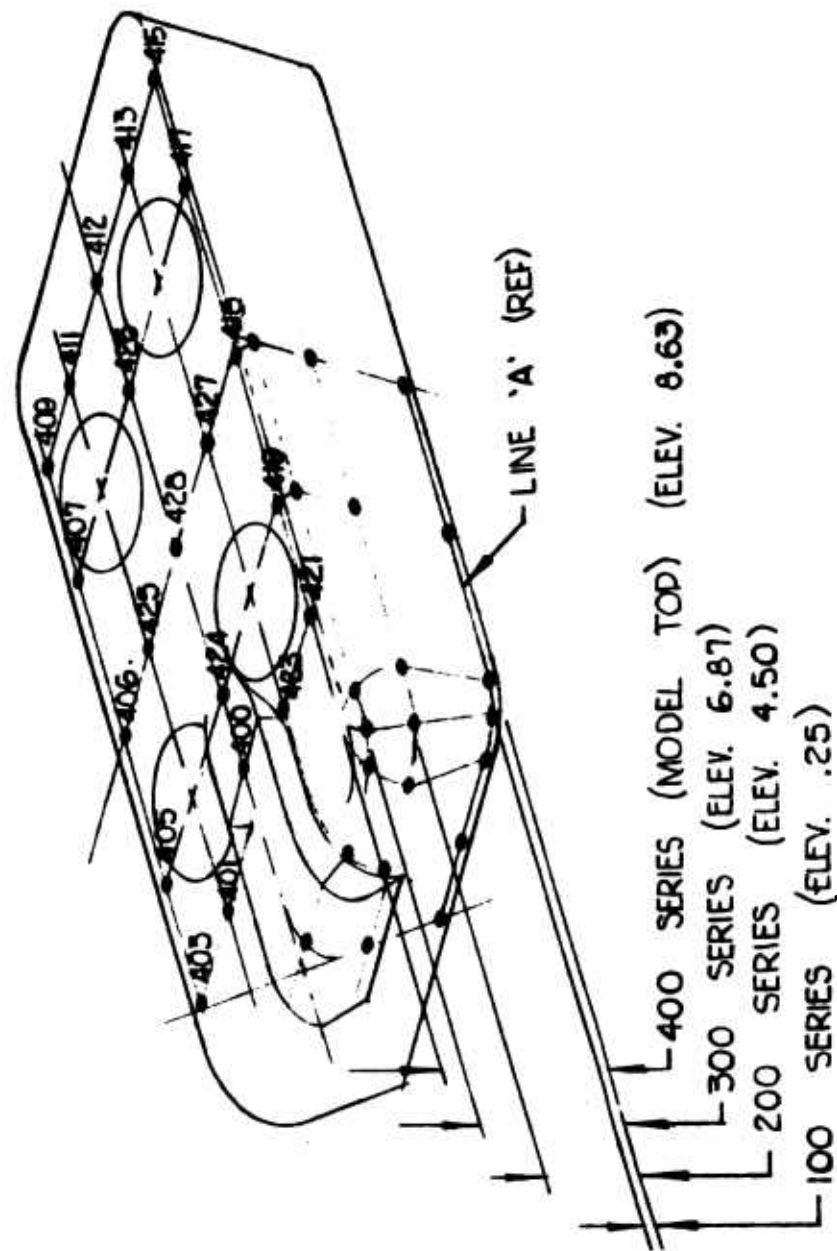
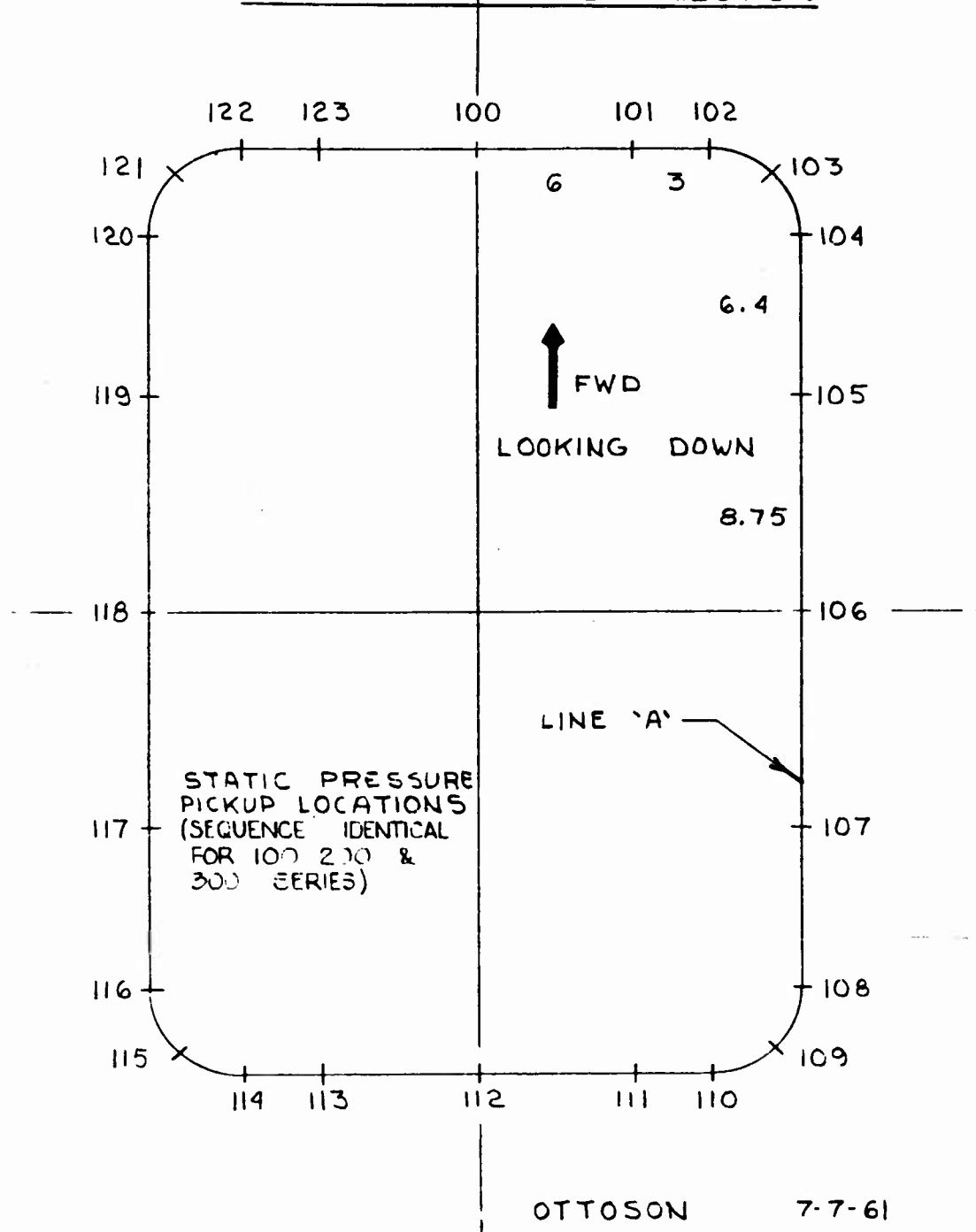


FIG 16

SIDE MODEL PRESSURE TAP DISTRIBUTION

FIG 17



PRESSURE DISTRIBUTION ABOUT MODEL IN FORWARD FLIGHT

$$C_p = 1.0 = \frac{P_{\text{LOCAL}} - P_{\text{AMBIENT}}}{q}$$

$$J$$

$$\frac{h}{S} = .64$$

$$\frac{q}{P_{\infty}} = .53$$

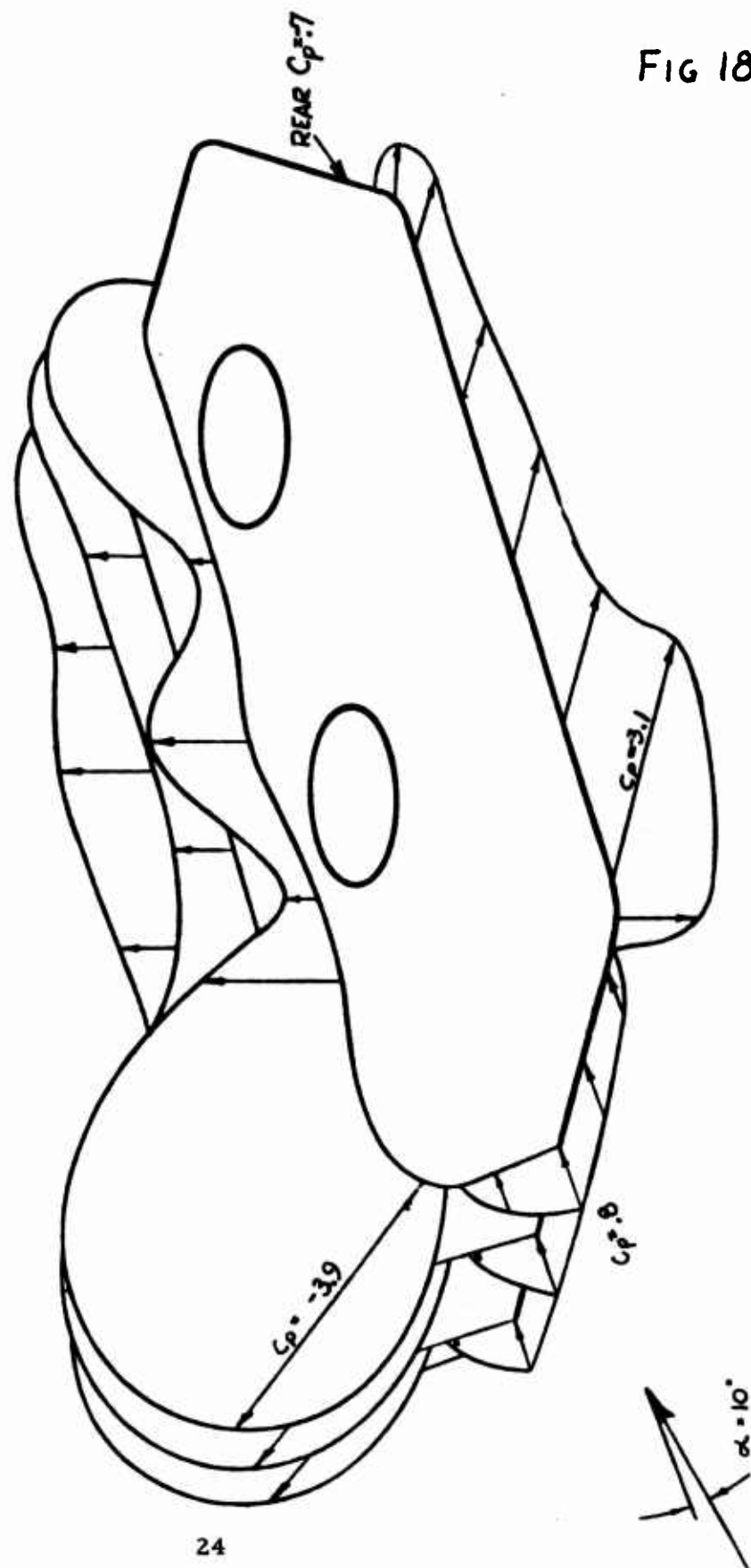


FIG 18

EXPERIMENTAL RESULTS

1. Effect of Forward Speed - Model Straight and Level

Before embarking on stability and control investigations, the effects of increasing airspeed on the longitudinal characteristics of the basic jet segmented model (J) in the straight and level attitude were determined.

a. Lift

The effects on lift at the design height ($h/S = 0.64$) are presented in Figure 19. The total lift (at constant input to the lift fans) increases linearly with flight dynamic pressure. At flight dynamic pressure equal to peripheral jet total pressure, the total lift has increased 60% over the hovering value. The cushion lift decreases almost linearly with increasing speed * and is reduced to 60% of the hovering value at $q = \bar{p}_{tj}$. The difference between total lift and cushion lift non-dimensionalized with q and reference area is shown in the lower portion of Figure 19, to result in an aerodynamic lift coefficient of about 0.7. The aerodynamic lift coefficient of the faired and sealed model with solid wall jet simulation was about 0.3. It would appear that the lift increment due to the inflow to the lift fans is of the same magnitude as that generated by the acceleration of the external flow around body-plus-jet shape.

b. Drag

The aerodynamically blunt body had surprisingly low form drag when faired and sealed. The coefficient based on frontal area is lower than that for the 1960 Ford Falcon automobile, which has been determined as 0.443. This can no doubt be attributed to the proportions since the air cushion model had a height $1/3$ of its width, while an automobile has a height of at least $1/2$ its width. It is interesting to note that at $\alpha = \phi = \psi = 0^\circ$ the drag coefficient of the faired model based on frontal area is 0.35 while at $\psi = 90^\circ$, the drag

* The lift loss takes place at the forward end of the base. The average base pressure falls to $1/2$ the hovering value at $q/\bar{p}_{tj} = 0.7$.

coefficient based on side area is 0.755. The increased length normal to the wind makes the flow more two-dimensional. The increase in drag of the blowing model over the faired model was formidable, amounting to a fourfold increase over the plain faired model or an eightfold increase over the faired model with a simulated jet curtain (not attached to the model).

<u>Configuration</u>	<u>D/qS</u>	<u>D/qS_{frontal}</u>
F	.087	0.35
F with sim. jet	.047	0.19
J	.380	1.52

The significance of this result is that the high drag of an air cushion vehicle does not come primarily from the relatively poor body form, but rather from the momentum drag of the air used in the lift producing system. A comparison of measured and computed momentum drag is presented in Figure 20. The comparison is complicated by several factors. Due to the use of tip jet fans, 20% of the total exit flow was fed in from outside the tunnel so that the momentum drag from this portion should not have appeared on the wind tunnel balance. One-hundred percent momentum drag curves have been computed for the full exit air quantity and for the inlet air quantity (exit air-feed pipe air). The latter calculation should be the correct one. Experimentally, it is difficult to decide what drag to attribute to the momentum loss of the lift air. If one subtracts the faired model drag from the blowing model drag, account is not taken of the shielding of the bottom surface by the jet. The faired model with a rigid simulated jet probably does not accurately account for the true situation. Both methods were used and presented in Figure 20. It would appear that the most practical way to compute the total drag of a blowing model would be as follows:

$D \text{ faired model} + K \cdot \rho \cdot V_{\infty} \cdot Q \text{ inlet}$ where $K = 1.08$
up to $q/\bar{p}t_j = 0.5$ increasing to 1.16 at $q/\bar{p}t_j = 1.0$.

c. Pitching Moment

The longitudinal trimming problem with increasing forward speed is presented in Figure 21. The influence of flight ram pressure is to reduce the base pressure near the front of the vehicle. The cushion center of pressure moves aft (more than 8% of the length by $q/\bar{p}_{tj} = 1.0$) causing a nose down pitch. The total moment on the vehicle, however, may be described as an 8% forward shift of the effective center of pressure. This means that the non-cushion contribution provides a pitch up tendency amounting to a 16% forward shift in effective center of pressure. This is due to the air load distribution on the body, part of which comes from acceleration of the air around the body, and part from acceleration of air into the intakes. The relative contributions are shown in Figure 22.

The lower part of Figure 21 presents information on a configuration evolved late in the test period to cure the pitch up. The forward intakes, front jet, front half of the side jets, and all segmenting jets except the rear longitudinal one are sealed over. A skirt of length equal to 10% of the vehicle length is added along the sides and around the rear of the vehicle. The front of the skirt is left open. The cushion center of pressure is still aft of the C. G. but now moves forward with increasing forward speed. The lower nose up moment of $J/2 S^{3/4}$ due to external air load is shown in Figure 23. The total model center of pressure is now within 1% length of the center of gravity for $q/\bar{p}_{tj} = 0.4$. At low speeds, there is an appreciable nose down pitching moment.

The effect of adding propulsion nacelles and tail surfaces to the basic jet segmented model is shown in Figure 24. The effective center of pressure in pitch lies from 6 to 10% forward of the center of gravity for all these configurations. The effect of skirt and jet modifications are shown in Figure 25. Shutting off the forward jets without addition of the skirt produces a nose down pitch (C. P. 10% aft of C. G.). Addition of the $3/4$ skirt results in longitudinal trim.

The presence or absence of lateral segmenting jets does not affect the longitudinal trim achieved with the J/2 S 3/4 configuration.

d. Performance

The performance in straight and level flight at $h_1/S = 0.64$ is compared in Figure 26 for the basic J configuration and the high speed J/2 S 3/4 configuration. Performance in forward flight concerns the weight, speed, power relationship. It can be expressed as $W V/P$. Since weight = lift and $P/V = \text{drag}$, this relationship is usually expressed as the lift drag ratio L/D . The power required to produce the lifting jet (volume flow x pressure rise) when divided by the forward speed will give a drag equivalent of the lifting power. Total drag is the sum of this plus the momentum drag of the air which was fed to the tip jet fans from outside the tunnel plus the measured drag. The total measured lift is used in the numerator. The basic J configuration levels out at an L/D of 1.7 in the upper speed range. The L/D of the J/2 S 3/4 configuration continues to increase to the highest speed tested where the value is 3.4 or just double that of the J configuration. It should be noted that these L/D values do not reflect the effect of internal losses on the lift system power. Typical internal losses on an actual vehicle will reduce the L/D values shown here. As explained in the model description section, the internal losses in the model were very high compared to an actual vehicle and for that reason are not included in the analysis.

The third configuration presented in Figure 26 is the three-quarter skirt arrangement with all jets and inlets sealed. There is no power applied to direct production of lift. The lift is produced by a combination of ram pressure within the three-quarter skirt, and also by flow acceleration over the upper part of

the model. The L/D values presented are for zero angle of attack. Since $p_{tj} = 0$, this information should strictly speaking not be presented on a scale of q/p_{tj} . The q values of the F S 3/4 configuration are identical to those for J/2 S 3/4 configuration and are therefore presented at the same values of the abscissa. The limited L/D values of air-cushion vehicles are brought into focus in this comparison where even a very crude aerodynamic configuration gains in L/D by closing down the air-cushion feature. The lift coefficient at $\alpha = 0^\circ$ and $q = 36 \text{ lbs/ft}^2$ was 0.7 for F S 3/4, was 0.9 for J, and was 1.4 for J/2 S 3/4. It should be noted that the L/D of the F S 3/4 configuration increased to 4.5 at $\alpha = +4^\circ$ and a lift coefficient of 1.12.

Improvements in cruise L/D must not be obtained by limiting the allowable planform loading too drastically nor by losing slow speed and hovering flight capability. These first forward flight experiments by Aeronutronic point the way to an approach to the problem, but many practical problems remain. The J/2 S 3/4 configuration is a promising improvement but it should be remembered that it was evolved from a configuration designed from a hovering viewpoint. It would be interesting to start with a configuration designed for high cruise efficiency and then develop the modifications necessary to achieve high planform loadings coupled with low speed and hover capability. It might look considerably different from any existing air-cushion vehicle as well as different from the improved J/2 S 3/4 configuration evolved under this contract.

Figure 27 summarizes L/D values for several configurations at several combinations of height and speed. The upper plot shows the improvement in L/D with decreasing height for the basic J configuration. At an h_l/S of 0.184 the L/D is about the same as that of the J/2 S 3/4 configuration at an $h_l/S = 0.64$. This is not surprising since the clearance between the base and the ground for J at an $h_l/S = 0.184$ is identical to the clearance between the skirt and the ground for J/2 S 3/4.

The central plot reveals that the fully skirted configuration has an L/D at $h_l/S = 0.64$ equal to that of the J configuration at $h_l/S = 0.184$ for the same reason stated above. Likewise the clearance of the skirt at $h_l/S = 0.87$ is equal to the clearance of the base on the J configuration at $h_l/S = 0.412$ and again the L/D's are very comparable. The lower plot reveals that at an h_l/S of 0.64 the same L/D values were achieved with half the peripheral jet as were achieved with the full peripheral jet over most of the speed range. Comparison of the middle and lower plots indicates that a small penalty is paid at $q/\bar{p}t_j = 0.55$ in going from the S configuration to the J/2 S $3/4$ configuration at $h_l/S = 0.64$ and 0.87. Again, it should be remembered that all L/D values neglect the internal losses in the lift system.

The cost in L/D incurred by using base segmenting jets for stability is presented in Figure 28. The cost varies from 4 to 8% for the J/2 configurations and from 10 to 13% for the J configuration. The cost for a given configuration expressed in percent decreases as h_l/S increases.

e. Hovering Performance

Hovering performance of an air-cushion vehicle can be expressed by the ground effect power factor. This relates the quantity:

$$\frac{(\text{LIFT})^{3/2}}{(\text{POWER}) (\text{PLAN AREA})^{1/2}} \quad \text{of the air-cushion vehicle}$$

to that of a ducted rotor operating out of ground effect. A fractional value means a savings in power due to ground effect. Figure 29 indicates a reduction to 30% of the power of the ducted rotor out of ground effect at an $h_l/S = 0.184$. At $h_l/S = 0.6$ the power savings due to ground effect is nil for the J configuration. It should be remembered that the internal losses have not

been included in this calculation. A practical vehicle at $h_l/S = 0.5$ will require more power than the ideal ducted rotor out of ground effect. It should be noted that designing the vehicle specifically for hovering would result in hovering superiority over the ideal rotor out of ground effect to much higher heights. Since the purpose of the vehicle is transportation, the hovering mode must be compromised in favor of forward flight considerations. If a skirt of length equal to 10% of the vehicle length should be practical, the G curve can be shifted as indicated by the S configuration curve. At values of base h_l/S of 0.64 and .87, G values with skirt comparable to those obtained without skirt at h_l/S of 0.240 and 0.620 respectively can be obtained. The lower curve reveals that the cost in hovering performance due to stabilization by means of base segmenting jets varies from 17% at $h_l/S = 0.184$ to 6% at $h_l/S = 0.87$ for the J configuration. The jets were designed for forward flight and thus are further from optimum at high heights than at low heights. Thus, the cost of the segmenting jets does not appear as high at large values of h_l/S . Also, the level of stability achieved with the segmenting jets at low height is much larger than that achieved at high height.

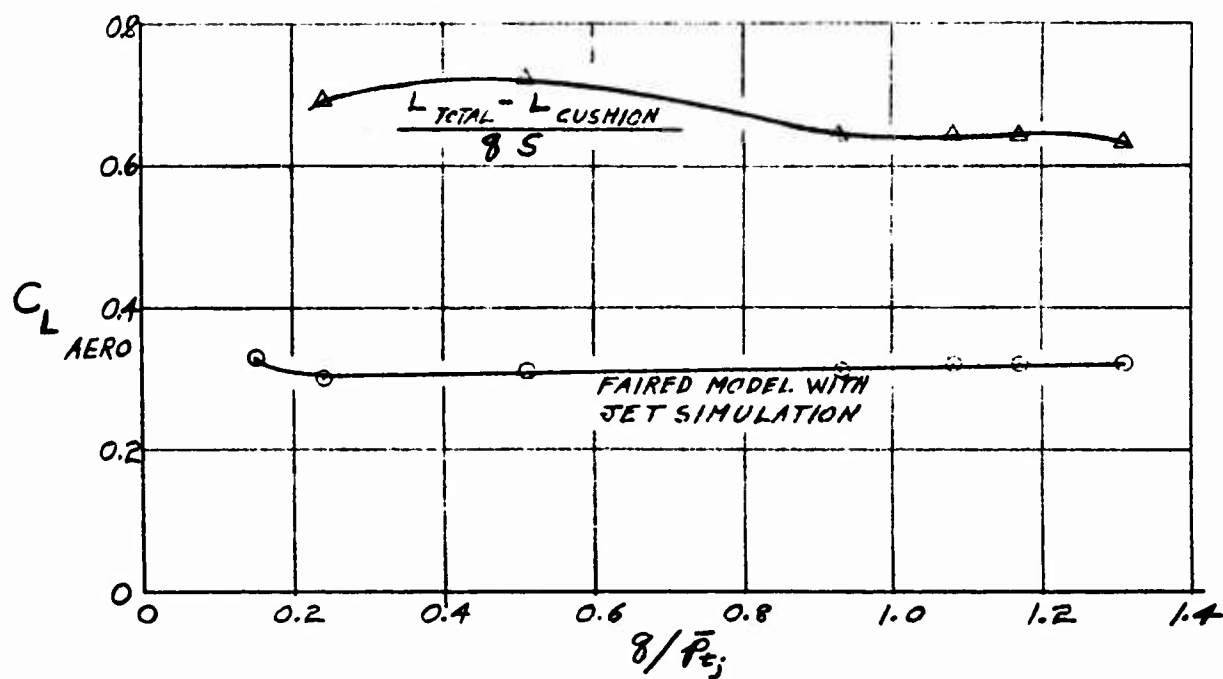
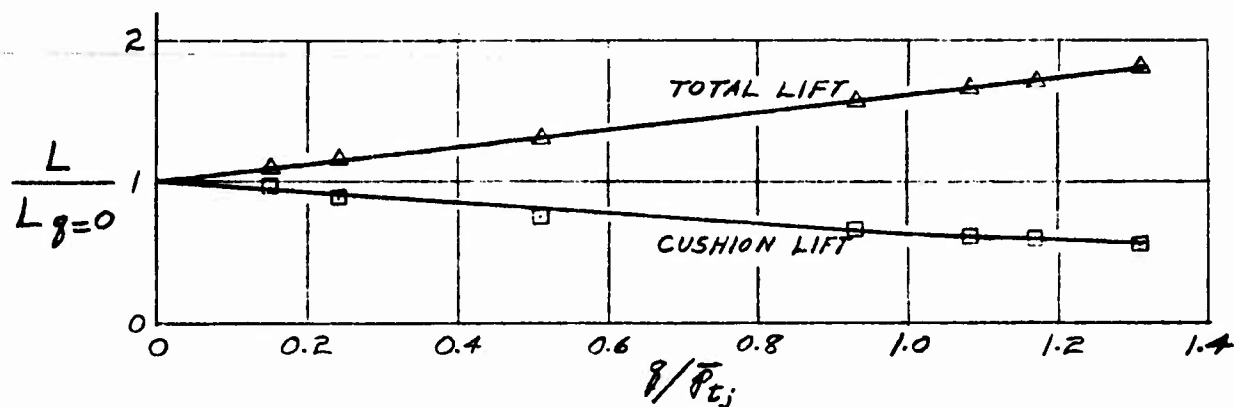
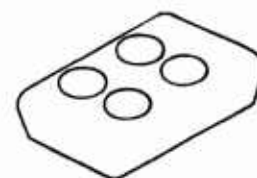
FIG 19

EFFECT OF FLIGHT SPEED ON LIFT

CONFIGURATION J

$$h l / S = 0.64$$

$$\alpha = \phi = \psi = 0^\circ$$



COMPARISON OF CALCULATED MOMENTUM DRAG
WITH MEASURED DIFFERENCE BETWEEN
BLOWING MODEL AND FAIRED MODEL

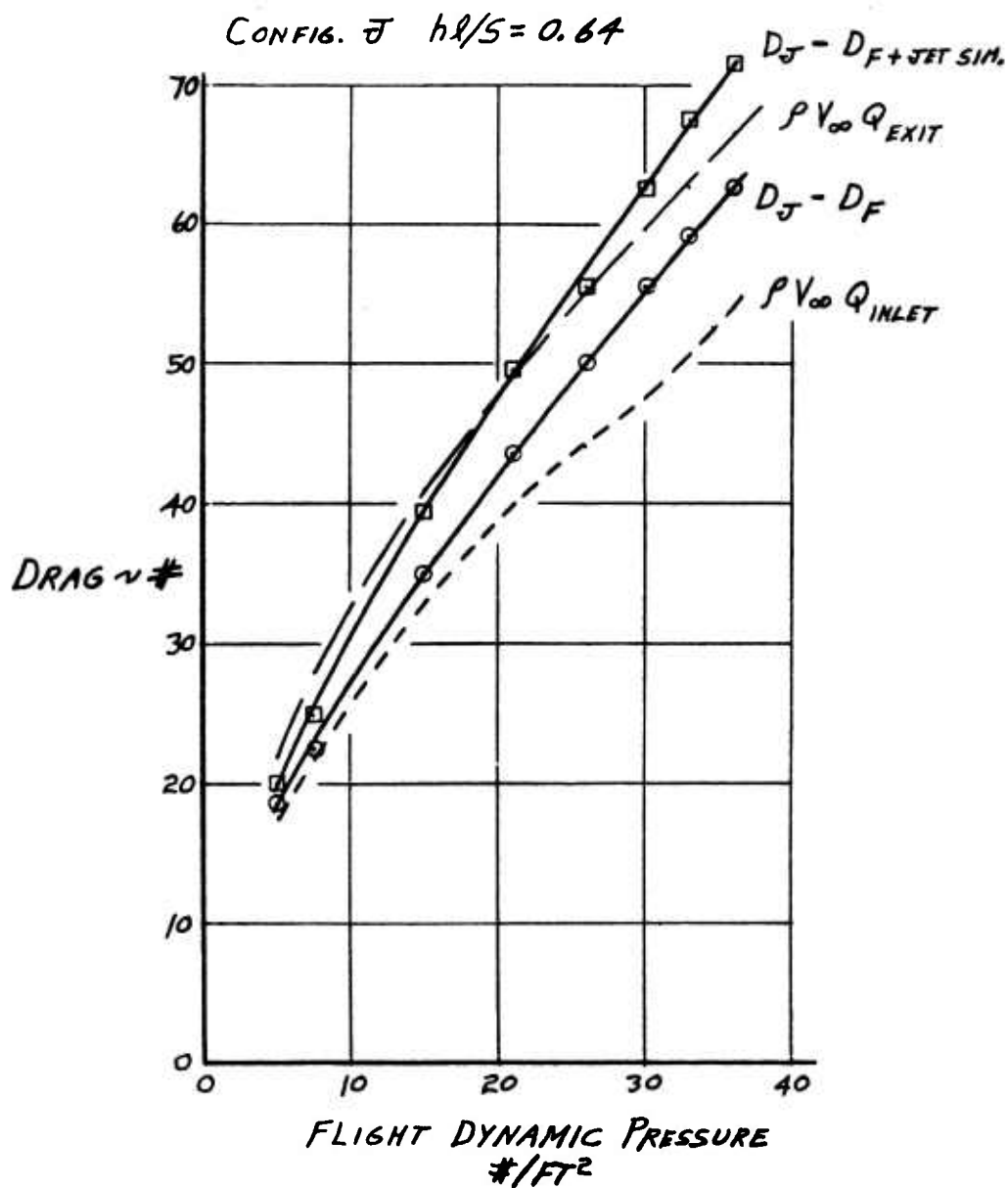
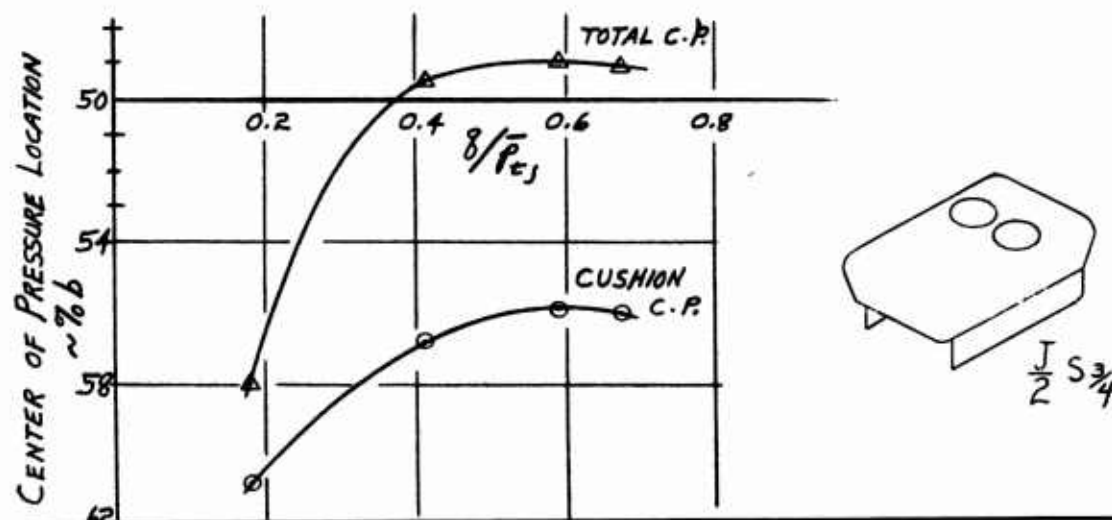
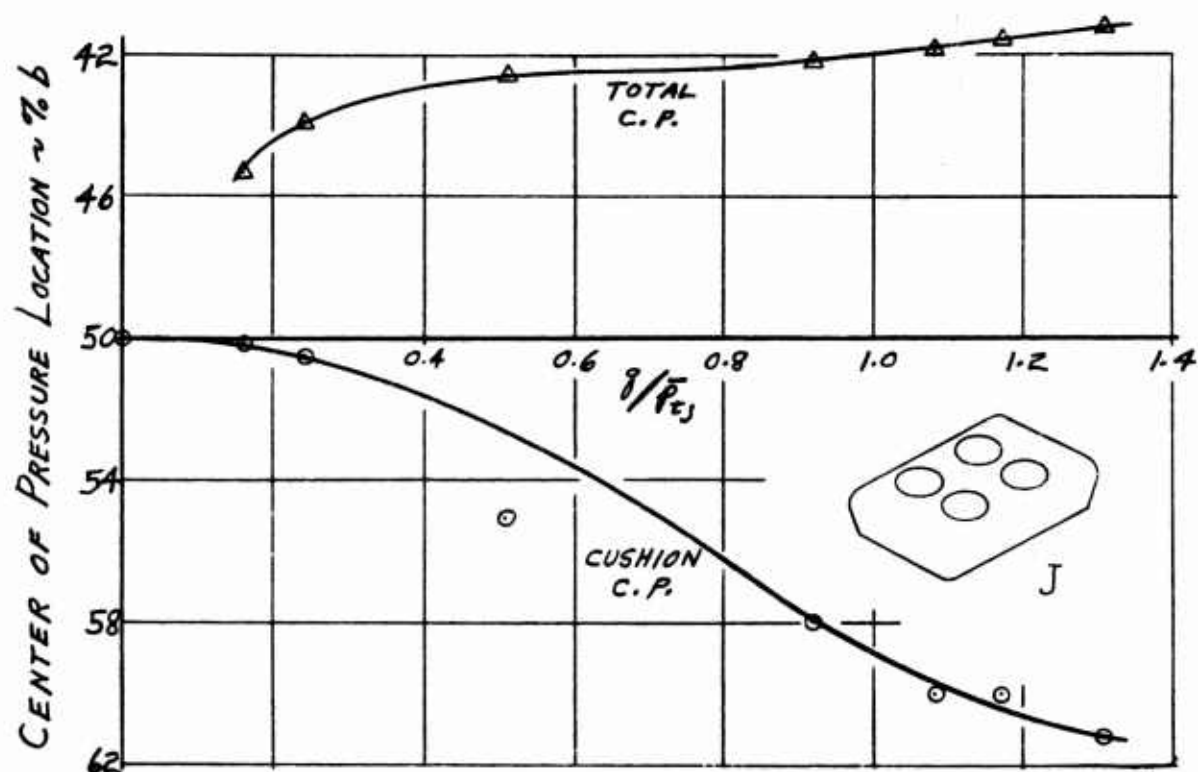


Fig 21

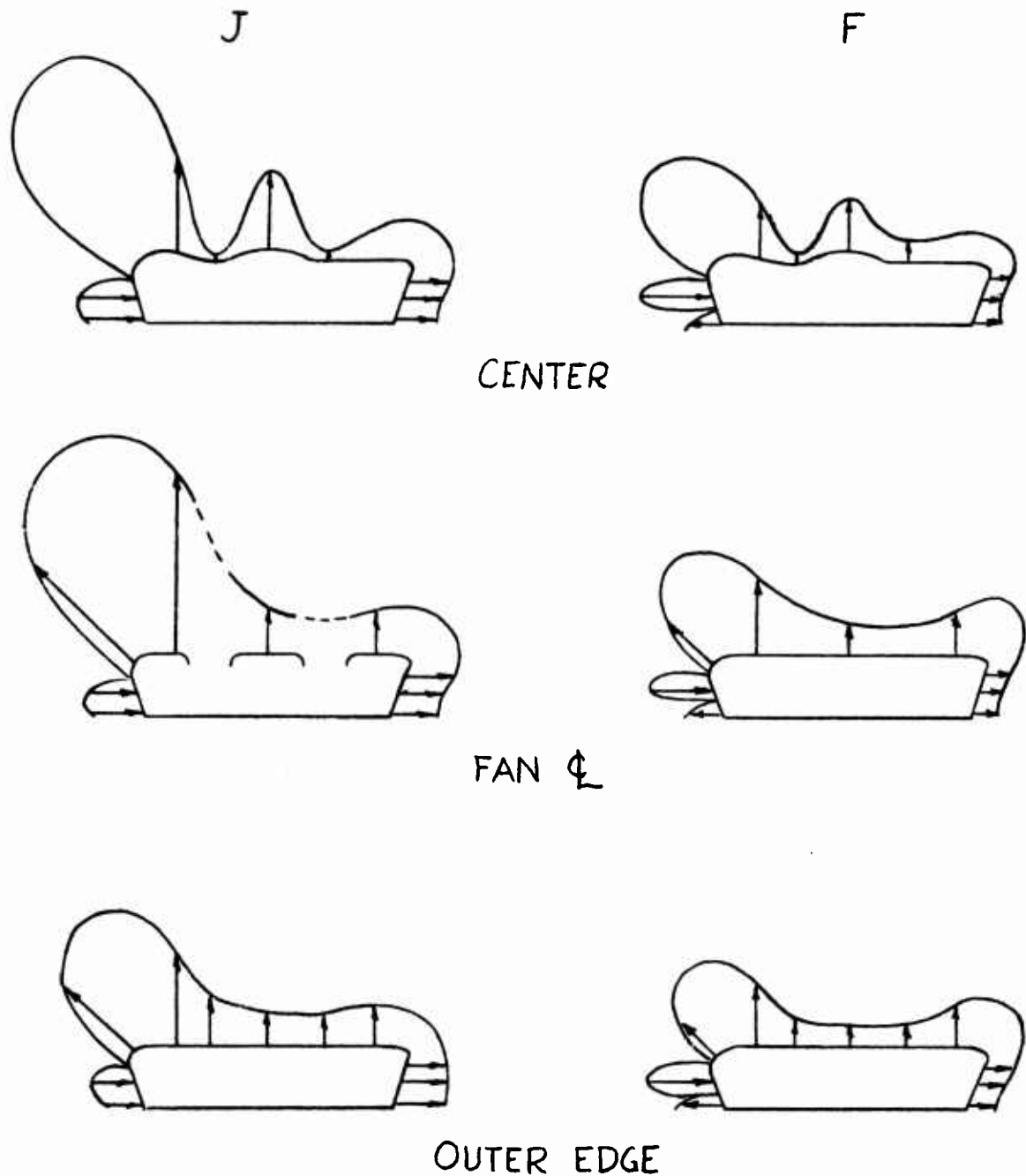
EFFECT OF FLIGHT SPEED ON CENTER OF PRESSURE LOCATION



LONGITUDINAL PRESSURE DISTRIBUTION
FOR BASIC AND FAIRED CONFIGURATIONS
AT ZERO ANGLE OF ATTACK

FIG. 22

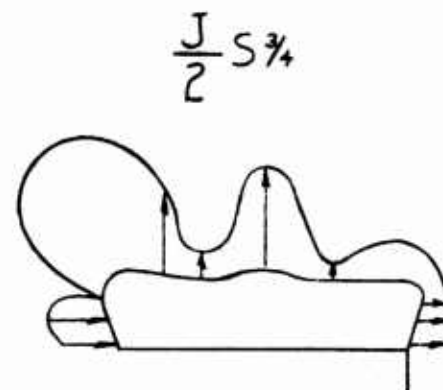
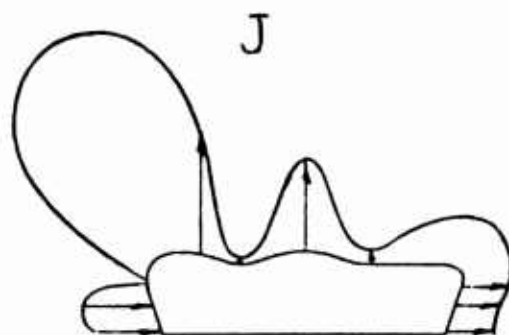
$$q=15 \quad \frac{h_l}{S} = .64$$



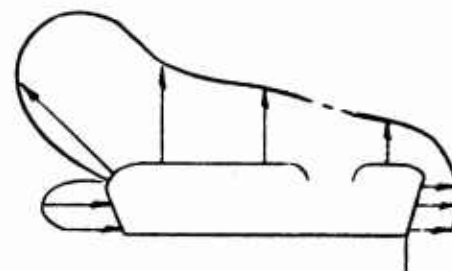
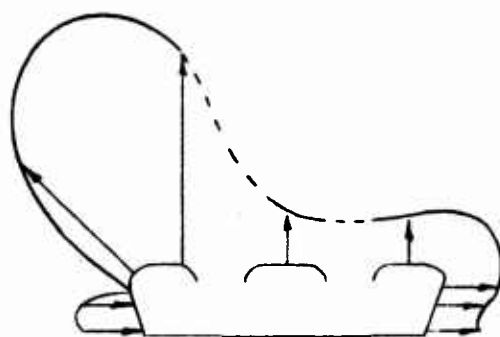
LONGITUDINAL PRESSURE DISTRIBUTION
FOR BASIC AND HIGH SPEED CONFIGURATIONS
AT ZERO ANGLE OF ATTACK

Fig 23

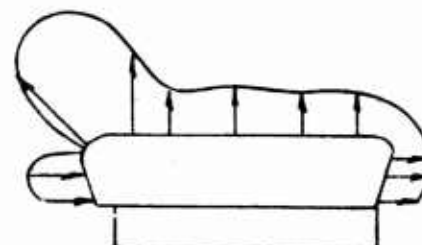
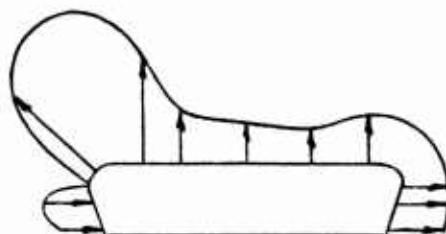
$$g = 15 \quad \frac{h}{s} = .64$$



CENTER



FAN \downarrow



OUTER EDGE

LONGITUDINAL TRIM PROBLEM

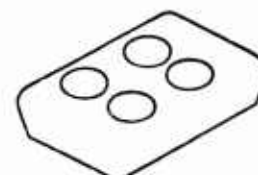
FIG 24

ZERO ANGLE OF ATTACK

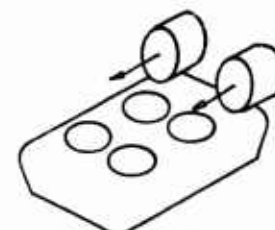
$$\frac{h}{S} = 0.64$$

CONFIGURATION $\frac{q}{P_{tj}}$ C.P. LOCATION FROM C.G.

J .55 7.7% FWD
1.10 9.0% FWD



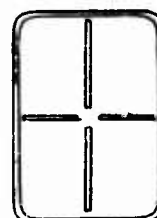
JP_F .55 6.0% FWD
1.10 9.0% FWD



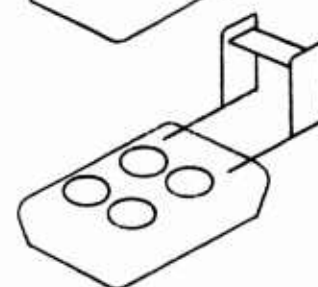
JP_FT_{i=0} .55 8.0% FWD



JVT_{i=0} .55 9.0% FWD



J_{EXT}T_{i=0} .55 10.5% FWD



LONGITUDINAL TRIM
ZERO ANGLE OF ATTACK

PROBLEM
 $\frac{h \cdot l}{S} = 0.64$

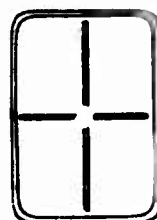
Fig 25

CONFIGURATION $\frac{q}{P_{tj}}$ C.P. LOCATION
FROM C.G.

J

.55
1.10

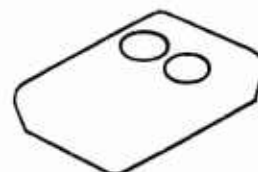
7.7% FWD
9.0% FWD



$\frac{J}{2}$

.55
1.20

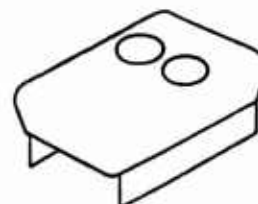
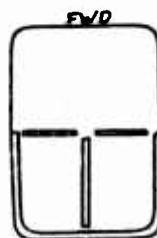
10.0% AFT
9.0% AFT



$\frac{J}{2} + i S \frac{3}{4}$

.42
.72

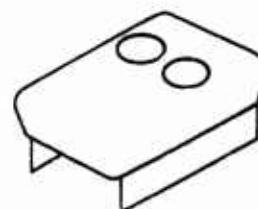
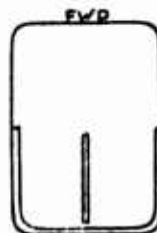
1.0% FWD
1.0% FWD



$\frac{J}{2} S \frac{3}{4}$

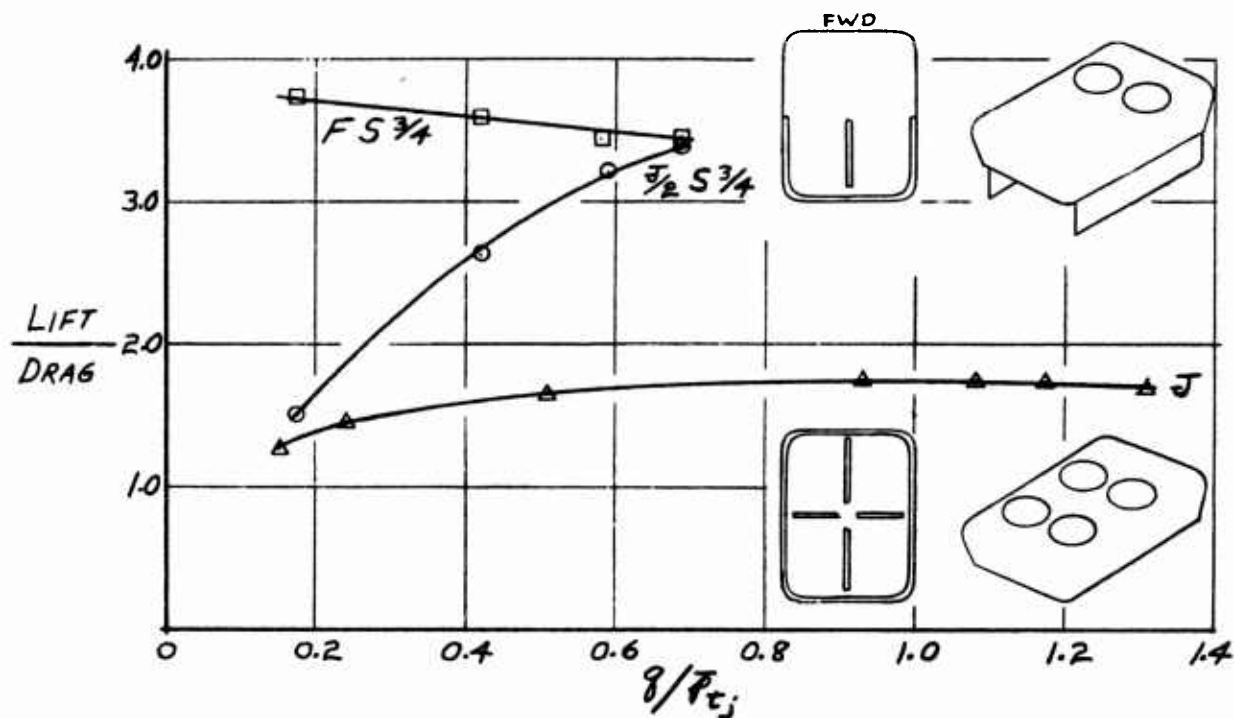
.42
.72

0.5% FWD
1.0% FWD



COMPARISON OF LIFT DRAG RATIO
FOR STANDARD AND HIGH SPEED CONFIGURATIONS

$$h_l/S = 0.64 \quad \alpha = 0^\circ$$

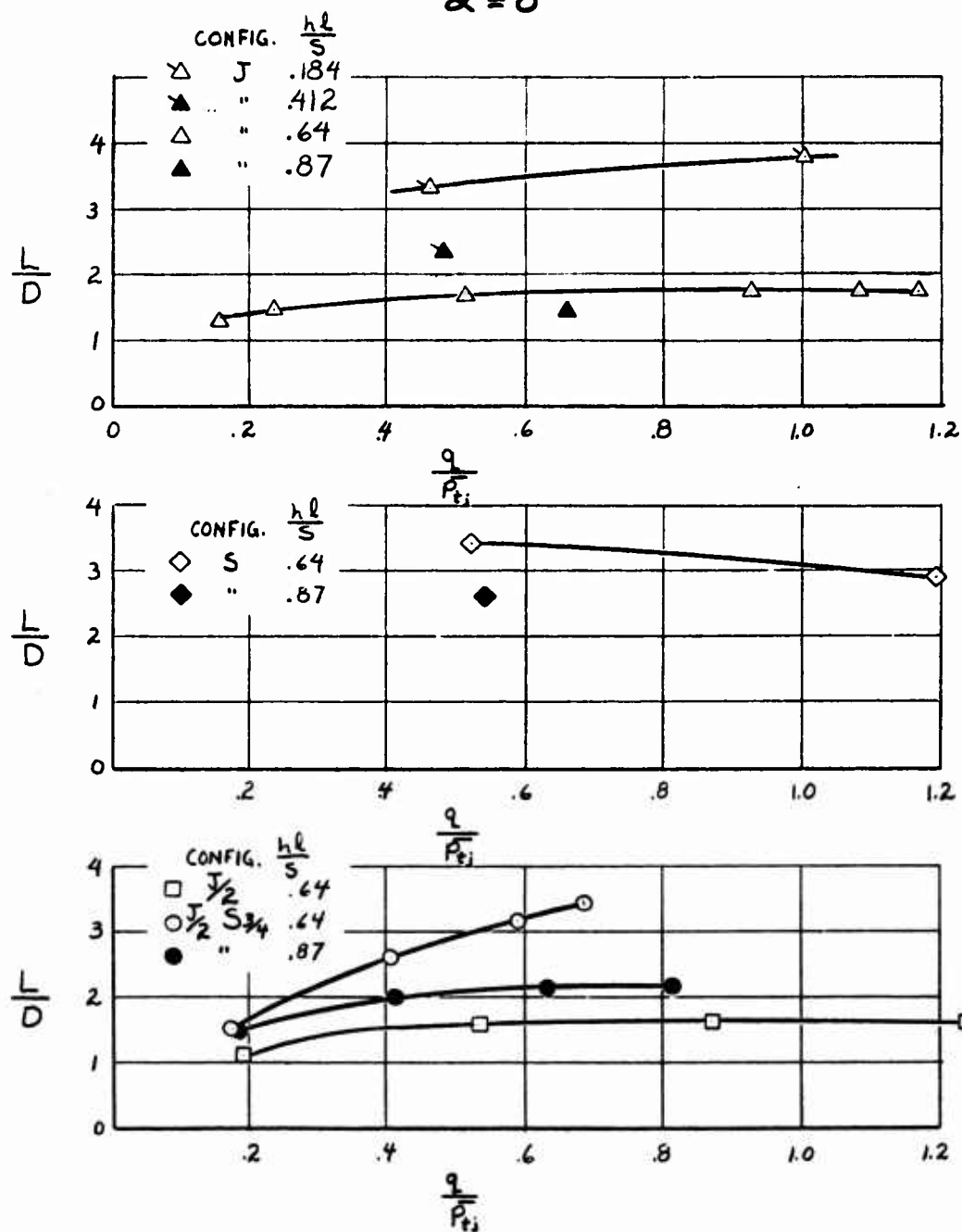


$$\frac{\text{LIFT}}{\text{DRAG}} = \frac{\text{TOTAL MEASURED LIFT}}{\frac{550 \text{ HP}}{V_{FS}} + \text{TOTAL MEASURED DRAG} + 0.2 \rho Q_{\text{EXIT}} V_{FS}}$$

Fig 27

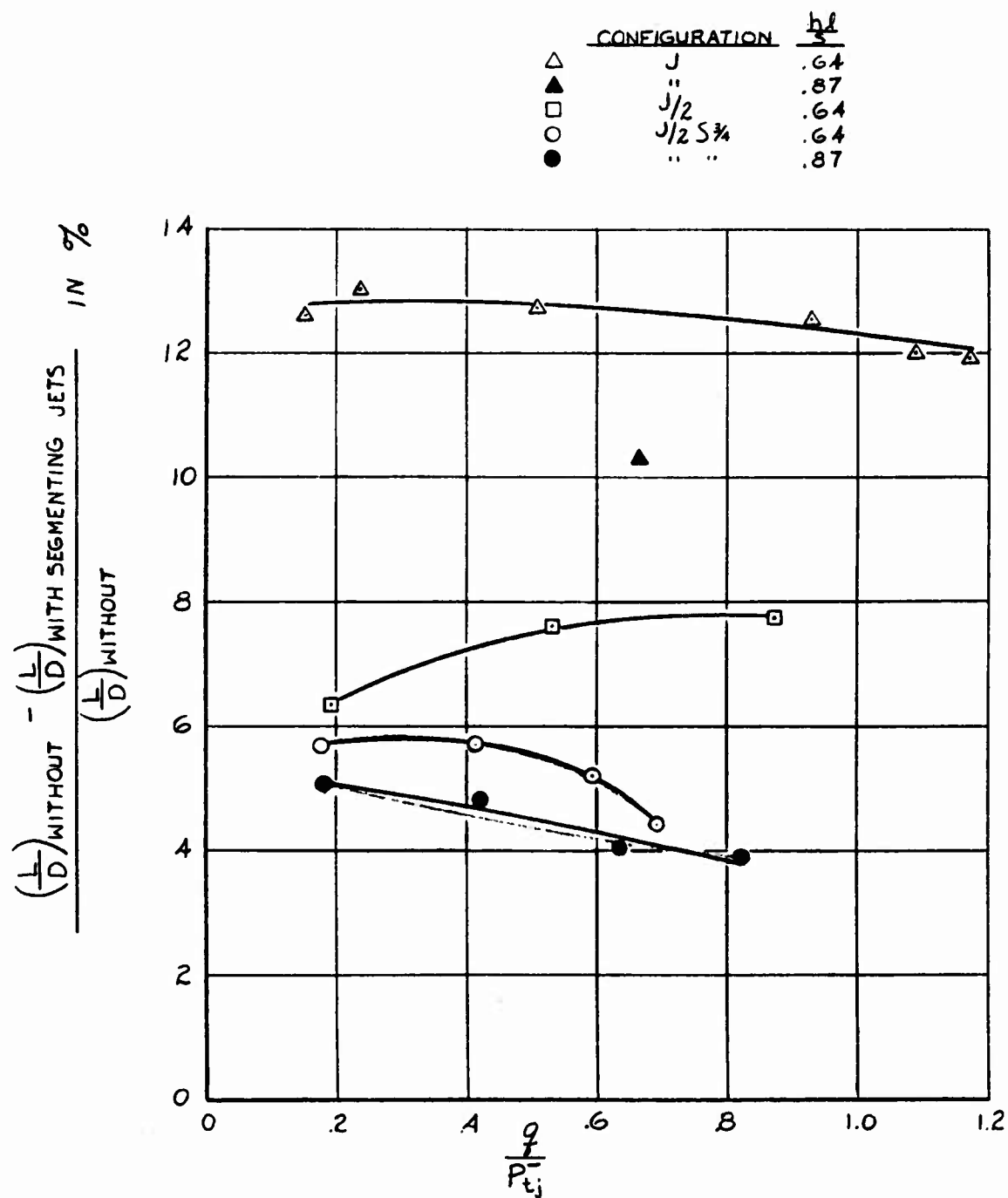
EFFECT OF HEIGHT AND SPEED ON $\checkmark D$

$\alpha = 0$



PERFORMANCE COST OF SEGMENTING JET STABILIZATION

Fig 28



GROUND EFFECT POWER FACTOR IN HOVERING - BASED ON EXIT POWER

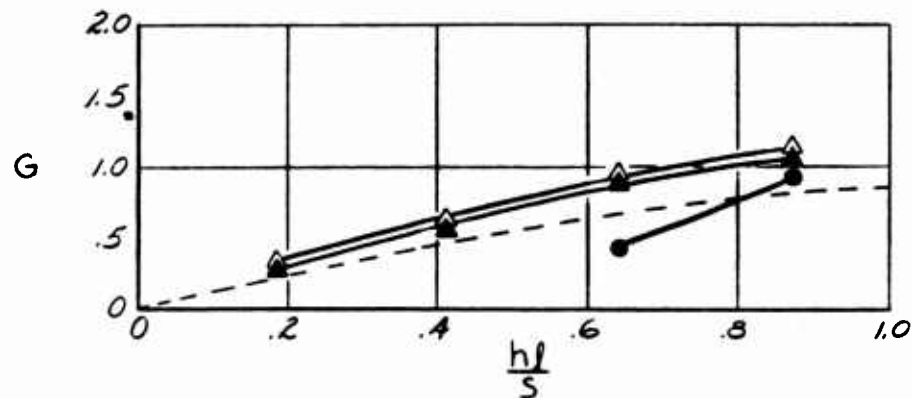
FIG 29

$g=0$

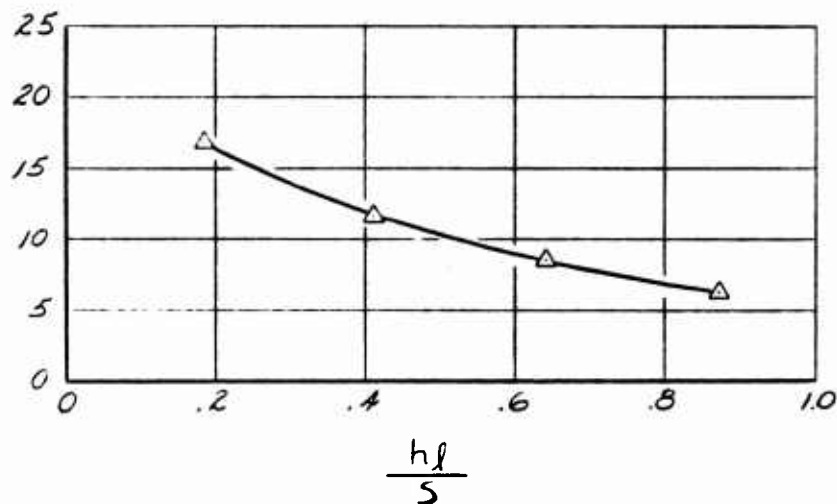
--- ENVELOPE OF OPTIMUM HOVERING
CONFIGURATIONS-AERONUTRONIC EXPERIMENTS
REF. 2

J \triangle WITH SEGMENTING JETS
▲ WITHOUT " "

S ● WITHOUT SEGMENTING JETS



$\frac{G_{\text{WITH SEGMENTING JET}} - G_{\text{WITHOUT}}}{G_{\text{WITHOUT}}} \sim \%$



2. Static Longitudinal Stability

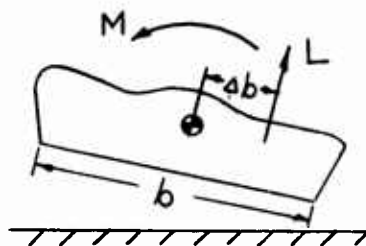
a. Method of Analysis

The requirement for static longitudinal stability is that the moment generated due to a displacement in pitch be in a direction opposing the original displacement. A negative slope to the curve of pitching moment vs. angle of pitch fulfills this requirement. A glance at the basic data will therefore be sufficient to reveal static stability or instability. Expression of the degree of static stability requires a bit more analysis.

Air cushion vehicles do not have a definite attitude-speed relationship under constant lift as do aircraft. The aircraft method of determining a static margin

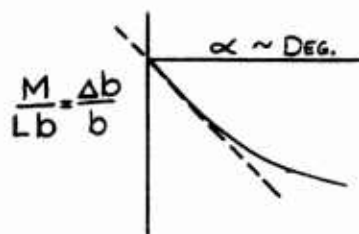
$\partial C_M / \partial C_L$ and neutral point (C. G. location where $\partial C_M / \partial C_L = 0$) is not therefore applicable to air cushion vehicles in the pitch mode. In addition, the air cushion vehicle, similar to VTOL aircraft, encounters the problem of coefficient definition in hovering and very low speed flight. It is no longer meaningful to non-dimensionalize in terms of flight dynamic pressure q .

Both of the above problems can be neatly solved in the following manner. The most fundamental view one can employ is to remember that a moment is the product of a force acting at an arm. If we take the force com-



ponent normal to the model and consider that the moment about the C. G. can be attributed to this force, it is possible to solve for the arm Δb between the center of gravity and the effective center of pressure.

If we now plot this effective center of pressure location $\frac{\Delta b}{b}$ against angle of attack α we can take



the slope of the curve as the measure of static stability for small angles. By multiplying the slope by 100, we can express the stability as center of pressure shift (expressed in percent of length) per degree of tilt. This method can be employed in hovering as well as at all values

of forward speed. The lift and moment can arise from cushion pressure, flight dynamic pressure or some undetermined combination of both and not affect the method. Of course, in reality some of the moment may come from drag loads acting with an unknown arm about the C.G. The proposed method when used consistently does provide the correct sign for the stability, provides a quantitative stability value by which different configurations and flight conditions may be compared, and presents a clear physical picture which does not require a previous knowledge of expected coefficient magnitude to interpret.

b. Results

The static longitudinal stability parameter is presented (as a function of height and speed) for the basic jet segmented configuration in Figure 30. Note that static stability exists for all heights tested (through $h_1/S = 0.87$, which represents a base height of 20% of the vehicle diameter) and at all speeds tested through $q/\bar{P}_{t_1} = 1.1$. A pronounced decrease in magnitude of the parameter occurs with increasing height and a somewhat smaller decrease occurs with increasing speed. Examination of the stability parameter obtained from plots of the base-plus-jet lift and moment integrations reveals that while the cushion normal forces provide the majority of the stabilization at a given height and speed, there is a significant stable contribution coming from elsewhere. This result was somewhat unexpected as it had been

anticipated that the upper body would have a destabilizing tendency.[†] Perhaps the manner in which chord forces change with attitude may be responsible.

The stability parameter is presented for the skirted and flap segmented configuration in Figure 32. Again, the model is stable at all heights and speeds tested. At $h_l/S = .87$ where the skirt and flaps extend half way to the ground, the stability derivative is identical to that of the jet segmented model at $h_l/S = 0.87$. At an $h_l/S = 0.64$ where the skirt and flaps extend two-thirds the way to the ground, the stability is somewhat higher than for the jet segmented model at the same height and this effect is most pronounced at the high speed.

The stability parameter values for the half cushion, three-quarter skirt, configuration are presented in Figure 33. This configuration was evolved to cure the serious pitch up problem at forward speed. The stability is very high in hovering with the front skirt back in place and the cushion fed only through the rear jets. In forward flight with the front skirt open, slight instability exists at all heights and speeds. Additional study would be required to achieve improved stability, trim, and performance over the entire range.

The effect of Beta vanes on the static longitudinal stability of the basic jet segmented model is shown in Figure 34 as a function of speed for an $h_l/S = 0.64$. The vanes tend to reduce the stability, the 60° vanes having a greater effect than the 30° vanes. It should be noted that in all three cases, the front jet was closed off for the high speed point.

The addition of propulsion nacelles to the basic jet segmented configuration is seen in Figure 35 to have very little effect on longitudinal stability. An isolated

[†] Note the effect of angle of attack on the pressure distribution in Figure 31. The pitching moment due to this distribution increases at $+\alpha$ and decreases at $-\alpha$.

ducted fan is known to have a high rate of change of normal force with angle of attack. The fact that a change in stability did not occur when the fans were added must mean that the unit does not feel an aerodynamic angle of attack when the model pitches. This is due to the influence of the body on the local flow field. The air which flows by the rear propulsion fans does not flow parallel to the ground but rather flows parallel to the model body.

The effect of location on longitudinal effectiveness of a horizontal tail (when added to the basic jet segmented model) is shown in Figure 36. At the top of the page the lift curve slope of the isolated tail is given. The effective lift curve slopes of the tail in several locations were deduced from differences in the slope

$\partial C_M / \partial \alpha$ tail on and tail off knowing the tail length. The effective lift curve slopes so obtained are then compared to the isolated tail value to obtain the fraction of geometric angle of attack change the tail actually feels when placed on the model. The tail is almost completely ineffective as a stabilization device when placed between the rear propulsion fans. It is 64% as effective as an isolated tail when placed between vertical tails at the rear of the model. When extended a half model length behind its normal position, the effectiveness increases to 86% of the isolated tail value. It appears that the location of aerodynamic stabilization fins is quite critical for air-cushion vehicles in the pitch mode.

The effect of several modifications (investigated in the search for a cure for the pitch up problem) upon static longitudinal stability is presented in Figure 37. Closing off the front jet, front longitudinal segmenting jet, and front part of the side jets and adding the three-quarter skirt produces neutral stability in place of the strong stability available for the standard configuration.

Removal of the lateral segmenting jets and addition of tilted propulsion fans causes a small destabilizing and stabilizing tendency respectively. The magnitude of the change is very small, however. Additional configurations are presented in Figure 38. Replacing the lateral segmenting jet with a solid flap produces strong static stability. Tapering the forward portion of the side skirt walls destabilizes the model.

Summing up, the static longitudinal stability appears adequate over the range of heights and speeds tested for the basic jet segmented and flap segmented configurations. The high speed model which cured the pitch up problem and doubled the L/D was statically unstable in pitch. The propulsion fans did not change the longitudinal stability when added to the basic model. The stability contribution of the horizontal tail was drastically reduced when mounted above the propulsion fans as compared to mounted between vertical tails.

EFFECT OF HEIGHT AND SPREAD ON
STATIC LONGITUDINAL STABILITY FIG 30

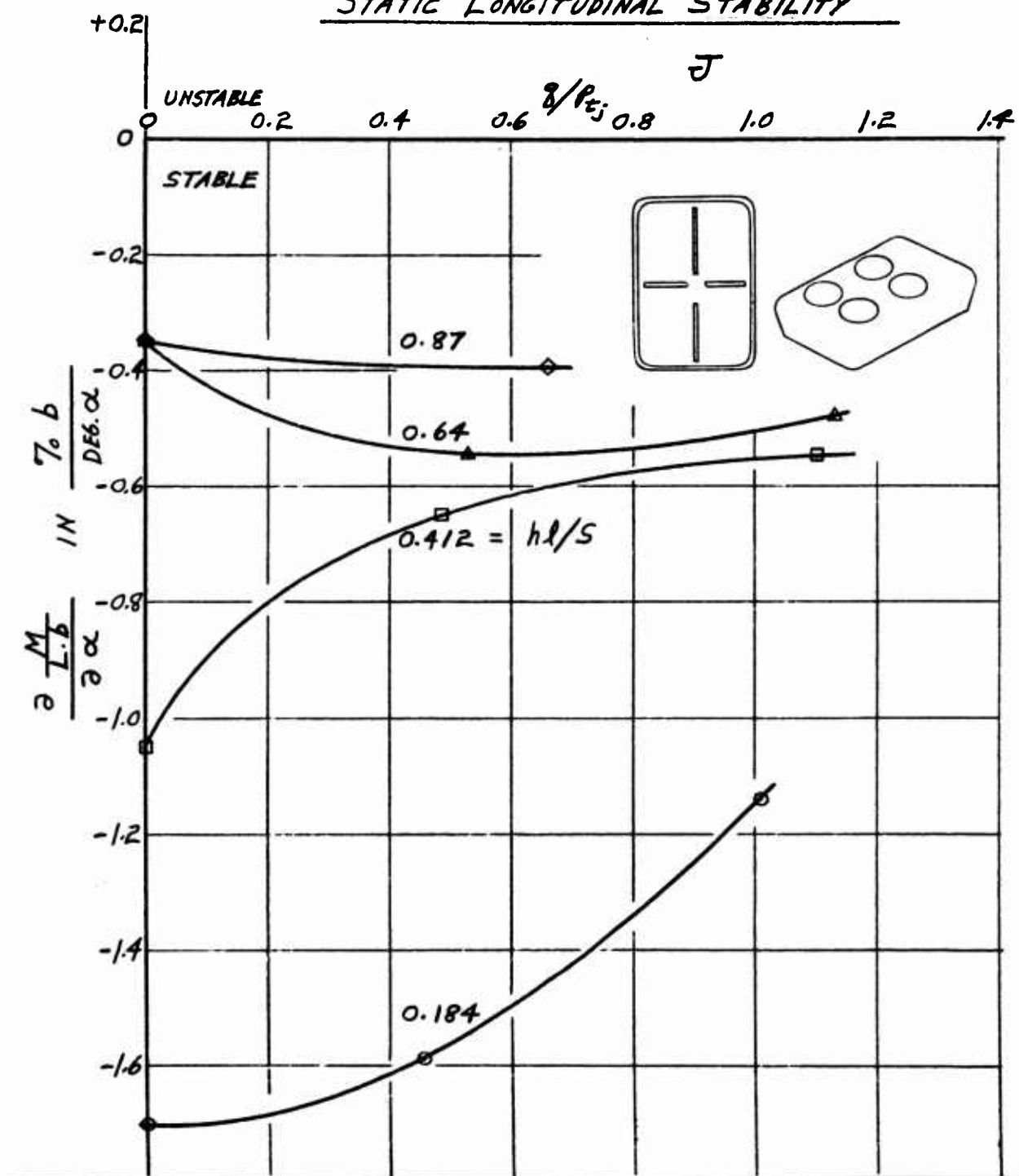



FIG 3

EFFECT OF PITCH ON PRESSURE DISTRIBUTION IN PLANE OF FAN ϕ

$$J \quad \frac{hl}{S} = .64$$

$$C_p = 1.0$$


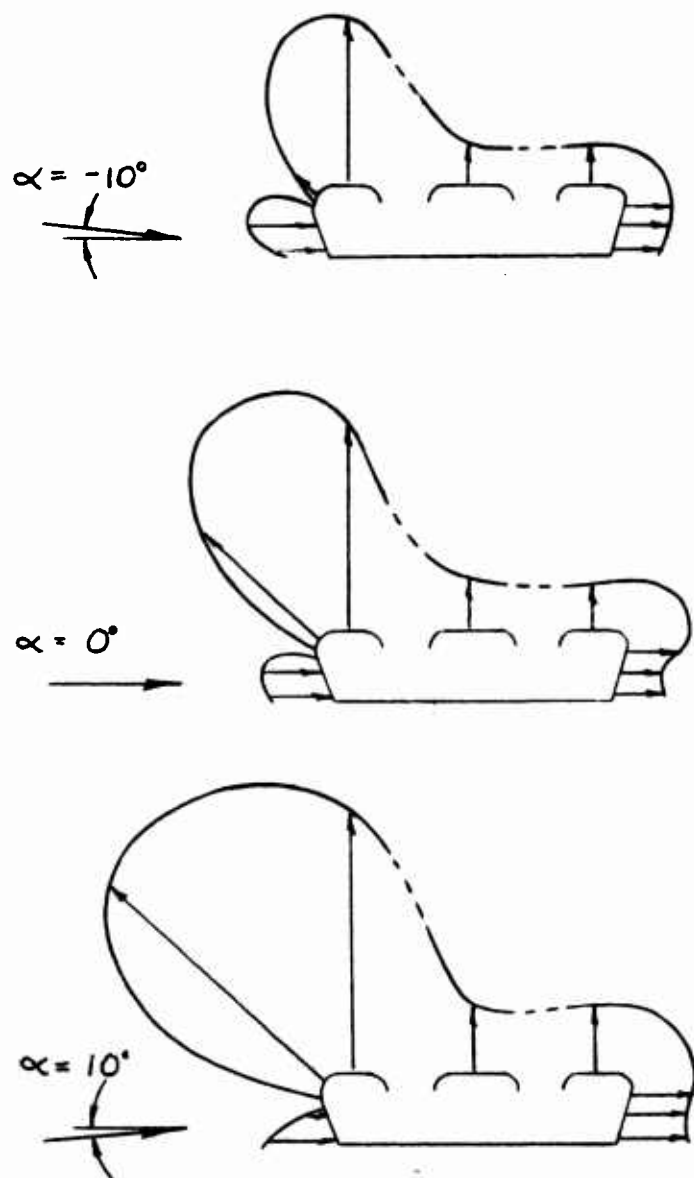
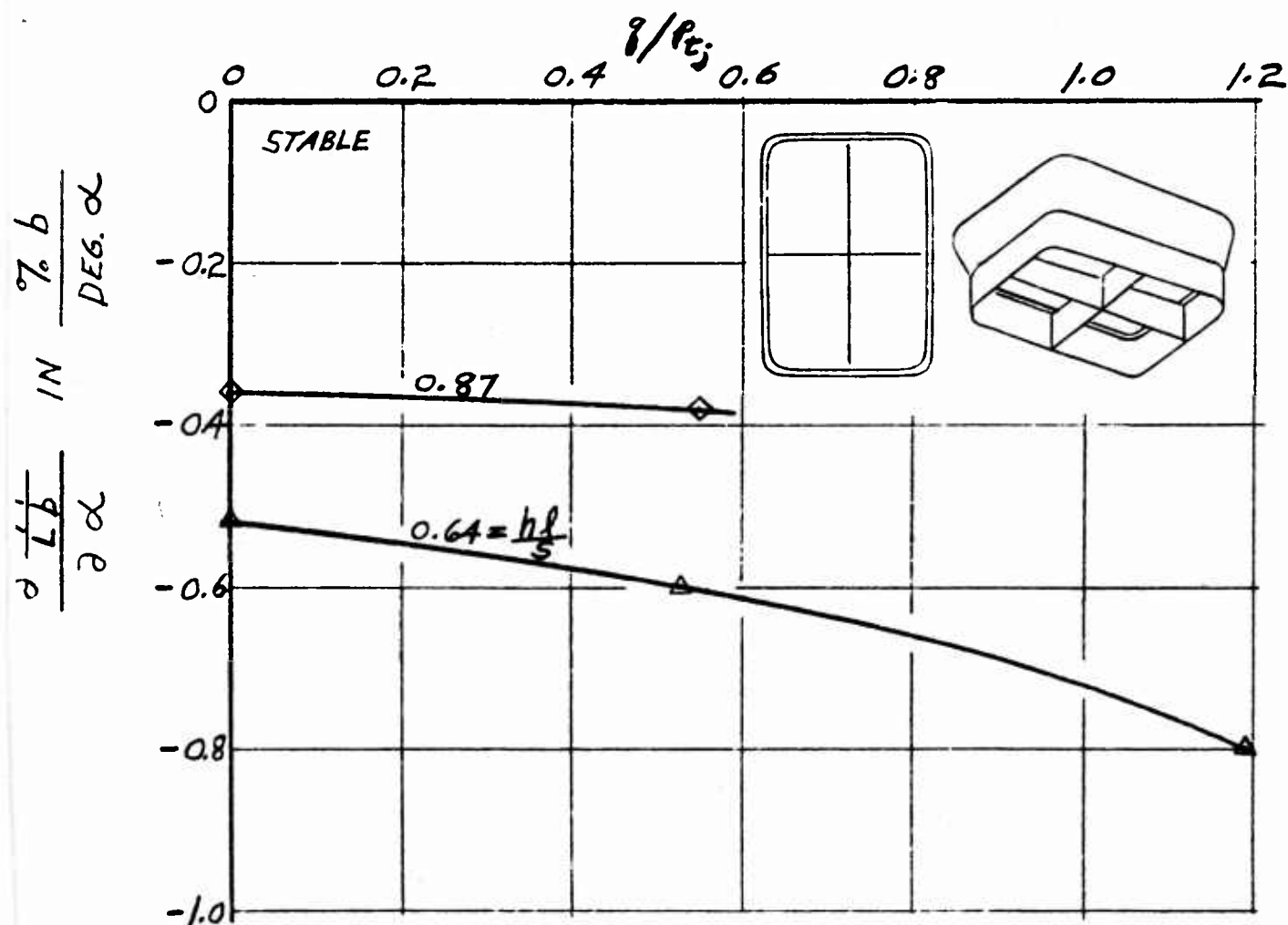


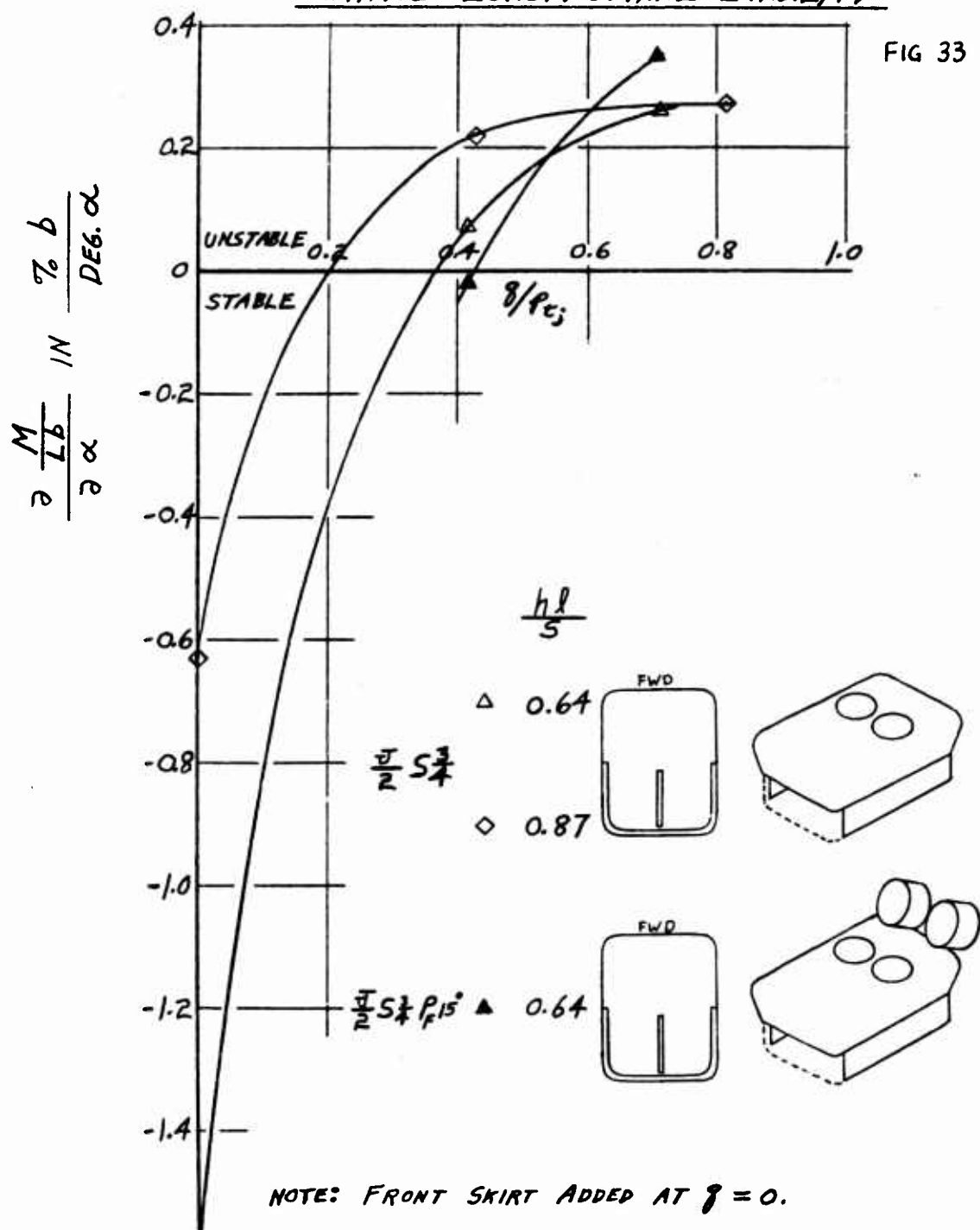
FIG 32

EFFECT OF HEIGHT AND SPEED ON
STATIC LONGITUDINAL STABILITY

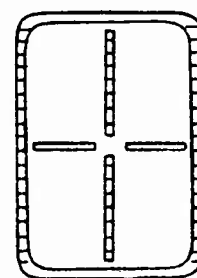
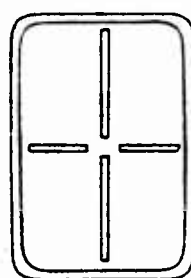
S



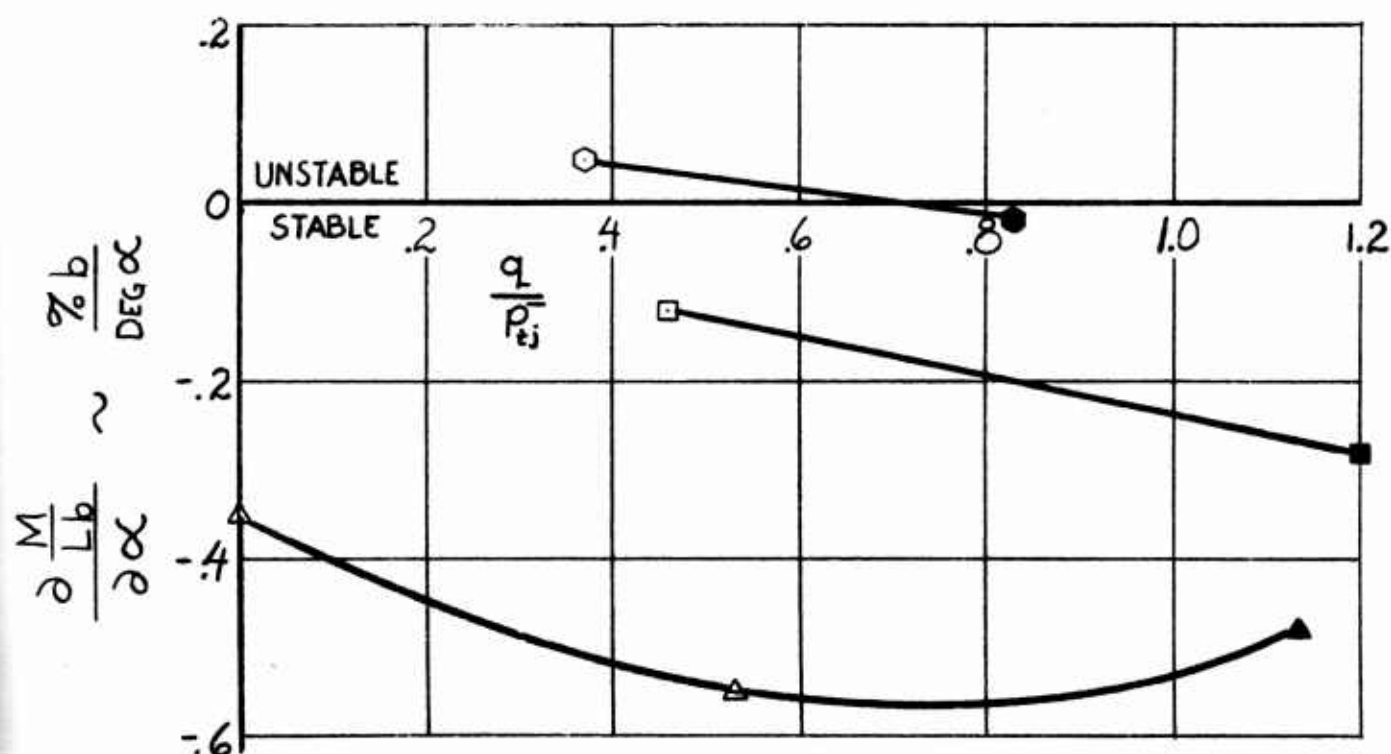
EFFECT OF HEIGHT AND SPEED ON STATIC LONGITUDINAL STABILITY



EFFECT OF β VANES ON STATIC LONGITUDINAL STABILITY

 $\triangle J$ $\square J\beta_{30^\circ}$ $\circ J\beta_{60^\circ}$ 

$$\frac{h l}{S} = 0.64$$



SOLID SYMBOL DENOTES FRONT JET CLOSED

STATIC LONGITUDINAL STABILITY

FIG 35

$$\frac{h\ell}{S} = 0.64 \quad \frac{q}{P_i} = .55$$

CONFIGURATION $\frac{\partial \frac{M}{Lb}}{\partial \alpha} \sim \frac{\% b}{\text{DEG } \alpha}$

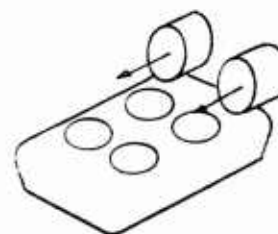
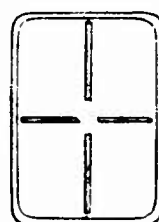
J

-0.54



JP_F

-0.45



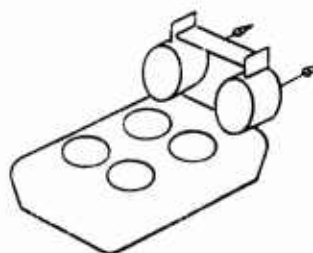
JP_R

-0.65



JP_RT

-0.50



HORIZONTAL TAIL EFFECTIVENESS

FIG 36

A. STABILITY

$$\frac{h\ell}{S} = 0.64$$

$$\frac{q}{P_{Tj}} = .55$$

CONFIGURATION

$$\frac{\partial C_L}{\partial \alpha}_{TAIL}$$

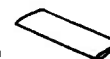
$$1 - \frac{d\epsilon}{d\alpha}$$

ISOLATED TAIL

0.055

1.0

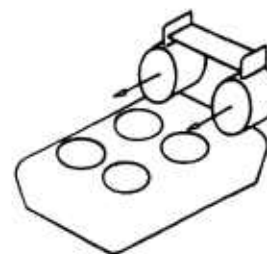
R = 2.78



J_{PfT}

0.002

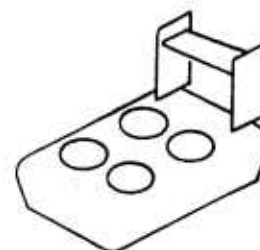
0.036



J_{VT}

0.0352

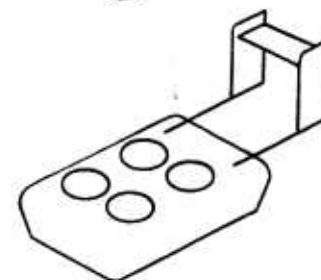
0.64



J_{EXTT}


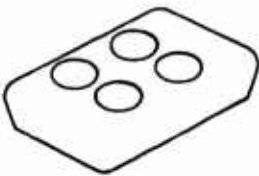
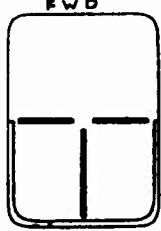
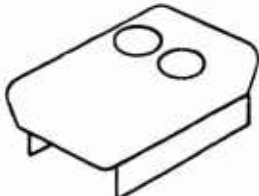

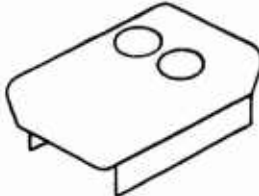


0.047

0.855



STATIC LONGITUDINAL STABILITY $\frac{h\ell}{S} = 0.64$

FIG 37

CONFIGURATION	$\frac{\partial \frac{M}{Lb}}{\partial \alpha} \sim \frac{\% b}{\text{DEG } \alpha}$		$\frac{q}{P_{Tj}}$
J	-0.54		 <p>.55</p>
$\frac{J}{2} + i S \frac{3}{4}$	0.0		 <p>.42</p>
$\frac{J}{2} S \frac{3}{4}$	+0.07		 <p>.42</p>
$\frac{J}{2} S \frac{3}{4} P_F + 15^\circ$	-0.02		 <p>.42</p>

STATIC LONGITUDINAL STABILITY

FIG 38

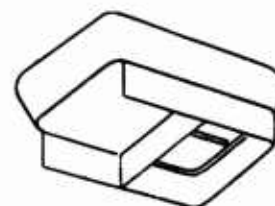
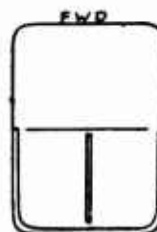
$$\frac{hl}{S} = 0.64$$

$$\frac{q}{P_{Tj}} = .42$$

CONFIGURATION $\frac{\partial \frac{M}{Lb}}{\partial \alpha} \sim \frac{\% b}{\text{DEG } \alpha}$

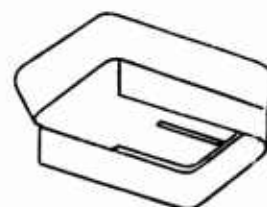
$\frac{J}{2} + \text{FL. } S \frac{3}{4}$

-0.75



$\frac{J}{2} S \frac{3}{4}$

+0.07



$\frac{J}{2} S \frac{3}{4}$ TAPERED

+0.30



3. Static Lateral Stability

a. Method of Analysis

A stable air-cushion vehicle has a restoring moment due to pure roll angle in hovering and at forward speed just as it has due to pure pitch angle. This is different than an airplane which has no moment imposed due to pure roll angle (until slip takes place). The same type of analysis used in pitch will therefore be used in roll.

b. Result

The static lateral stability parameter for the basic jet segmented configuration is presented in Figure 39 as a function of height and speed. The model is statically stable in roll at all heights and speeds. The usual decrease in stability with increase in height is apparent at low speeds but at high speeds the level of stability is relatively independent of height. As in the pitch case, the cushion provides a large portion of the stability, but there is also a large non cushion stable contribution.

Similar stability data are presented for the skirted and flap segmented model in Figure 40. The skirts and flaps extended half way to the ground at $h_1/S = 0.87$ and two-thirds the way to the ground at $h_1/S = 0.64$. The values of the stability parameter are very similar to those for the jet segmented model at the same base height.

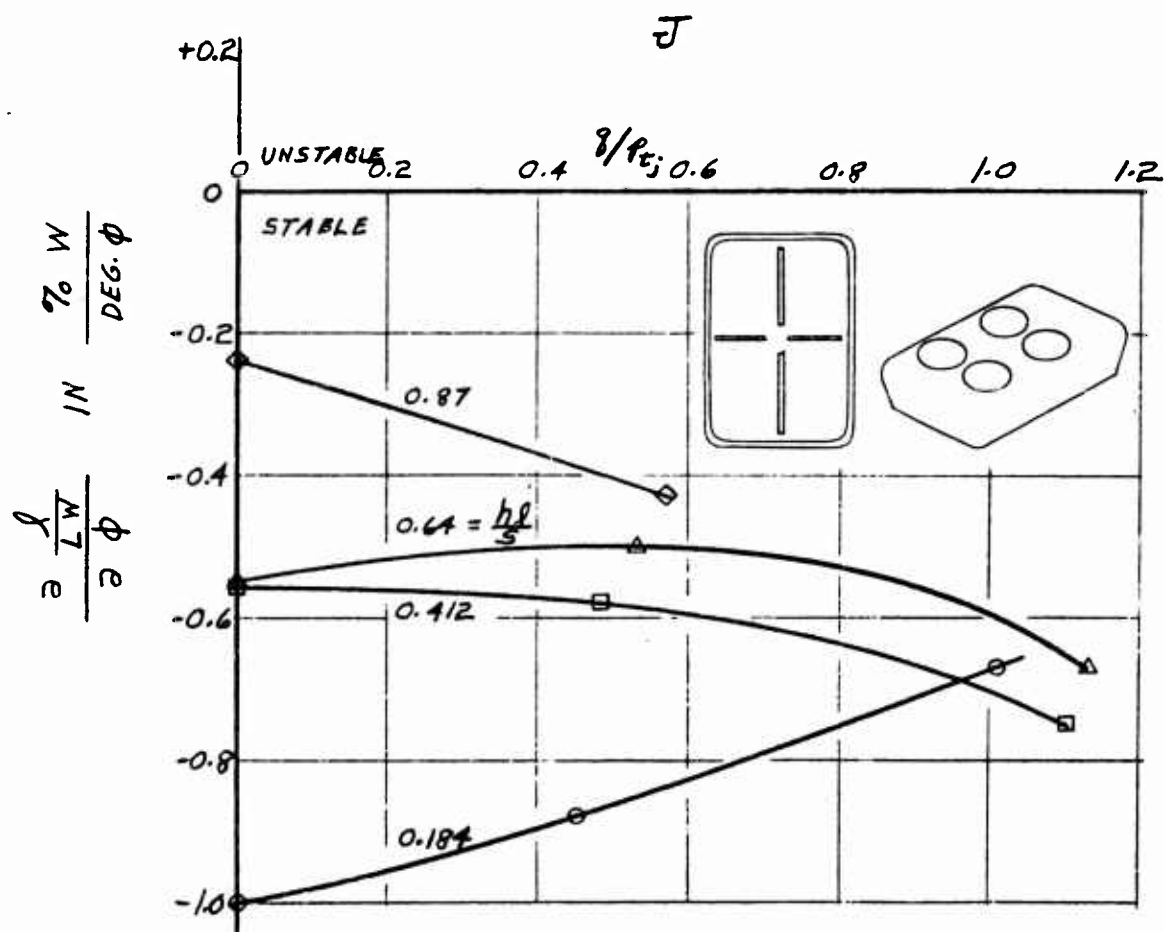
Static lateral stability derivatives are presented in Figure 41 for the high speed configuration. In hovering, with the front skirt added, and the cushion fed from the rear half of the model, a high degree of instability exists. At forward speed, however, the single rear segmenting jet appears to be adequate and strong stability exists.

The effect of a few additional configuration changes on static lateral stability at $h_l/S = 0.64$ and $q/p_{t_j} = 0.55$ is presented in Figure 42. All configurations are stable. The Beta vanes seem to actually improve the lateral stability slightly.

Summing up, there appear to be no static lateral stability problems over the range of height and speed investigated, except for the hovering case of the high speed configuration. This could be corrected by opening the forward longitudinal segmenting jet. It should be emphasized that the degree of stability required is still quite open to question.

EFFECT OF HEIGHT AND SPEED ON STATIC LATERAL STABILITY

FIG 39



EFFECT OF HEIGHT AND SPEED ON
STATIC LATERAL STABILITY

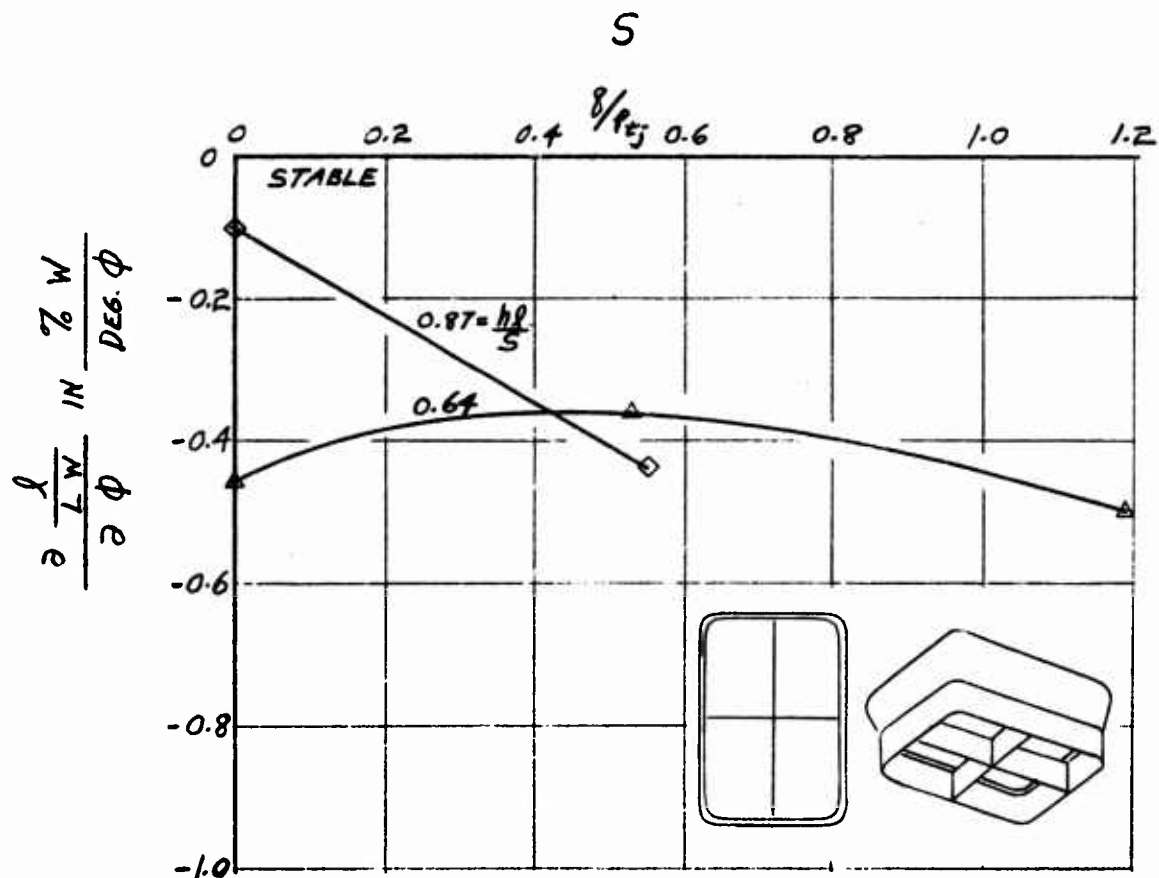
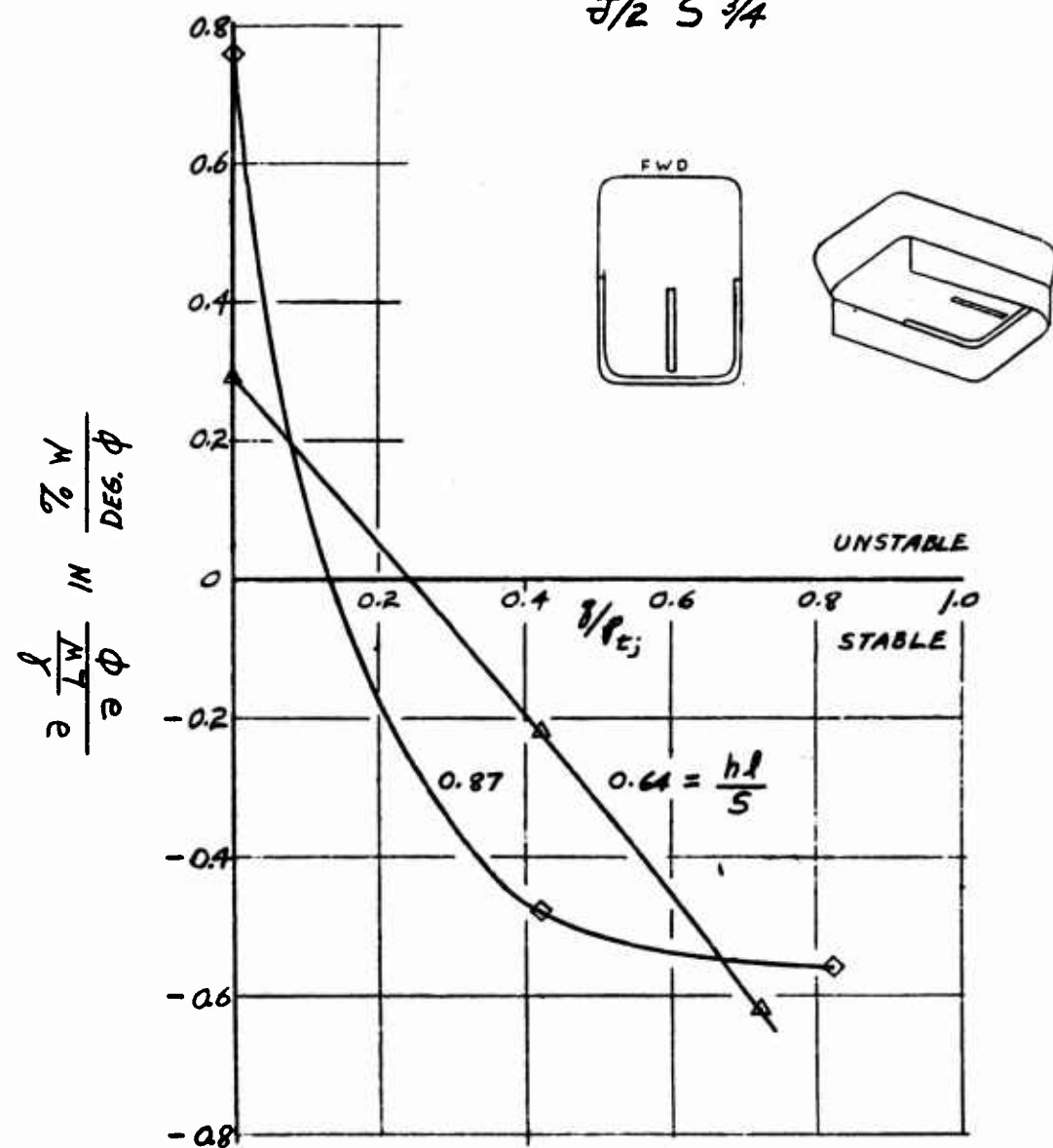


FIG 41

EFFECT OF HEIGHT AND SPEED
ON STATIC LATERAL STABILITY

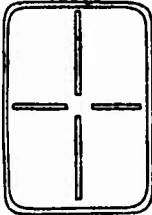
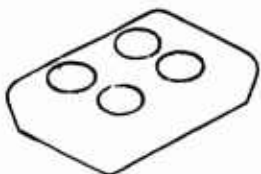





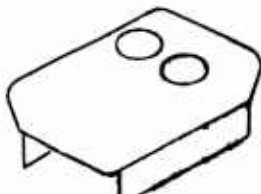
 $\frac{S}{2} S \frac{3}{4}$


NOTE: FRONT SKIRT ADDED AT $\eta = 0$

STATIC LATERAL STABILITY

FIG 42

$$\frac{hL}{S} = 0.64$$

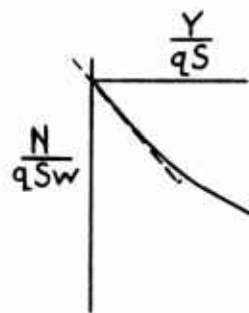
CONFIGURATION	$\frac{\partial \frac{L}{W}}{\partial \phi} \sim \frac{\% W}{\text{DEG } \phi}$		$\frac{q}{P_{Tj}}$
J	-0.5 %		 .55
J P _F J P _R	-0.42 % -0.30 %		 .55
J B _{30°} J B _{60°}	-0.67 % -0.59 %		 .55
I S ₃	-0.22 %		 .42

4. Static Directional Stability

a. Method of Analysis

The directional behavior of an air-cushion vehicle is different from its longitudinal and lateral behavior. The cushion loads themselves would be expected to be relatively independent of yaw angle. The directional contributions of the body, fins, and propulsion fans would not be expected to be greatly influenced by the presence of the ground or cushion. It would seem therefore that an airplane type directional neutral point location presentation might be suitable for the yaw case.

The wind axis drag and side force coefficient on the model are resolved into a body axis side force coefficient. The yawing moment coefficient is then plotted against the body axis side force coefficient.



The slope of this line,

$$\frac{\partial C_N}{\partial C_Y} = \frac{\partial N/qSw}{\partial Y/qS}$$

represents the fraction of the characteristic width which the neutral point in yaw lies behind the center of gravity. The width of the vehicle was used as the characteristic length in

non-dimensionalizing the yawing moment similar to aircraft practice where the wing span is used in both roll and yaw. Since the neutral point is visualized as a location along the length of the model, the value of

$\frac{\partial C_N}{\partial C_Y}$ is converted from percent of width to percent of length and added or subtracted from 50% which is the moment center (C. G.) to obtain the absolute neutral point location on the model. This method appears to work well, does not lead to any paradoxes, and has a simple and clear significance.

The stability derivatives in pitch and roll were presented for small angles near zero since it is desirable to keep an air-cushion vehicle level to keep good ground clearance. It may, however, be desirable to yaw an air-cushion vehicle to relatively large angles in the course of a turn maneuver. The directional neutral point location is therefore given for a range of yaw angles.

b. Results

Directional neutral points for various faired model configurations are presented in Figure 43. The basic body shape is directionally unstable and becomes increasingly so with increasing yaw angle. Addition of propulsion fans provides directional stability. There is a slight decrease in the degree of stability as the yaw angle increases. The neutral point moves from 73% at $\psi = 0^\circ$ to 67% as the yaw angle approaches 45° . Windmilling one propulsion fan for directional control causes a small decrease in directional stability. Reversing one fan for directional control causes a larger decrease in directional stability but the neutral point still lies well aft of the center of gravity.

Directional neutral points for various blowing model configurations are presented in Figure 44. The blowing model is about neutrally stable at small angles.[‡] The propulsion fans do an excellent job of directional stabilization through a wide range of yaw angles. A pair of vertical tails stabilize the model up to 15° where tail stall occurs leading to neutral stability at higher angles. The half cushion high speed model with three-quarter skirt and propulsion fans tilted 15° (for longitudinal trim) exhibits high directional stability up through 45° of yaw angle.

[‡] The instability at large angles can be explained by the pressure distributions of Figure 45.

The effect of propulsion fan mode on the directional neutral point location of the blowing model is presented in Figure 46. Again, as in the case of the faired model, windmilling one fan for directional control reduces directional stability slightly and reversing one fan for increased directional control makes the stability neutral at small angles. When both fans are reversed for braking, the model becomes directionally unstable. The reason for this is that the strong flow created by the reversed fan overcomes locally the effect of the windstream. The shrouded props which act as an efficient tail surface are now experiencing flow in the wrong direction so they contribute a destabilizing moment.

The vertical tails are analyzed in the upper portion of Figure 47. The effective lift curve slope of the tail is deduced from the change in $\partial C_N / \partial \psi$ tail on - tail off and the tail volume coefficient. The effective aspect ratio is almost twice the geometric value. The broad flat body does a good job of endplating, and acts as almost a perfect reflection plane.

The propulsion fans are analyzed in the lower portion of Figure 47. The flight condition is $h_l/S = 0.64$, $q/\bar{P}_{tj} = 0.55$, and thrust equal to drag. The change in $\partial C_N / \partial \psi$ due to the nacelles when converted to a nacelle lift curve slope through use of the "tail" volume based on the projected side area ($d \times c$ for each nacelle) yields a value of 0.111. This reference area has been used in other studies of ducted fans. Perhaps a "rolled out" reference area would be more meaningful in which case the lift curve slope would be $0.111/\pi$.

Summing up, it appears that rear mounted propulsion fans do an excellent job of providing static directional stability for air-cushion vehicles with horizontal lift fan intakes through angles of yaw at least as great as 45° . See Figure 57 for the shape of the C_N vs. ψ curve for angles greater than 45° . One remaining problem is the directional instability which occurs with full reversal of the propulsion fans for maximum braking.

DIRECTIONAL

$q = 15$

NEUTRAL

POINT

FIG 43

$\frac{hL}{S} = 0.64$

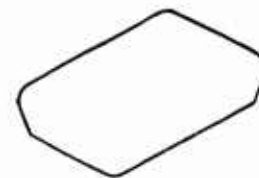
CONFIGURATION

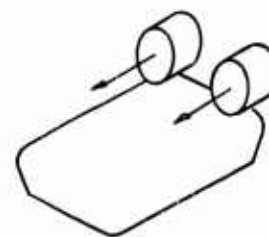
 ψ

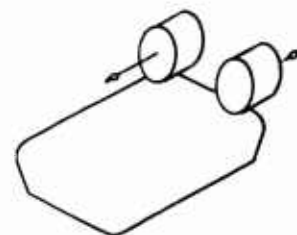
N.P. ~ %b

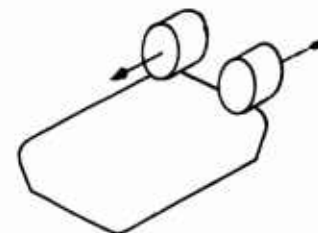
F

 $-5^\circ \text{ TO } 15^\circ$
 $15^\circ \text{ TO } 45^\circ$

43 %
27 %
 FP_F
 $-5^\circ \text{ TO } 5^\circ$
 $5^\circ \text{ TO } 15^\circ$
 $15^\circ \text{ TO } 45^\circ$

73 %
70 %
67 %
 FP_{DWM}
 $-5^\circ \text{ TO } 15^\circ$
 $15^\circ \text{ TO } 45^\circ$

68 %
65 %
 FP_{DR}
 $-5^\circ \text{ TO } 15^\circ$
 $15^\circ \text{ TO } 45^\circ$

61 %
66 %

NOTE: NP > 50 %b
NP AT 50 %b
NP < 50 %b

STABLE
NEUTRAL
UNSTABLE

DIRECTIONAL NEUTRAL POINT

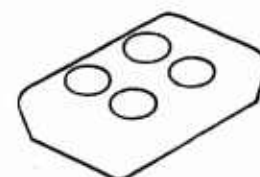
FIG 44

$$\frac{hl}{S} = 0.64$$

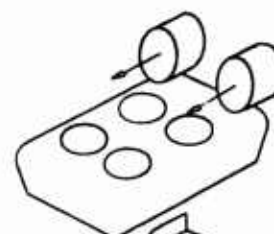
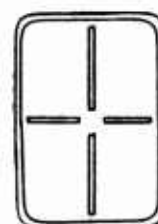
CONFIGURATION ψ NP ~ %b

J -5° to 5° 52%
 5° to 15° 40%
 15° to 45° 24%

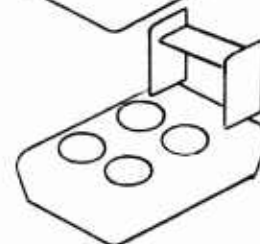
$$\frac{q}{P_i} = .55$$



JP_F -5° to 45° 67%

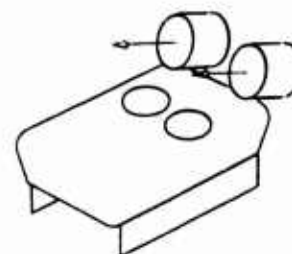


JVT -5° to 5° 64%
 5° to 15° 60%
 15° to 45° 50%



$$\frac{q}{P_i} = .42$$

$\frac{J}{2} S_{\frac{3}{4}} P_F + 15^\circ$ -5° to 5° 67%
 5° to 15° 69%
 15° to 45° 77%



NOTE: NP > 50% b STABLE
 NP AT 50% b NEUTRAL
 NP < 50% b UNSTABLE

EFFECT OF YAW ON PERIPHERAL PRESSURE DISTRIBUTION
IN THE PLANE OF THE BASE

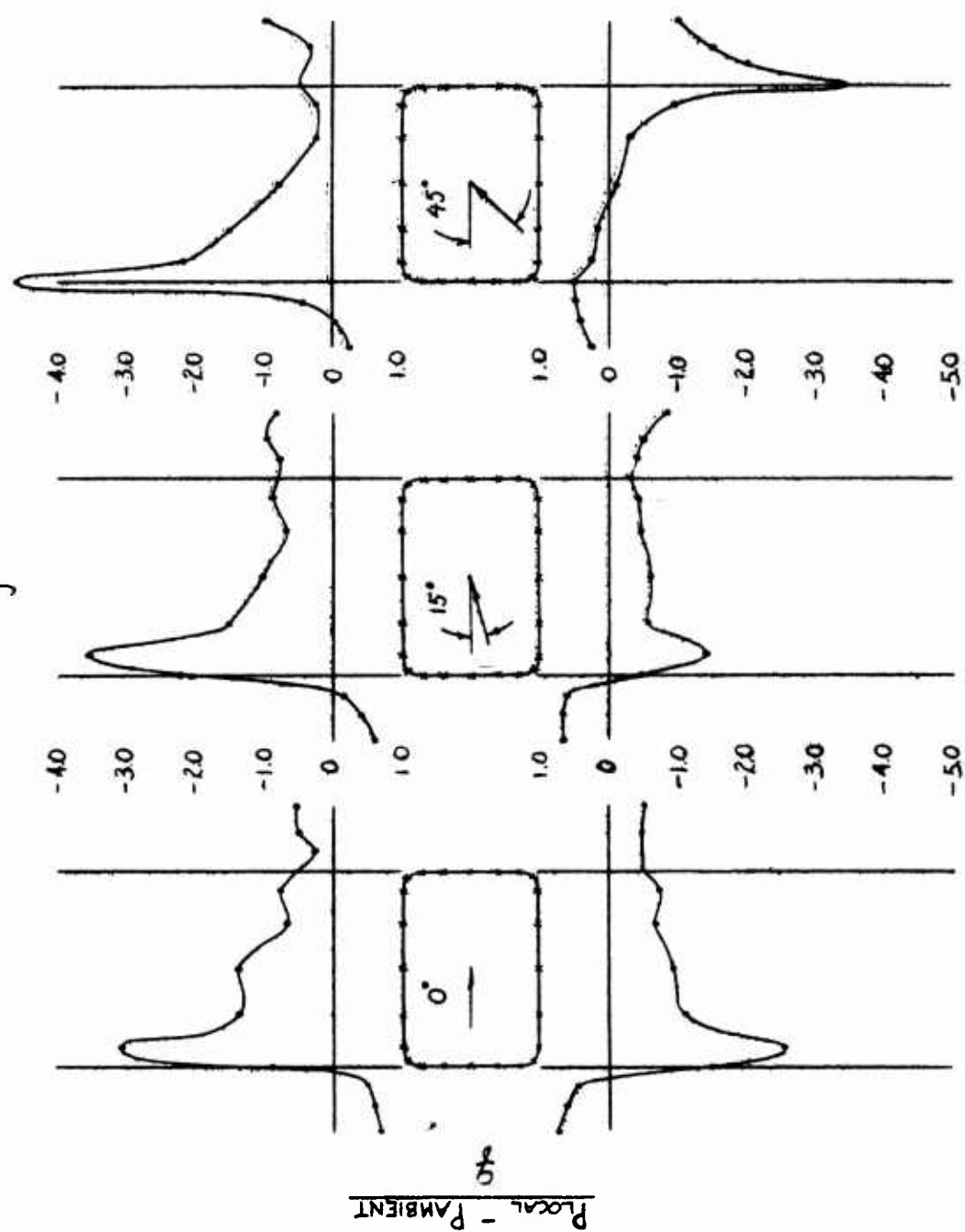


FIG 45

DIRECTIONAL NEUTRAL POINT

Fig 46

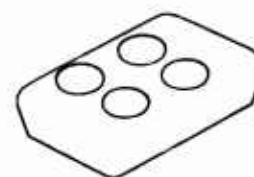
$$\frac{hl}{S} = 0.64$$

$$\frac{q}{P_{tj}} = .55$$

CONFIGURATION ψ N.P. ~ %b

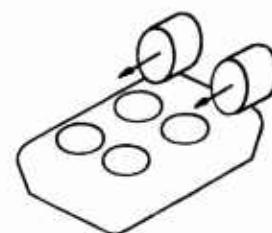
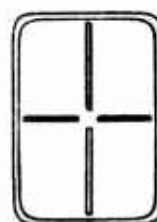
J

-5° to 5° 52%
5° to 15° 40%
15° to 45° 24%



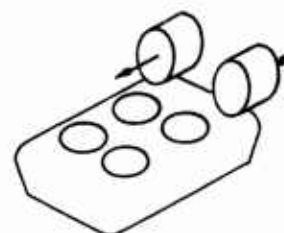
JP_F

-5° to 45° 67%



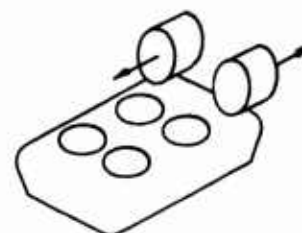
JP_{DM}

-5° to 15° 64%
15° to 45° 61%



JP_{DR}

-5° to 5° 50%
5° to 45° 60%



NOTE: NP > 50% b STABLE
NP AT 50% b NEUTRAL
NP < 50% b UNSTABLE

DIRECTIONAL STABILIZATION

FIG 47

A. VERTICAL TAILS $\frac{h l}{S} = 0.64$ $\frac{q}{P_{t_i}} = 0.55$

$$\frac{\partial C_L}{\partial \alpha}_{\text{TAIL}}$$

0.061

EFFECTIVE AR
GEOMETRIC AR

1.95



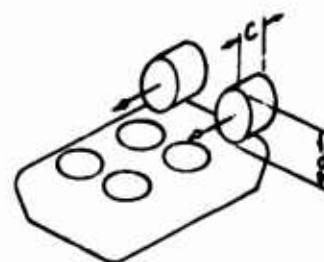
B. PROPULSION FANS & NACELLES

$\frac{h l}{S} = 0.64$ $\frac{q}{P_{t_i}} = 0.55$

THRUST -- DRAG

$$\left(\frac{\partial C_L}{\partial \alpha} \right)_{\text{NAC}} = 0.111$$

BASED ON PROJECTED
SIDE AREA = $d \cdot C$



5. Cross Stability Terms in Yaw

a. Method of Analysis

Due to the complexity of the problem and the early state of the art, the decision was made to rotate the model in one plane at a time. Thus, all runs were either pure pitch, pure roll, or pure yaw. All six force and moment components were measured but in most cases of single axis rotation, three components are sufficient to describe the behavior. Spot checks of the data reveal that side force, rolling moment, and yawing moment are negligible in pure pitch. Likewise, changes in drag, pitching moment and yawing moment are negligible in pure roll.

For the pure yaw case, however, it is not sufficient to merely look at the drag, side force, and yawing moment. Appreciable changes occur in rolling moment and pitching moment as the model is yawed. The yawing moment characteristics have already been covered in the directional stability section. The remaining components will now be discussed.

The forces in the horizontal plane were measured as side force perpendicular to the flight path and drag along the flight path. These were then expressed as lateral and longitudinal acceleration by dividing by the vehicle weight which was taken equal to the wind axis lift at the start of the maneuver ($\psi = 0^\circ$).

The rolling moment due to yaw is expressed as a lateral center of pressure shift in percent of model width by dividing the rolling moment coefficient by the lift coefficient where both items are in the body axis system. The pitching moment due to yaw is expressed as a longitudinal center of pressure shift in percent of model length by dividing the pitching moment coefficient by the lift coefficient. Again both items are in the body axis system.

b. Results for $q/p_{tj} = 0.55$

All configurations exhibit a strong roll in to the turn coupled with a nose down change in trim. The flight path lateral acceleration increases rapidly up to $\psi = 45^\circ$ and then falls slightly at higher yaw angles.

The J configuration is shown in Figures 48 and 49 to develop a maximum lateral acceleration of 0.13 g. The drag is relatively constant with yaw angle. The body axis roll due to yaw increases linearly with ψ and amounts to an 11% lateral center of pressure shift at $\psi = 90^\circ$. The longitudinal center of pressure which was 8% out of trim at $\psi = 0^\circ$ reduces to only 1% out of trim at $\psi = 90^\circ$.

The addition of vertical tails (JVT) produces side force of 1/4 g in the wind axis system and has a history of drag and longitudinal center of pressure shift similar to the J configuration. The lateral center of pressure shift of JVT is higher than for J, rising to 18% at $\psi = 90^\circ$.

The addition of propulsion fans (configuration JPF) led to some surprising results. At $\psi = 0$ the fans RPM were adjusted so that the net drag was zero, i. e., thrust = +0.28 g was equal and opposite to drag = -0.28 g.

When the configuration with the fan RPM set as noted above was oriented at $\psi = 45^\circ$, the wind axis lateral force (the force which produces the turn maneuver) was one "g", a rather surprisingly high value. The drag force (0.28 g @ $\psi = 0$) was 0.75 g at $\psi = 90^\circ$.

The addition of propulsion fans JPF leads to a maximum wind axis side force @ $\psi = 45^\circ$ of one g.

The lateral center of pressure shift increases even more rapidly than for the tailed version, rising to a value of 22% at $\psi = 90^\circ$. The change in longitudinal

center of pressure is also larger changing from 6% nose up at $\psi = 0^\circ$ to 11% nose down at $\psi = 90^\circ$.

The skirted and flap segmented configuration (S) is shown in Figures 50 and 51 to have flight path lateral acceleration, drag, and longitudinal center of pressure shift very similar to the J configuration. The lateral center of pressure shift is, however, significantly lower, especially at low angles of yaw. The J/2 S 3/4 has characteristics similar to the S configuration. Addition of propulsion fans to the J/2 S 3/4 configuration again produces large changes in lateral acceleration, drag, lateral and longitudinal center of pressure shift.

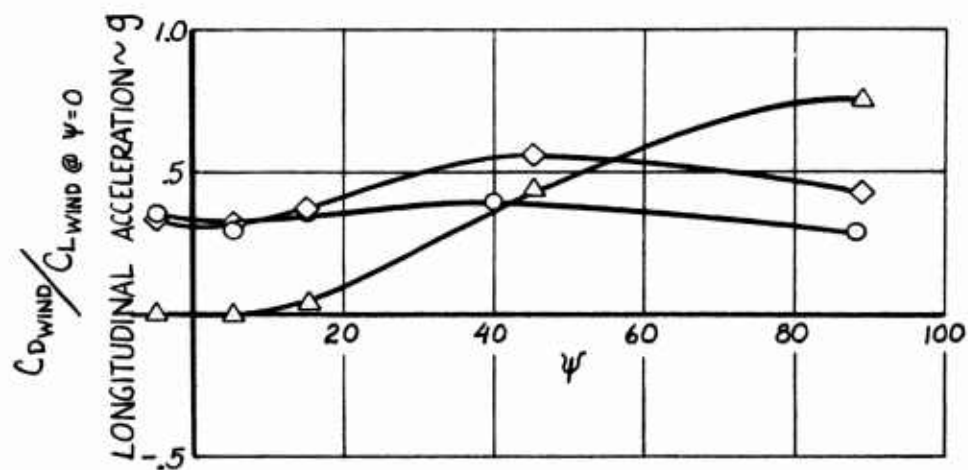
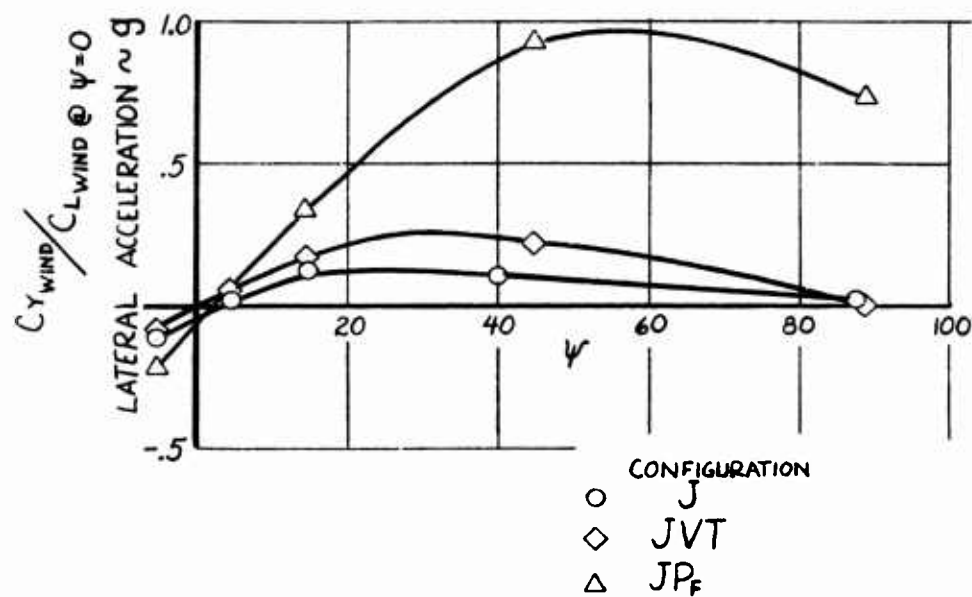
Half the lateral center of pressure shift is coming from the propulsion fans which act as very efficient fins high above the center of gravity. Even if the propulsion fans (which are desirable from the propulsion, and yaw control standpoint) were removed, there is still a very large lateral center of pressure shift remaining. At large yaw angles the cushion loads produce negative roll due to yaw. It is concluded that the momentum drag of the intake air produces the large positive roll due to yaw just as it produced the pitch up problem at forward speed. It should be remembered that the yaw runs were made with the model level. Under combined angles, the results may differ.

Summing up, then, it is apparent that if large angles of yaw are to be employed in turning maneuvers, more study will be necessary to solve the problems uncovered in these preliminary experiments. The strong lateral acceleration is of course welcome but the lateral center of pressure shift at large yaw angles is greater than can be overcome with the lateral jet control employed in this experiment. Likewise, the longitudinal center of pressure shift is greater than can be trimmed out with control systems investigated to date.

EFFECT OF YAW ON LATERAL AND LONGITUDINAL ACCELERATION

FIG 48

$$\frac{h\ell}{S} = .64 \quad \delta/\rho_{ej} = .55$$



EFFECT OF YAW ON
ROLL TRIM AND PITCH TRIM
 $h/s = .64$ $g/P_0 = .55$

FIG 49

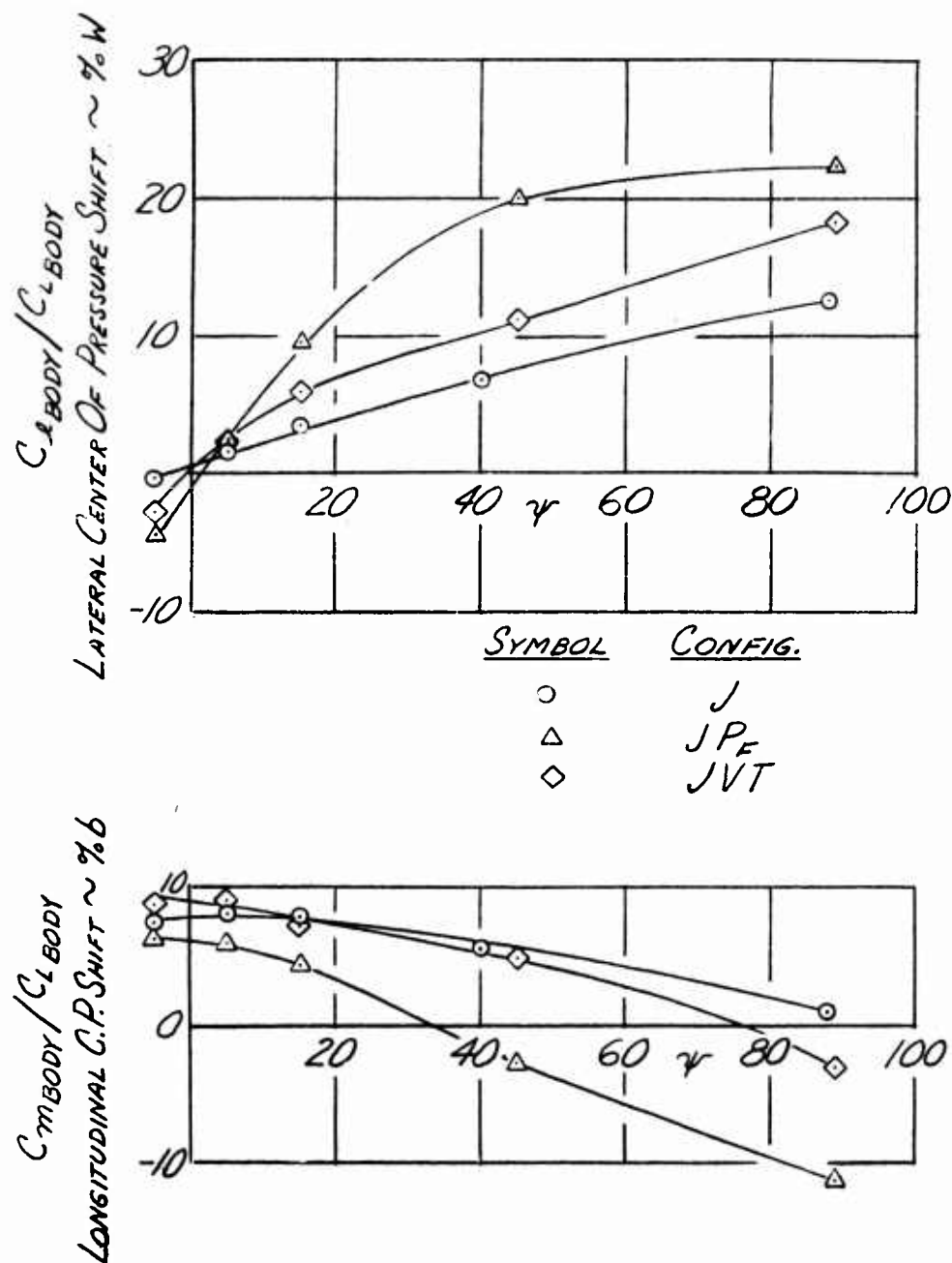
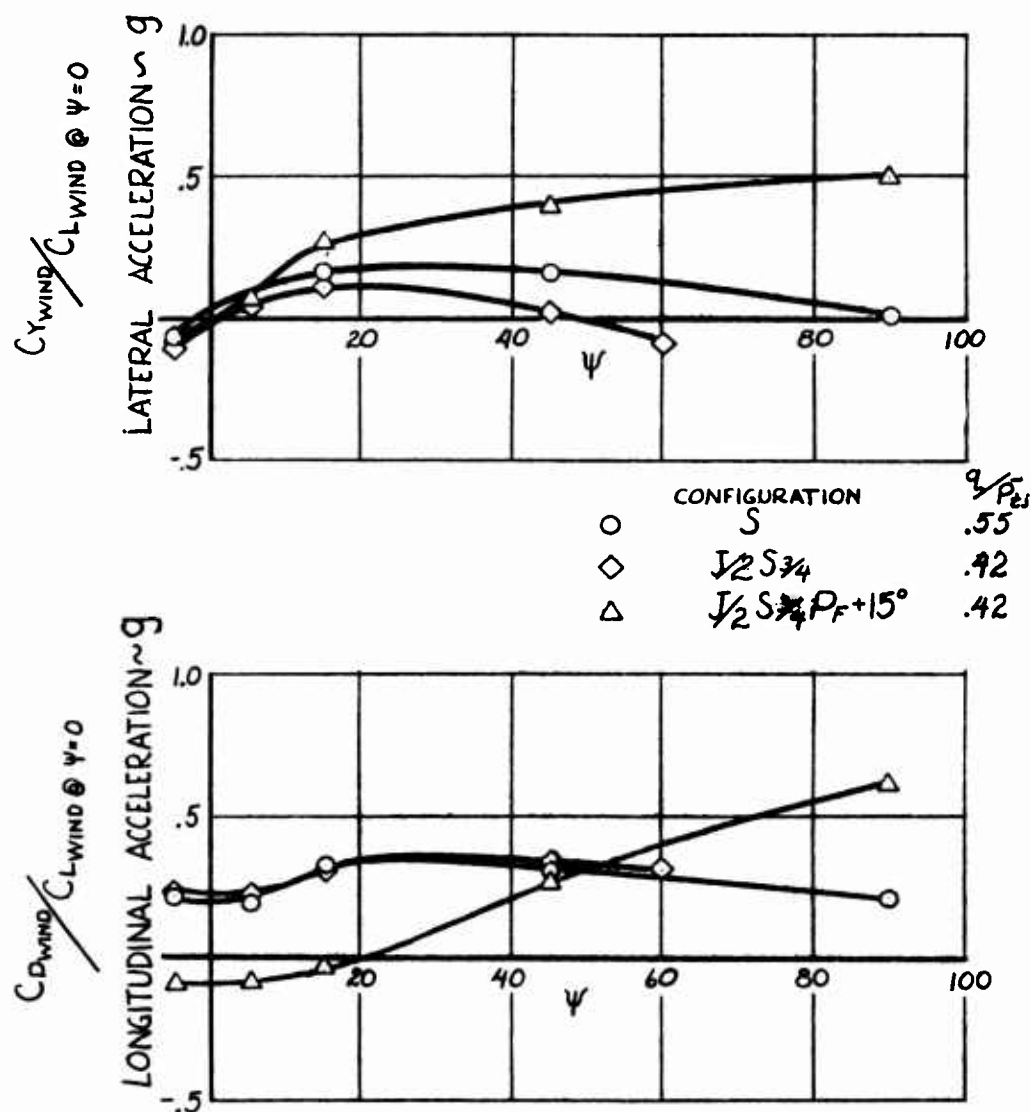


FIG 50

EFFECT OF YAW ON LATERAL AND LONGITUDINAL ACCELERATION

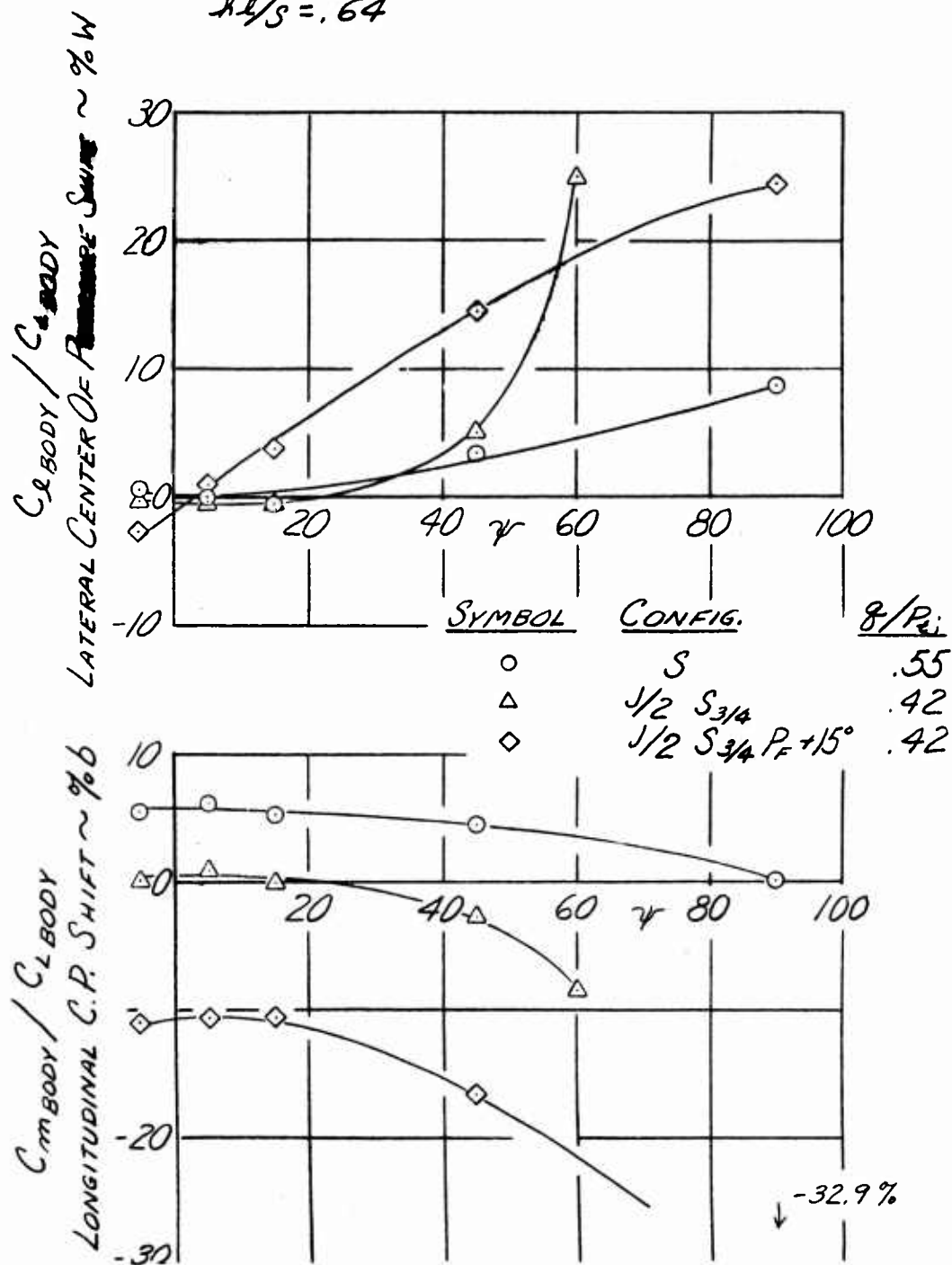
$$\frac{hL}{S} = .64$$



EFFECT OF YAW ON ROLL TRIM AND PITCH TRIM

FIG 51

$$h/s = .64$$



6. Longitudinal Control

a. Method of Analysis

The method used previously to define the magnitude of the pitch up problem was also used to define longitudinal control power. The pitching moment produced by control action was divided by the lift acting perpendicular to the body. The resulting shift in effective center of pressure was expressed in percent of vehicle length.

b. Results

A comparison of several longitudinal control schemes is presented in Figure 52. A horizontal tail with area equal to 11.5% of the planform area and a length of half the vehicle characteristic length produces a center of pressure shift of 2.3% of the vehicle length forward and aft of the C. G. when the tail is deflected 10° nose down and nose up respectively. These results are increased to 3% when the tail is mounted between vertical tails. The control power is increased proportional to the tail arm increase obtained by placing the tail assembly behind the vehicle on booms.

Full closure of the front or rear jet in hovering provides a shift in center of pressure of 8% of the vehicle length at a cost of 26% of the lift. In forward flight, closure of the front jet has very little effect on lift or pitching moment. The center of pressure shift is only 1.5% compared to the requirement of 8% to cure the pitch up. Closure of the rear jet produced a center of pressure shift of 8% at a cost of 25% of the lift. This trim change is of course in the opposite direction to that required to cure the pitch up.

The bottom sketch presents the effect of tilting the propulsion nacelles. A 15° tilt provides an 11.5% center of pressure shift at a flight q of 15 lbs/ft² and a 6% shift at a q of 36 lbs/ft². The fans were providing thrust 10% greater than drag at the lower speed and 10% less than the drag at the high speed. These center of pressure shifts were greater than computed values based on thrust component only, but were 80% of the computed

values which included both thrust term and normal force term. The propulsion nacelle apparently does not feel the full angle of attack.

Results of an analysis of the horizontal tail effectiveness is presented in Figure 53. The rate of change of tail lift with tail incidence is deduced from the change in pitching moment and the tail volume coefficient. These values are compared to the value of $C_{L\alpha}$ for an isolated tail. When placed above the propulsion nacelles, the horizontal tail is found to be 80% as effective as the isolated tail when used as a control device. When placed between vertical tails at the same tail length it is 96% effective and when the tail length is doubled, it achieves 98% of maximum effectiveness. Compare these values with those of horizontal tail effectiveness when used as a stabilization device as given in Figure 36. The choice of location of a tail when required to augment stability is more critical than choice of location when it need serve only a control function. The reasons are given in the section on longitudinal stability.

7. Lateral Control

The method of analysis is identical to the longitudinal control case except that the center of pressure shift is expressed in percent of vehicle width.

Results are shown in Figure 54 for the basic jet segmented model and for the same model with propulsion fans operating. The basic model achieves a shift in center of pressure of 13% of the width in hovering when one complete side jet is closed. In forward flight the shift is reduced to 10% of the width. Control effectiveness is equally strong at a 10° roll angle as it is at 0° in hovering and at q/\bar{p}_{tj} equal to 0.55. At the high speed ($q/\bar{p}_{tj} = 1.10$) there is a large loss in lateral control power at $\phi = 10^\circ$.

The addition of propulsion fans has a slightly unfavorable interference. The center of pressure shift being reduced from 10% to 9% at $q/\bar{p}_{tj} = 0.55$ and to 8% at $q/\bar{p}_{tj} = 1.10$. Again, the reduction in control power at $\phi = 10^\circ$ is apparent at high speed.

Additional details on jet lateral control are presented in Figures 55 and 56. The upper part of Figure 55 reveals that with the control jet half open very little center of pressure shift is obtained for the lift that is lost. This is due to the poor internal flow in the wind tunnel model. In the space available, it was not possible to turn the high speed flow efficiently in the approach to the nozzle. Many vehicle configurations will also be faced with this problem. In the remainder of the runs, the intermediate control position was taken as only a quarter open. The curves of lift loss vs. center of pressure shift are now easier to fair. It should be noted that a shift in lateral center of pressure of 10% of the vehicle width comes at a loss of 30% of the lift.

8. Directional Control and Braking

The effect of both windmilling and reversing one propulsion fan on the yawing moment coefficient over a 90° range of yaw angles is presented in Figure 57 for the jet segmented model with propulsion fans. This configuration has perhaps an undesirably high degree of directional stability. Windmilling one propulsion fan allows the vehicle to be trimmed to a 12° yaw angle with little decrease in static directional stability. Reversing one propulsion fan allows directional trim over the full 90° yaw angle range. The directional stability does become neutral at small yaw angles, however, with one fan fully reversed.

The braking effect of the propulsion fans is quite good. With the fans windmilling within the nacelles, it was somewhat disappointing to find that the net propulsion thrust was only zero. A non-shrouded prop would have produced some drag in addition. Due to the high drag of the basic jet segmented configuration, however, reducing propulsive thrust to zero causes a longitudinal deceleration of 0.28 g. If both fans are reversed (and run at the same RPM at which they had cancelled out, the drag when thrusting) a longitudinal deceleration of 0.75 g results. It must be remembered that full reversal of both propulsion fans leads to directional instability at small yaw angles. Since control power and radius of gyration in yaw are large, the situation may perhaps be acceptable.

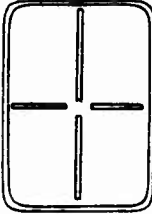
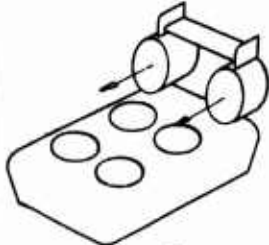
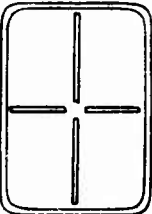
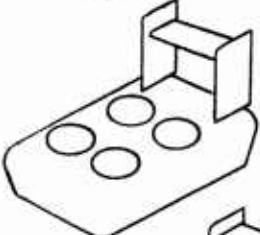

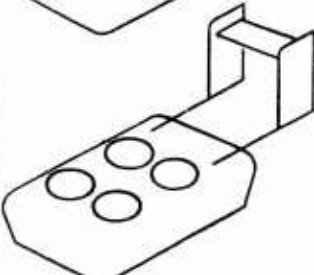

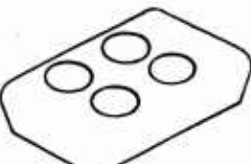

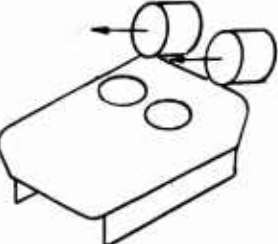
Summing up the control power situation for air-cushion vehicles at $h_l/S \approx 0.40$:

1. Closure of fore and aft jets does not constitute a practical longitudinal control in forward flight. A horizontal tail of reasonable size does not appear adequate. Tilting of propulsion fans appears to be the best solution to date if mechanically practical.
2. Closure of side jets provides better lateral than longitudinal control at forward speed but the lift penalty is unacceptable. The control function must be divorced from the lift function.
3. Differential propulsion fan thrust is a suitable method of directional control and braking.

LONGITUDINAL CONTROL POWER ZERO ANGLE OF ATTACK

FIG 52

$$\frac{hL}{S} = 0.64$$

METHOD	$\frac{q}{P_{Tj}}$	C.P. SHIFT ~%b			
		Nose Up	Nose Down		
JP _F T	+10° i _t	.55			
	-10° i _t	.55	2.5%		
JVT	+10° i _t	.55			
	-10° i _t	.55	3.0%		
J _{EXT} T	+10° i _t	.55			
	-10° i _t		5.7%		
J		0.00			
	FRONT JET	.55	8.4%		
	CLOSURE	1.10	1.7%		
			1.5%		
	REAR JET	.55	8.0%		
	CLOSURE	1.10	9.0%		
$\frac{J}{2} S_{\frac{3}{4}} P_F + 15^\circ$.42			
		.72	11.5%		
			6.0%		

HORIZONTAL TAIL EFFECTIVENESS

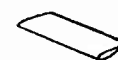
FIG 53

B. CONTROL POWER

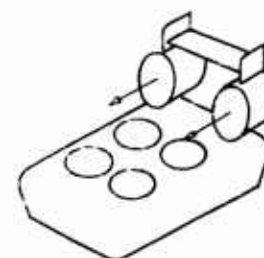
$$\frac{h l}{S} = 0.64 \quad \frac{q}{P_{tj}} = 0.55$$

CONFIGURATION	$\frac{\partial C_L}{\partial i_t}$	$\frac{\partial C_L / \partial i_t}{\partial C_L / \partial \alpha}$
---------------	-------------------------------------	----------------------------------------------------------------------

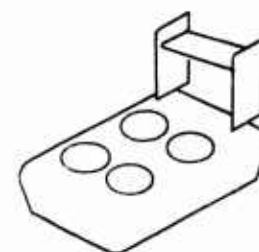
ISOLATED TAIL	0.055	1.0
---------------	-------	-----



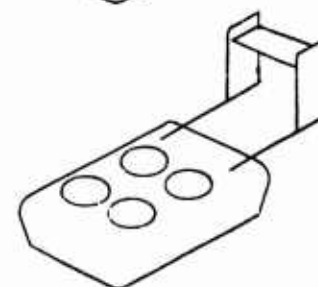
J_{P_T}	0.044	0.8
-----------	-------	-----



J_{V_T}	0.053	0.965
-----------	-------	-------



J_{EXT}	0.0536	0.975
-----------	--------	-------



LATERAL CONTROL POWER

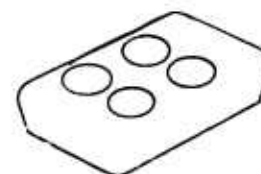
FIG 54

CENTER OF PRESSURE SHIFT \sim % WIDTH
DUE TO CLOSING ONE SIDE JET

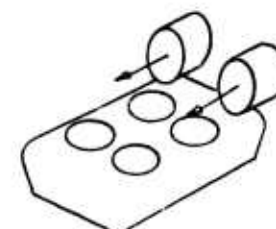
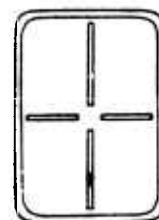
$$\frac{h_l}{S} = 0.64$$

CONFIGURATION	$\frac{q}{P_{tj}}$	ϕ	$\Delta C.P. \sim \% W$
---------------	--------------------	--------	-------------------------

J	0	0°	13.4%
		10°	13.9%
J	.55	0°	10.0%
		10°	10.0%
J	1.10	0°	10.0%
		10°	3.2%



JP _f	.55	0°	9.0%
		10°	7.3%
JP _f	1.10	0°	8.0%
		10°	5.0%



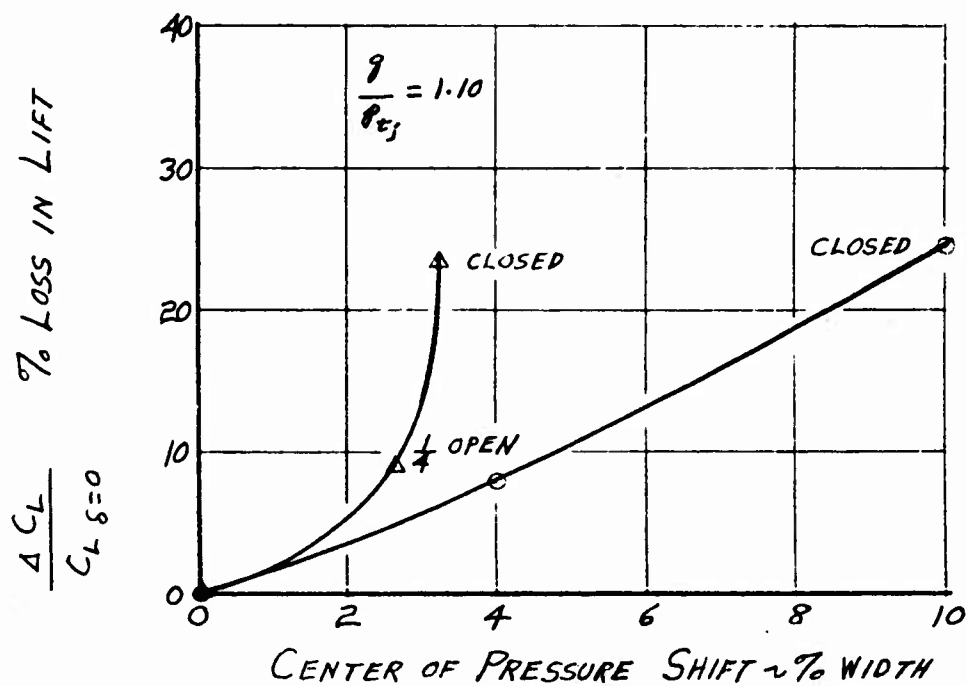
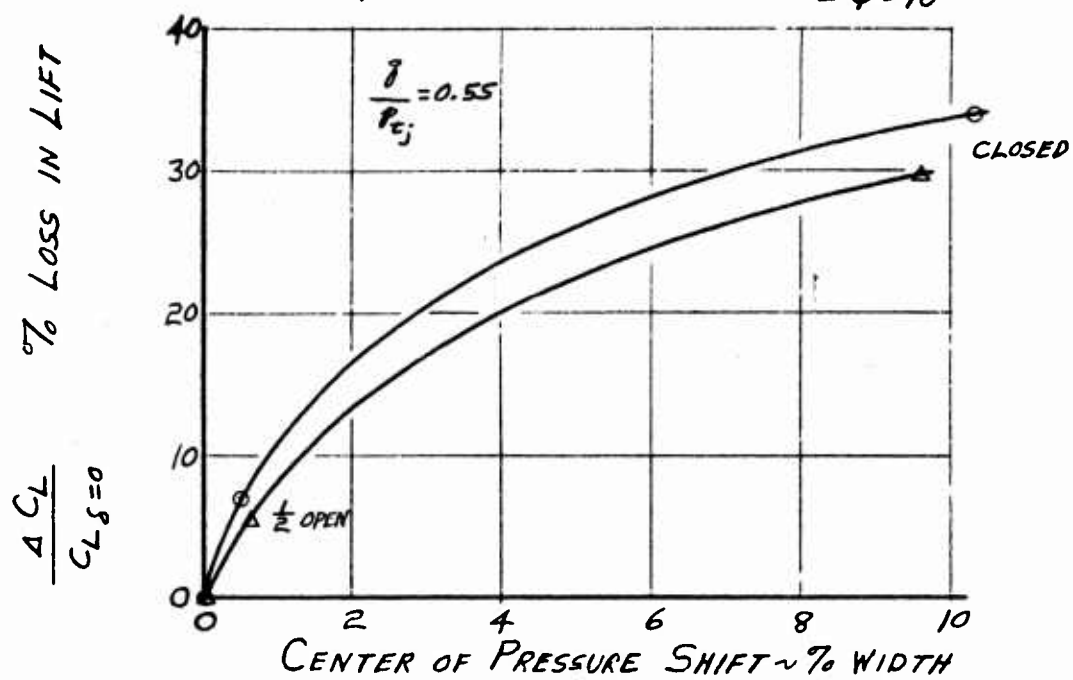
POWER AND COST OF LATERAL CONTROL

$$hl/S = 0.64 \quad \bar{\sigma}$$

$$\circ \phi = 0^\circ$$

$$\triangle \phi = 10^\circ$$

FIG 55



POWER AND COST OF LATERAL CONTROL

FIG 56

$$hl/S = 0.64 \quad \bar{J}PF$$

$$\circ \phi = 0^\circ$$

$$\triangle \phi = 10^\circ$$

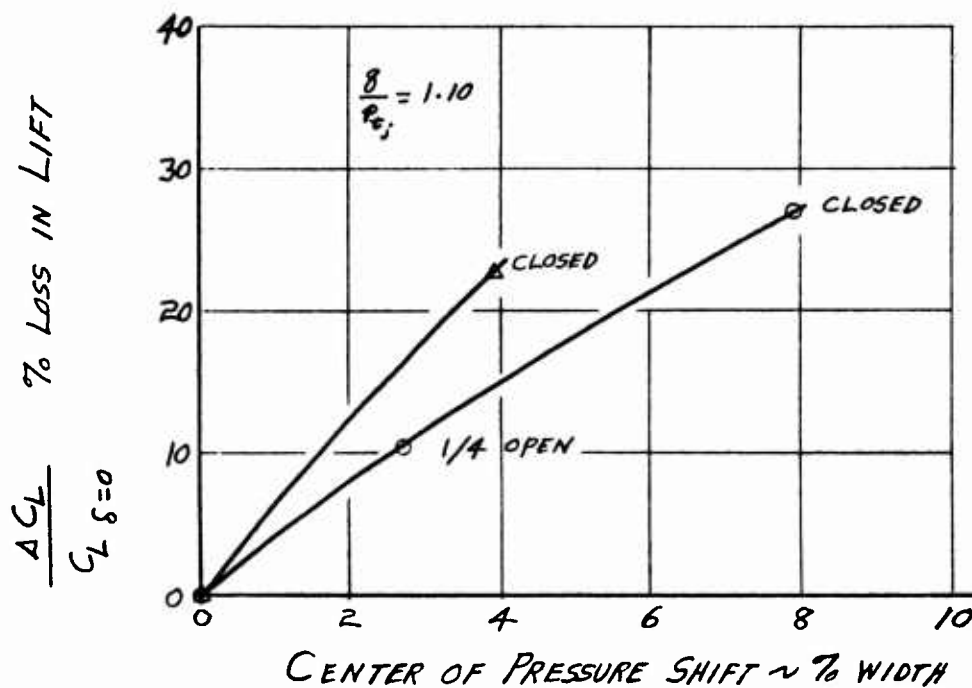
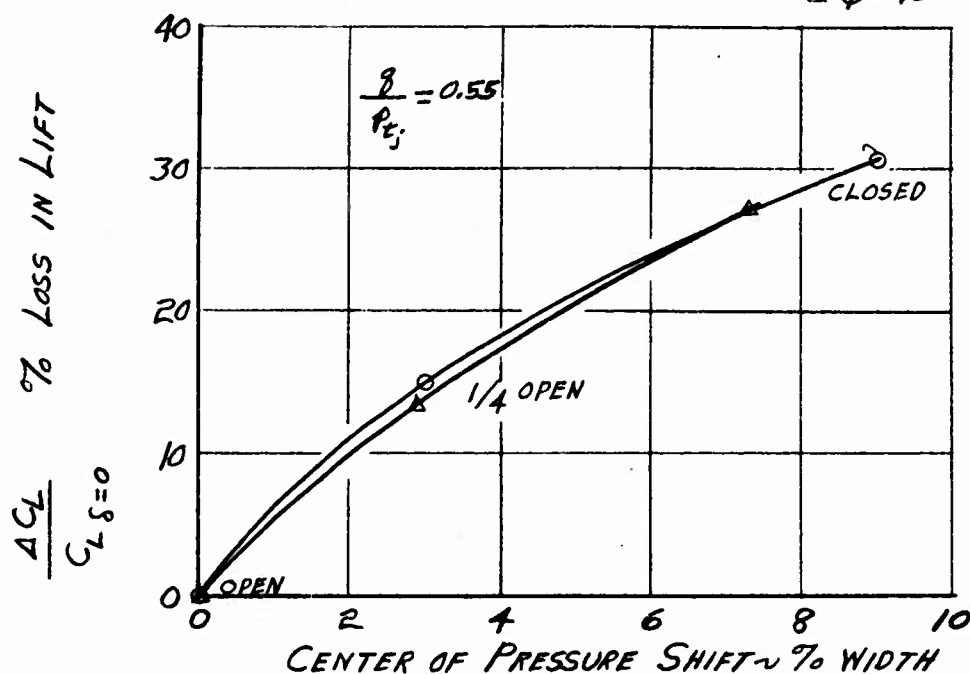
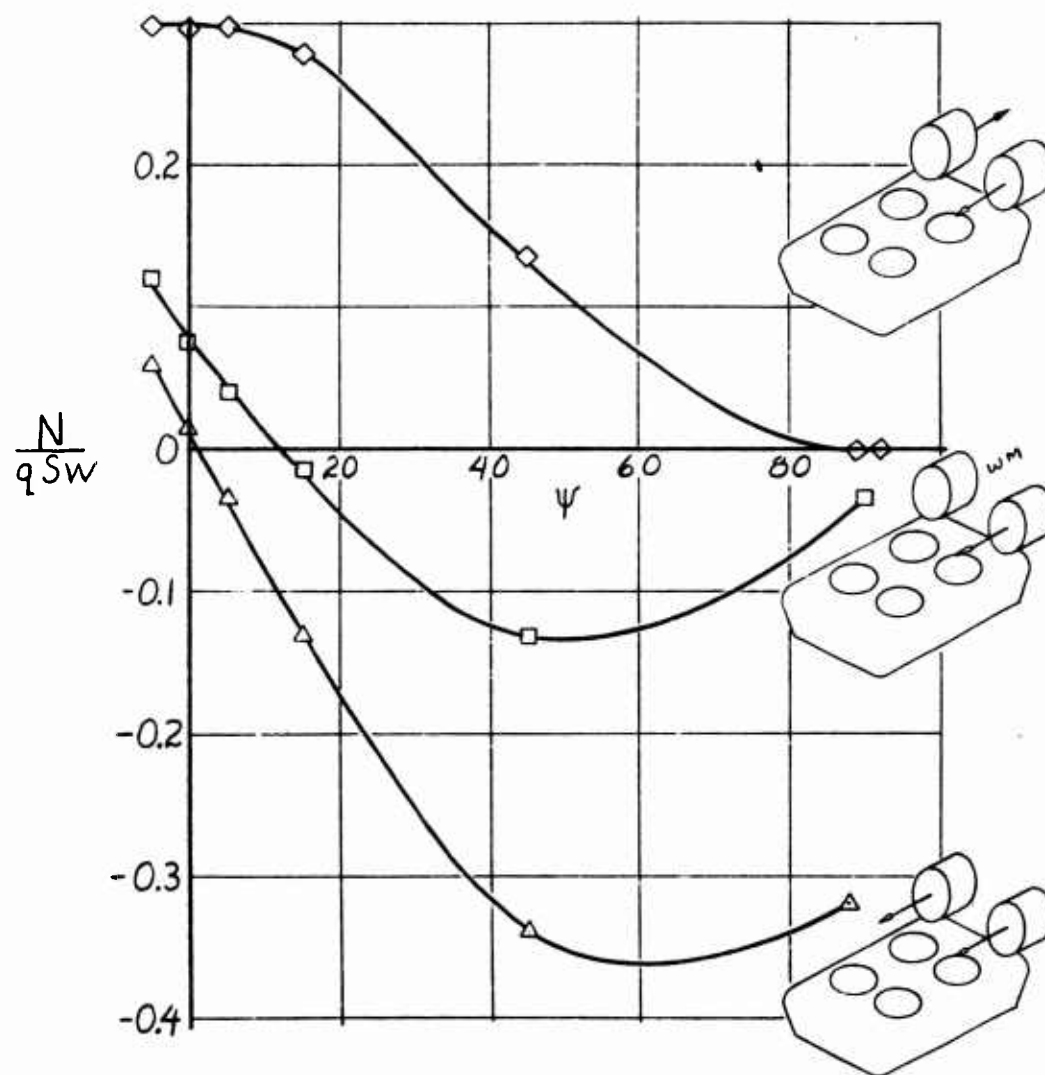


FIG 57

DIRECTIONAL CONTROL POWER

JP

 $q = .55$ $\frac{h\ell}{S} = .64$ 

ACKNOWLEDGEMENTS

The support of U. S. Army Transportation Research Command is greatly acknowledged.

The model design was ably executed by Mr. R. H. Ottoson and constructed by Mr. F. F. Kerns. The generosity of Vought Aeronautics in loading four tip jet fans and four pressure scani-valves contributed much to the success of the program. The quality of the Vought tunnel facilities and competence of Vought personnel was also a major factor in the success of the program. In particular, the Vought Project Engineer, Mr. J. Flechtner, was of major assistance.

The pressure data was integrated on Aeronutronic computers under the able guidance of Mr. D. Stewart. The force data was put in form for analysis through the efforts of Mrs. J. Herron and Mr. K. Kuperus. The final presentation of data was enhanced by the art work of co-author Mr. D. E. McNay. Valuable contributions to the analysis were provided by Department Manager, M. F. Southcote.

BIBLIOGRAPHY

1. Carmichael, B. H.
Aeronutronic, a Division of Ford Motor Company
HOVERING STATIC STABILITY AND PERFORMANCE
EXPERIMENTS, THREE-DIMENSIONAL ANNULAR JET
MODELS
Aeronutronic Publication No. U-1443
15 November 1961

3. Carmichael, B. H.
Aeronutronic, a Division of Ford Motor Company
HOVERING TWO-DIMENSIONAL ANNULAR JET
PERFORMANCE EXPERIMENTS
Aeronutronic Publication No. U-1053
November 1960

DISTRIBUTION

USAWC	1
USATMC(FTZAT), ATO	1
USAPRDC	1
DCSLOG	1
Rsch Anal Corp	1
ARO, Durham	2
OCRD, DA	2
Ofc of Maint Engr, ODDR&E, OSD	1
NATC	1
ARO, OCRD	1
DCSOPS	1
USAERDL	2
USAOTAC, Center Line	3
OrdBd	1
QMRECOMD	1
CofT	3
USATCDG	1
USATMC	19
USATSCH	4
USATRECOM	77
TCLO, USAERDL	1
TCLO, USAABELCTBD	1
USATRECOM LO, USARDG(EUR)	3
CNO	1
CNR	3
BUWEPS, DN	1
BUWEPS, DN (RA-4)	1
ACRD(OW), DN	1
USNSRDF	1
USNPGSCH	1
BUSHP, DN	1
USNOTS	1
Dav Tay Mod Bas	2
MCLFDC	1
MCEC	1
USASGCA	1
Canadian LO, USATSCH	3
BRAS, DAQMG(Mov&Tn)	4
USASG, UK	1
Langley Rsch Cen, NASA	3

NASA, Wash., D. C.	6
Ames Rsch Cen, NASA	2
Lewis Rsch Cen, NASA	1
USGPO	1
ASTIA	10
USAMRDC	1
HUMRRO	2
DDRE	1
Maritime Administration	1
Human Engineering Lab	1

Aeronutronic Division, Ford Motor Company, Newport Beach, California
OVERLAND AIR-CUSHION VEHICLE STABILITY AND CONTROL WIND TUNNEL EXPERIMENTS, by B. H. Carmichael, D. E. McNay.
Report No U-1447, November 1961 (Contract DA44-177-TC-709) Task 9R99-01-005-02. 102p. incl. illus. (TCREC Technical Report 62-35)

1. Fluid Dynamics, Aerodynamics
2. Stability & Control

Unclassified Report

The static stability in pitch, roll, and yaw of a generalized annular jet (GEM) has been determined in hover and forward flight at ratios of h/d

(over)

Aeronutronic Division, Ford Motor Company, Newport Beach, California
OVERLAND AIR-CUSHION VEHICLE STABILITY AND CONTROL WIND TUNNEL EXPERIMENTS, by B. H. Carmichael, D. E. McNay.
Report No U-1447, November 1961 (Contract DA44-177-TC-709) Task 9R99-01-005-02. 102p. incl. illus. (TCREC Technical Report 62-35)

1. Fluid Dynamics, Aerodynamics
2. Stability & Control

Unclassified Report

The static stability in pitch, roll, and yaw of a generalized annular jet (GEM) has been determined in hover and forward flight at ratios of h/d

(over)

Aeronutronic Division, Ford Motor Company, Newport Beach, California
OVERLAND AIR-CUSHION VEHICLE STABILITY AND CONTROL WIND TUNNEL EXPERIMENTS, by B. H. Carmichael, D. E. McNay.
Report No U-1447, November 1961 (Contract DA44-177-TC-709) Task 9R99-01-005-02. 102p. incl. illus. (TCREC Technical Report 62-35)

1. Fluid Dynamics, Aerodynamics
2. Stability & Control

Unclassified Report

The static stability in pitch, roll, and yaw of a generalized annular jet (GEM) has been determined in hover and forward flight at ratios of h/d

(over)

Aeronutronic Division, Ford Motor Company, Newport Beach, California
OVERLAND AIR-CUSHION VEHICLE STABILITY AND CONTROL WIND TUNNEL EXPERIMENTS, by B. H. Carmichael, D. E. McNay.
Report No U-1447, November 1961 (Contract DA44-177-TC-709) Task 9R99-01-005-02. 102p. incl. illus. (TCREC Technical Report 62-35)

1. Fluid Dynamics, Aerodynamics
2. Stability & Control

Unclassified Report

The static stability in pitch, roll, and yaw of a generalized annular jet (GEM) has been determined in hover and forward flight at ratios of h/d

(over)

exceeding 0.1, the normal stability limit. The effects of modifications to the basic configuration, including full and partial skirting, were determined. In addition to stability data, control forces and some performance and pressure distribution data were obtained. The hovering and the forward flight investigations are presented in separate reports (TCREC Tech Rpts 62-35 and 62-36). A report, Vought Aeronautics LSWT 105, dated December 1961, containing basic wind tunnel test data is available, on loan, from the Research Reference Center, USA TRECOM.

exceeding 0.1, the normal stability limit. The effects of modifications to the basic configuration, including full and partial skirting, were determined. In addition to stability data, control forces and some performance and pressure distribution data were obtained. The hovering and the forward flight investigations are presented in separate reports (TCREC Tech Rpts 62-35 and 62-36). A report, Vought Aeronautics LSWT 105, dated December 1961, containing basic wind tunnel test data is available, on loan, from the Research Reference Center, USA TRECOM.

exceeding 0.1, the normal stability limit. The effects of modifications to the basic configuration, including full and partial skirting, were determined. In addition to stability data, control forces and some performance and pressure distribution data were obtained. The hovering and the forward flight investigations are presented in separate reports (TCREC Tech Rpts 62-35 and 62-36). A report, Vought Aeronautics LSWT 105, dated December 1961, containing basic wind tunnel test data is available, on loan, from the Research Reference Center, USA TRECOM.

exceeding 0.1, the normal stability limit. The effects of modifications to the basic configuration, including full and partial skirting, were determined. In addition to stability data, control forces and some performance and pressure distribution data were obtained. The hovering and the forward flight investigations are presented in separate reports (TCREC Tech Rpts 62-35 and 62-36). A report, Vought Aeronautics LSWT 105, dated December 1961, containing basic wind tunnel test data is available, on loan, from the Research Reference Center, USA TRECOM.

Aeronutronic Division, Ford Motor Company, Newport Beach, California
OVERLAND AIR-CUSHION VEHICLE STABILITY
AND CONTROL WIND TUNNEL EXPERIMENTS,
by B. H. Carmichael, D. E. McNay.
Report No U-1447, November 1961 (Contract DA44-177-TC-709) Task 9R99-01-005-02. 102p. incl. illus. (TCREC Technical Report 62-35)

1. Fluid Dynamics, Aerodynamics
2. Stability & Control

Aeronutronic Division, Ford Motor Company, Newport Beach, California
OVERLAND AIR-CUSHION VEHICLE STABILITY
AND CONTROL WIND TUNNEL EXPERIMENTS,
by B. H. Carmichael, D. E. McNay.
Report No U-1447, November 1961 (Contract DA44-177-TC-709) Task 9R99-01-005-02. 102p. incl. illus. (TCREC Technical Report 62-35)

1. Fluid Dynamics, Aerodynamics
2. Stability & Control

Unclassified Report

The static stability in pitch, roll, and yaw of a generalized annular jet GEM has been determined in hover and forward flight at ratios of h/d (over)

Aeronutronic Division, Ford Motor Company, Newport Beach, California
OVERLAND AIR-CUSHION VEHICLE STABILITY
AND CONTROL WIND TUNNEL EXPERIMENTS,
by B. H. Carmichael, D. E. McNay.
Report No U-1447, November 1961 (Contract DA44-177-TC-709) Task 9R99-01-005-02. 102p. incl. illus. (TCREC Technical Report 62-35)

1. Fluid Dynamics, Aerodynamics
2. Stability & Control

Aeronutronic Division, Ford Motor Company, Newport Beach, California
OVERLAND AIR-CUSHION VEHICLE STABILITY
AND CONTROL WIND TUNNEL EXPERIMENTS,
by B. H. Carmichael, D. E. McNay.
Report No U-1447, November 1961 (Contract DA44-177-TC-709) Task 9R99-01-005-02. 102p. incl. illus. (TCREC Technical Report 62-35)

1. Fluid Dynamics, Aerodynamics
2. Stability & Control

Unclassified Report

The static stability in pitch, roll, and yaw of a generalized annular jet GEM has been determined in hover and forward flight at ratios of h/d (over)

Unclassified Report

The static stability in pitch, roll, and yaw of a generalized annular jet GEM has been determined in hover and forward flight at ratios of h/d (over)

exceeding 0.1, the normal stability limit. The effects of modifications to the basic configuration, including full and partial skirting, were determined. In addition to stability data, control forces and some performance and pressure distribution data were obtained. The hovering and the forward flight investigations are presented in separate reports (TCREC Tech Rpts 62-35 and 62-36). A report, Vought Aeronautics LSWT 105, dated December 1961, containing basic wind tunnel test data is available, on loan, from the Research Reference Center, USA TRECOM.

exceeding 0.1, the normal stability limit. The effects of modifications to the basic configuration, including full and partial skirting, were determined. In addition to stability data, control forces and some performance and pressure distribution data were obtained. The hovering and the forward flight investigations are presented in separate reports (TCREC Tech Rpts 62-35 and 62-36). A report, Vought Aeronautics LSWT 105, dated December 1961, containing basic wind tunnel test data is available, on loan, from the Research Reference Center, USA TRECOM.

exceeding 0.1, the normal stability limit. The effects of modifications to the basic configuration, including full and partial skirting, were determined. In addition to stability data, control forces and some performance and pressure distribution data were obtained. The hovering and the forward flight investigations are presented in separate reports (TCREC Tech Rpts 62-35 and 62-36). A report, Vought Aeronautics LSWT 105, dated December 1961, containing basic wind tunnel test data is available, on loan, from the Research Reference Center, USA TRECOM.

exceeding 0.1, the normal stability limit. The effects of modifications to the basic configuration, including full and partial skirting, were determined. In addition to stability data, control forces and some performance and pressure distribution data were obtained. The hovering and the forward flight investigations are presented in separate reports (TCREC Tech Rpts 62-35 and 62-36). A report, Vought Aeronautics LSWT 105, dated December 1961, containing basic wind tunnel test data is available, on loan, from the Research Reference Center, USA TRECOM.

UNCLASSIFIED

UNCLASSIFIED